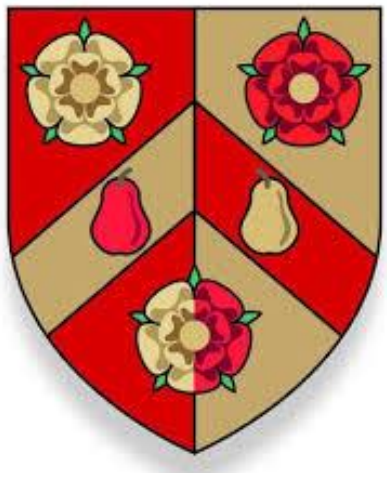

The University of Oxford

A thesis submitted for the degree of Doctor of Philosophy, Medical Sciences Division, University of Oxford

The Role of the cdk5 Pathway and NMDA Receptor Phosphorylation in Neurodegeneration in Hippocampal Sclerosis

Maysa M S Falah, BSc., MSc. Wolfson college.

Supervised by: Prof. John Jefferys & Prof. Arjune Sen.

Department of Pharmacology & Nuffield Department of Clinical Neurosciences.

DECLARATION

This thesis is a presentation of my original research work. Wherever contributions of others are involved, every effort is made to indicate this clearly, with due reference to the literature, and acknowledgement of collaborative research and discussions.

Maysa M S FALAH

Acknowledgments

This is a piece of written work that comes as a conclusion of a long and at times very difficult road. I am sincerely indebted to Professor John Jefferys for his eagerness to follow me across that road, with his unflagging advice and interest. I am also grateful to Professor Arjune Sen, who equally contributed to advising on various stages on this. I would like also to thank Prof. Matthew Walker and Dr Karri Lamsa.

A big Thanks from the heart to Prof. Frances Platt, Dr James Gray and the Platt group for all the advice, support and the valuable lab space.

Managing to remain on track despite the problems that occasionally arose, would not have been achieved without the help of family and friends. Special thanks are due to my family and friends for their unfailing support at times most overwhelming.

I would neither have started nor have concluded this effort if it wasn't for the patience and support of my father, Mashhour Falah and mother Amal Almallah.

Last, but not least, I want to present this work to the closest person to my heart whom I lost while I was working on my DPhil. To the soul of my mom Amal Almallah.

Table of contents

Table of Figures:

Chapter 1:

Chapter 2:

Chapter 3:

Chapter 4:

Chapter 5:

Abbreviations:

Microliter	μl
Nanogram	Ng
Nanolitre	Nl
Free, unbound calcium	Ca^{2+}
Sodium	Na^{+}
Cyclin-dependent kinases	CDKs
The serine-threonine kinase cyclin-dependent kinase 5	Cdk5
Hippocampal sclerosis	HS
Electroencephalogram	EEG
Lateral	Lat
Status Epilepticus	SE
Sudden unexpected death in epilepsy	SUDEP
Entorhinal cortex	EC

Temporal lobe epilepsy	TLE
N-Methyl-D-aspartate	NMDA
Fluoro Jade-C	FJ-C
Phosphate-buffered saline (Tween)	PBS(T)
G-protein-coupled receptors	GPCRs
Kainate receptors	KA receptors
University College London	UCL
Blood Brain Barrier	BBB

Chapter 1: Introduction

1.1. Epilepsy.

Epilepsy is a chronic disorder of the brain that affects people of all ages. It affects over 65 million people worldwide (Kini, Gee et al. 2016) and 603,000 people in the United Kingdom alone.

Epilepsy is characterised by recurrent seizures (Yuan, Gao et al. 2013). A seizure is the manifestation of an excessive discharge of a population of cortical neurons, which in turn is due to a sudden imbalance between excitatory and inhibitory processes in the neural network (Engelborghs, D'Hooge et al. 2000). Seizures are classified according to the site of onset in the brain and divide into focal (partial) or generalised seizures (Fisher, Cross et al. 2017). Seizures may be generalised when discharges arise from both hemispheres, and generalised epilepsy is thought to be predominantly genetic in origin. Seizures may also be focal arising from a specific part of the brain. In focal epilepsy, the symptoms and signs reflect the area of the brain that is affected, and focal epilepsy can arise from a multitude of causes – for example, infection, trauma, stroke or tumours. This discharge may produce physical symptoms and signs, in which case it is a clinical seizure. Sometimes such abnormal activity may only be apparent on an electroencephalogram (EEG), it is considered a subclinical seizure. Focal (partial) seizures demonstrate either clinical or EEG evidence of onset from a localised area within the cerebral hemisphere. They are further sub-classified according to whether awareness is impaired (complex partial seizure; focal impaired awareness seizure) or unimpaired (simple partial seizure; focal aware seizure). Generalized seizures originate simultaneously from both cerebral hemispheres, and clinical manifestations may involve both sides of the body (Bromfield 2006).

Among neurological diseases, epilepsy accounts for the highest rates of disability-adjusted life years in both men and women. Although epilepsy is self-remitting in up to 50% of cases, variable long-term prognostic patterns are seen based on the response to the available treatments. Epilepsy carries an overall increased risk of premature mortality with variable estimates across countries. Among deaths directly attributable to epilepsy or seizures, causes include sudden unexpected death in epilepsy (SUDEP), accidents, drowning, unintentional injuries, suicide, and status epilepticus (SE) (Beghi 2016). SE is defined as

seizures lasting for 5 minutes or more or recurrent seizures without recovery of consciousness to baseline between the attacks (Dubey, Kalita et al. 2017).

70% of adults with epilepsy will become seizure-free with current antiepileptic drugs. However, despite a significant increase in the number of anti-epileptic medications available, 30% of people will have drug-resistant epilepsy with seizures and would not respond to any currently available medication. Pharmacoresistant epilepsy is now defined as seizures which are not entirely controlled despite adequate trials of two or more anti-epileptic medications (Kwan and Sperling 2009, Schmidt and Schachter 2014).

1.2. The hippocampus and epilepsy.

The name hippocampus is originally Greek meaning seahorse, which it resembles in shape. Sometimes it is also referred to as Ammon's horn (Cornu Ammonis), which is derived from the unique image of an Egyptian god (Sendrowski and Sobaniec 2013). Together with the limbic cortex, amygdala, septal area and hypothalamus, the hippocampal formation forms the limbic system (Rajmohan and Mohandas 2007), which controls behavioural, emotional and memory processes (Rajmohan and Mohandas 2007, Sendrowski and Sobaniec 2013).

The hippocampus is one of several brain regions included in the hippocampal formation (Figure 1.1). The hippocampal formation is a C-shaped structure located adjacent to the inferior part of the temporal horn of the lateral ventricle, which consists of the hippocampus proper and the subiculum (Amaral and Witter 1989, Rajmohan and Mohandas 2007, Small, Schobel et al. 2011).

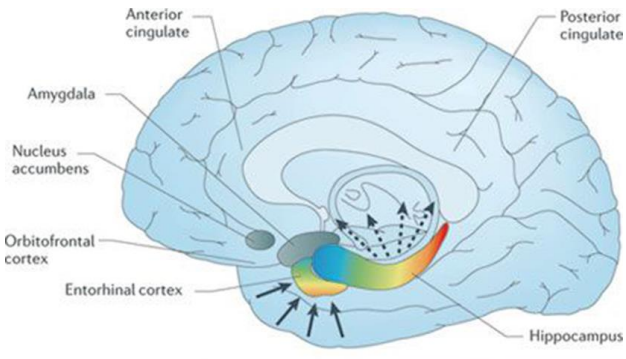

Figure 1.1: The hippocampal formation.

The hippocampal formation is made up of the entorhinal cortex and hippocampus (Small, Schobel et al. 2011).

Histologically, the hippocampus consists of four sectors that vary in size and nerve content: CA1 – CA4. The CA1 field contains small pyramidal cells; the small CA2 field is made up of small pyramidal cells as well, while the CA3 field consists of a broad, loose band of pyramidal neurons. The CA4 which is also referred to as a hilar region, is formed by loosely packed pyramidal cells, which are surrounded by the dentate gyrus (Sendrowski and Sobaniec 2013). Different hippocampal areas have different neuronal connections. The main afferent pathways of the hippocampus project to the thalamus and the hypothalamus. The main hippocampus afferent pathways initiate in the entorhinal cortex (EC), although there are additional pathways from the amygdala and various parts of the neocortex. The EC projects densely to the granule cells in the dentate gyrus and sends some less dense projections to the apical dendrites of CA3, and light projections to the apical dendrites of CA1. The dentate granule cell axons (mossy fibres) pass on the information from the EC on thorny spines that exit from CA3 pyramidal cells. Then, the CA3 axons project to CA1 extending all the way back into the deep layers of the EC - the Schaffer collaterals -which complete the circuit (Figure 1.2).

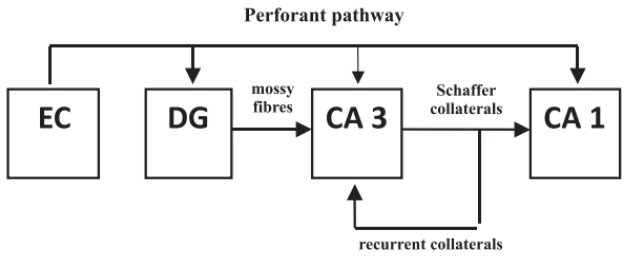

Figure 1.2: Circulation of nerve impulses between the separate hippocampal structures. Details in the text (Small, Schobel et al. 2011).

1.3. Temporal lobe epilepsy and hippocampal sclerosis.

Temporal lobe epilepsy (TLE) is the most common form of focal epilepsy (Al Sufiani and Ang 2012). In these patients, the epileptic focus is located in temporal lobe structures, such as the hippocampus, amygdala and parahippocampal gyrus (Sendrowski and Sobaniec 2013). temporal lobe epilepsy (TLE) can be pharmacoresistant particularly in cases where a substrate can be identified on brain imaging. The treatment of choice in appropriate

pharmacoresistant cases is surgical resection (Al Sufiani and Ang 2012, Sendrowski and Sobaniec 2013).

Hippocampal sclerosis (HS), is the most common pathological finding in patients with pharmacoresistant TLE (Al Sufiani and Ang 2012). Patients with HS often do not respond to any of the currently available anti-epileptic medications. The health burden includes cognitive and psychological co-morbidity as well as an increased risk of mortality (Bell, Lin et al. 2011, Laxer, Trinka et al. 2014).

HS is easily detected on magnetic resonance brain imaging (Bote, Blazquez-Llorca et al. 2008). Surgical resection of HS with either two-thirds temporal lobectomy or selective amygdalohippocampectomy (Boex, Seeck et al. 2011) can offer seizure freedom in up to 70% of cases. However, the rate of seizure freedom does diminish with time such that only 50% of cases remain seizure free for ten years postoperatively (Spencer and Huh 2008).

Histologically HS is characterised by gliosis, synaptic reorganisation, dispersion of the granular cell layer (40% of cases) and segmental neuronal loss in CA4, CA3, and CA1 areas of the hippocampus with relative sparing of CA2 and dentate gyrus (Blumcke, Thom et al. 2002). In more severe cases, neuronal loss in CA2 and dentate gyrus might also be seen (Proper, Oestreicher et al. 2000). The neuronal loss seen in HS might be the result of seizures, but also it is unclear to what extent these neurodegenerative changes may contribute to the perpetuation of the seizure activity in pharmacoresistant epilepsy.

HS can be diagnosed in patients preoperatively by clinical MR imaging; it usually shows hippocampal atrophy, T1 and T2 signal abnormality, and loss of the hippocampus and extra hippocampal structures(Jackson 1995, Henry, Chupin et al. 2011). Resection of tissue after surgery shows neuronal loss in hippocampal formation (Thom 2014) . Beside neuronal loss, the following can be detected: neuronal hypertrophy, astrogliosis, activation of pro-inflammatory factors like (COX-2, TGF-β, NFkB), increased expression of calpain, and increased expression of the α1c subunit comprising class C L-type Ca^{2+} channels, allowing for increased influx of Ca^{+2} (Das, Wallace et al. 2012) .

HS is classified into four grades based on the subfield distribution and extent of hippocampal neuronal loss and gliosis (Thom 2014). Several systems had previously been created to classify subtypes of HS. Thom et al., 2014 incorporated aspects of all previous schemes and

provided a classification system that was then validated through the neuropathology taskforce of the International League Against Epilepsy (ILAE) (Figure 1.3). In brief, Grade 0 refers to a hippocampus with no neuronal loss and no gliosis; Grade 1 to gliosis only without neuronal loss; Grade 2 refers to neuronal loss and gliosis in the CA4 or CA1 subfields, Grade 3 refers to neuronal loss and gliosis in CA1, CA4 and CA3 areas with sparing of CA2, while Grade 4 refers to extensive neuronal loss and gliosis in all subfields including the dentate gyrus. Sometimes other terms are used to describe HS, including Ammon's Horn sclerosis (refers to the neuronal loss in CA1–4 and not the dentate gyrus) and mesial temporal sclerosis (which implies more extended sclerosis of extrahippocampal tissues, such as the amygdala and parahippocampal gyrus; (Thom 2014)).

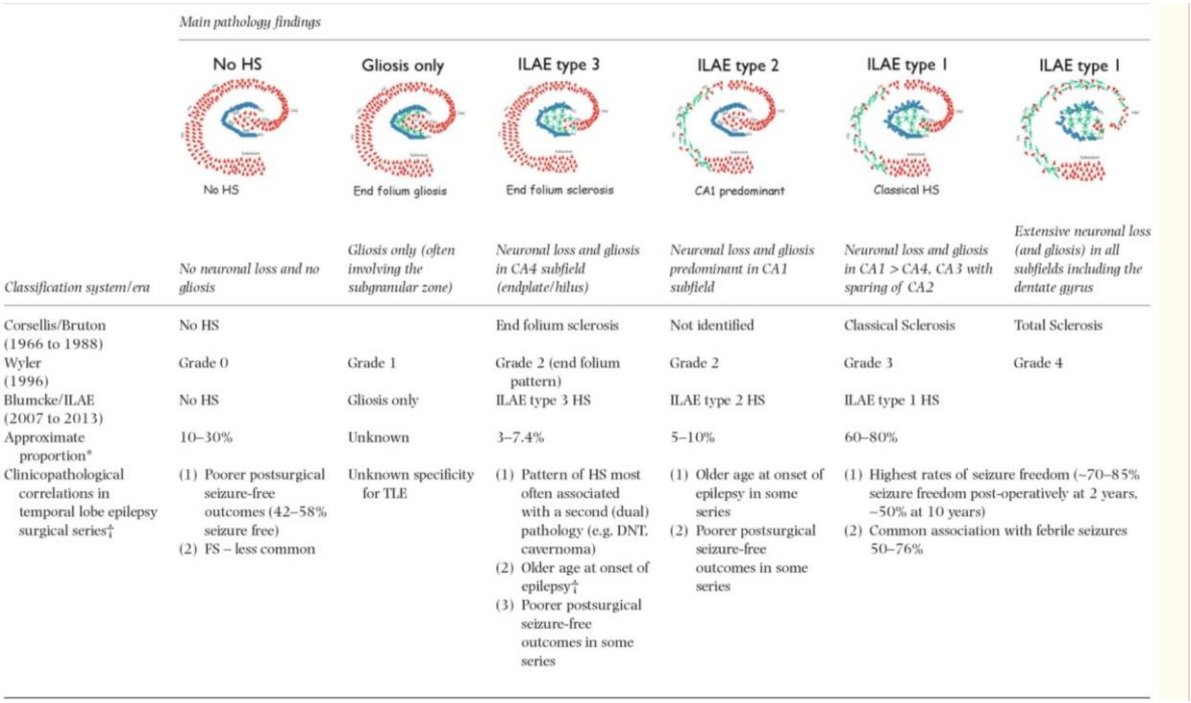

	Main pathology findings					
	No HS	Gliosis only	ILAE type 3	ILAE type 2	ILAE type I	ILAE type I
	No HS	End folium gliosis	End folium sclerosis	CA1 predominant	Classical HS	
Classification system/era	*No neuronal loss and no gliosis*	*Gliosis only (often involving the subgranular zone)*	*Neuronal loss and gliosis in CA4 subfield (endplate/hilus)*	*Neuronal loss and gliosis predominant in CA1 subfield*	*Neuronal loss and gliosis in CA1 > CA4, CA3 with sparing of CA2*	*Extensive neuronal loss (and gliosis) in all subfields including the dentate gyrus*
Corsellis/Bruton (1966 to 1988)	No HS		End folium sclerosis	Not identified	Classical Sclerosis	Total Sclerosis
Wyler (1996)	Grade 0	Grade 1	Grade 2 (end folium pattern)	Grade 2	Grade 3	Grade 4
Blumcke/ILAE (2007 to 2013)	No HS	Gliosis only	ILAE type 3 HS	ILAE type 2 HS	ILAE type 1 HS	
Approximate proportion*	10–30%	Unknown	3–7.4%	5–10%	60–80%	
Clinicopathological correlations in temporal lobe epilepsy surgical series†	(1) Poorer postsurgical seizure-free outcomes (42–58% seizure free) (2) FS – less common	Unknown specificity for TLE	(1) Pattern of HS most often associated with a second (dual) pathology (e.g. DNT, cavernoma) (2) Older age at onset of epilepsy† (3) Poorer postsurgical seizure-free outcomes in some series	(1) Older age at onset of epilepsy in some series (2) Poorer postsurgical seizure-free outcomes in some series	(1) Highest rates of seizure freedom (~70–85% seizure freedom post-operatively at 2 years, ~50% at 10 years) (2) Common association with febrile seizures 50–76%	

Figure 1.3: Summary by (Thom et al., 2014) of the various latest classification schemes adopted for the patterns of hippocampal sclerosis (HS) in epilepsy.

1.4. Neurodegeneration in hippocampal sclerosis (HS).

The neuronal loss seen in HS likely contributes to both the seizures and cognitive deficit that these patients experience. Despite considerable study, the mechanism of neuronal loss in HS is incompletely understood (Thom 2014). There are thoughts that excitotoxicity, necrosis and possibly apoptosis, can all contribute to neurodegeneration in this condition.

Calcium ions (Ca^{2+}) are thought primarily to be responsible for the excitotoxicity leading to necrotic and apoptotic damage in epilepsy (Arundine and Tymianski 2003, Niquet, Lopez-Meraz et al. 2012). An excessive synaptic release of glutamate, as can be seen in seizures, can lead to the deregulation of Ca^{2+} homeostasis. Glutamate activates postsynaptic receptors, including the ionotropic NMDA, AMPA, and kainate (KA) receptors. Upon activation, these receptors open their ion channels to allow the passage of K^+ and Na^+ ions to the cytoplasm. In addition to K^+ and Na^+, NMDA receptors allow an influx of Ca^{2+} as well. As a result, the excitatory postsynaptic potential (EPSPs) produced by NMDA receptors can increase the concentration of Ca^{2+} within the postsynaptic neuron.

Although transient elevations in cytoplasmic Ca^{2+} are essential to standard cell functions including cell growth, differentiation, and synaptic activity, the excessive influx of Ca^{2+} together with intracellular calcium-induced Ca^{2+} release will disrupt the Ca^{2+} regulatory mechanisms and lead to cell death (Arundine and Tymianski 2003). Excess Ca^{2+} influx can also trigger a range of neurotoxic cascades and pathways that will lead eventually to necrotic and apoptotic cell death. Those pathways include Ca^{2+} entry into the mitochondria, activation of calpains, caspases, and several other proteases, endonucleases, and kinases, which leads to damage of cells. The result is an overproduction of free radicals, malfunction/damage of the mitochondria and endoplasmic reticulum, acidosis, cell swelling, cytoskeletal breakdown, cell membrane disruption and DNA fragmentation. Such severe damage on many different levels all contribute to cell death (Arundine and Tymianski 2003, Szydlowska and Tymianski 2010, Niquet, Lopez-Meraz et al. 2012).

SE induced excitotoxicity usually leads to necrotic cell death. Numerous studies have shown that following seizure induced excitotoxicity, necrosis is the leading cause of neuronal death in the adult brain, particularly in the hippocampus.

As mentioned, excessive Ca^{2+} influx into neurons activates two Ca^{2+}-dependent enzymes, calpain I and neuronal nitric oxide synthase (nNOS). Calpain 1 activation will lead to mitochondrial swelling and rupture, a release of mitochondrial death factors like cytochrome c, apoptosis-inducing factor endonuclease G and the lysosomal release of cathepsins B and D and DNase II, those factors induce large-scale DNA cleavage and chromatin condensation which will lead eventually to cell death by necrosis. nNOS release will lead to formation of nitric oxide (NO), which reacts with superoxide (O_2^-) to form free radicals like peroxynitrite

($ONOO^-$) which damage cellular membranes, intracellular proteins and DNA leading to cell death by necrosis as well. NO will cause mitochondrial damage as well in three ways: reversible inhibition of respiration; irreversible inactivation of mitochondrial enzymes; and induction of the mitochondrial permeability transition

Cell death by apoptosis also still occurs after SE induced excitotoxicity (Figure 1.4). Upon mitochondrial dysfunction caused by excessive Ca^{2+} influx after seizures, apoptotic death pathways are activated, including pro-apoptotic Bcl-2 family proteins, ASK1/JNK/c-Jun,p53 and caspases, and other pathways triggered by the endoplasmic reticulum (ER) (Henshall and Simon 2005, Henshall 2007).

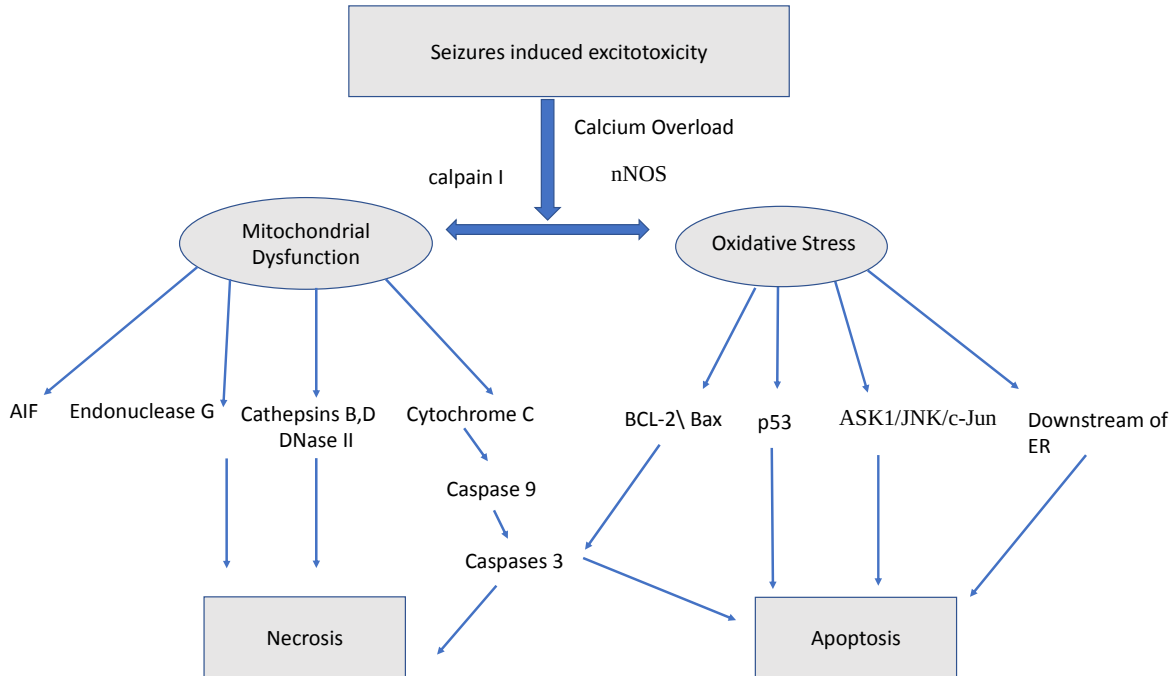

Figure 1.4: Mechanisms of necrosis and apoptosis.
Following hypoxia, excitotoxicity or seizures, Ca^{2+} entry into the mitochondria leads to mitochondrial swelling, outer membrane rupture, the release of mitochondrial death factors and activation of the intrinsic pathway. Apoptotic death pathways including pro-apoptotic Bcl-2 family proteins and caspases still occur which will lead eventually to cell death.

1.5. Neuroinflammation in HS:

There is increased evidence that inflammation presence in hippocampal sclerosis doesn't associate with the grade or degree of neuronal loss. Histologic evaluation showed the presence of lymphocytes within the perivascular space and the brain parenchyma within

the hippocampus, temporal cortex, and amygdala in HS patients brains. There was overexpression of transcription factors like NFkB in hippocampal foci patients as well (Jackson 1995, Crespel, Coubes et al. 2002).

Beside the inflammatory phenomenon , astrogliosis and activation of the microglia / macrophages lineage was shown in hippocampus with some very few cells of adaptive immunity (CD3/CD8 positive T-lymphocytes)(Jackson 1995).

Astrocytes has connection with neurons, nerve fibres and synapses. They are activated by intracellular Ca^{+2} and oscillations. Under normal conditions astrocytes are responsible to ensure most glutamate clearance in neuronal cells. They can synchronize the activity of neurons and control balance between excitation and inhibition and induce vasoconstriction and vasodilation and control blood cells.

Upon excitation they release gliotransmitters like glutamate and ATP through certain mechanisms including exocytosis, and that is when they start delivering excitation messages to the neighbour cells, glia and blood cells (Vermeiren, Najimi et al. 2005, Maragakis and Rothstein 2006, Verkhratsky, Rodriguez et al. 2013).

Astrocytes are activated in lots of diseases resulting in activation of common inflammatory pathways, and increased glutamate expression.

They express a defensive pathway in response to inflammation known as astrogliosis as a way of neuroprotection with negative outcomes. Astrogliosis is associated with an upregulation of GFAP, hypertrophy and proliferation of astrocytes (Vermeiren, Najimi et al. 2005, Maragakis and Rothstein 2006, Verkhratsky, Rodriguez et al. 2013).

1.6. Glutamate receptors and cell death.

1.6.1. Glutamate receptor.

Excitatory glutamate receptors are classified into two families: ionotropic (iGluR) and metabotropic (mGluR) (Willard and Koochekpour 2013). The metabotropic glutamate receptors (mGluR) are G-protein-coupled receptors (GPCRs) containing seven transmembrane domain structures that are activated by glutamate to initiate signalling cascades or cation influx. The mGluRs are sub-classified into the Group I, II and III subfamilies.

The ionotropic receptor family of glutamate receptors are ligand-gated ion channels. They are divided into the *N*-methyl-D-aspartate (NMDA), a-amino-3-hydroxy-5-methyl-4-isoxazolepropionic acid (AMPA), and kainate (KA) receptor subfamilies – each named according to the chemical agonist that selectively binds to the subfamily members (Hollmann and Heinemann 1994, Willard and Koochekpour 2013).

1.6.2. Ionotropic glutamate receptors.

In general, ionotropic glutamate receptors share the same basic structure; they are tetramers built from combinations of four core subunits, GluA1–4 (Willard and Koochekpour 2013, Greger, Watson et al. 2017). Ionotropic glutamate receptors are localised at excitatory central synapses and are activated by presynaptically released L-glutamate (Greger, Watson et al. 2017). They allow K^+ influx upon glutamate binding (Willard and Koochekpour 2013).

1.6.3. Ionotropic glutamate receptor and excitotoxicity.

The ionotropic glutamate receptors NMDA, AMPA and KA receptors mediate excitatory neurotransmission vital for different brain functions, including learning and memory formation (Karakas, Regan et al. 2015). The presynaptically released glutamate binds to the different subclasses of the ionotropic glutamate receptors and mediates opening of their cationic ion channels to generate synaptic current. It has also, though, been shown that these glutamate receptors have an essential role in underpinning the mechanisms of neurological diseases and disorders as varied as depression, schizophrenia, Alzheimer's and Parkinson's diseases, autism, epilepsy, and stroke (Karakas, Regan et al. 2015). Over activation by glutamate causes impairment of Ca^{2+} homeostasis, generation of free radicals, activation of the mitochondrial permeability transition and secondary excitotoxicity which will lead eventually to excitotoxicity and eventually apoptotic or necrotic cell death. Different receptor subtypes contribute differently to this cell death (Gasull, DeGregorio-Rocasolano et al. 2001, Dong, Wang et al. 2009).

1.7. The NMDA receptor.

1.7.1. NMDA structure.

The NMDA receptor (NMDAR) is located on most central neurons and is a proto-typical ionotropic receptor in morphology.

NMDA consists of heteromers of glycine-binding NR1, glutamate-binding NR2 and glycine-binding NR3 subunits, the assembly of two copies each of the NR1 and NR2 and/or NR3 subunits is needed for NMDA function(Furukawa, Singh et al. 2005).

There are two NR1 subunits and two NR2 subunits (NR2A-2D) (Dong, Wang et al. 2009). Each subunit is composed of four domains: the intracellular C-terminal domain, the transmembrane domain that contains the ion channel, the agonist binding domain and the N-terminal domain (Dong, Wang et al. 2009, Balu 2016). Once activated post-synaptic depolarisation, which relieves the Mg^{2+} blockade of the channel, occurs. Upon NMDAR channel opening, $Ca^{2+}$and Na^{+} enter the neuron, while potassium (K^{+}) exits (Figure 1.5; (Balu 2016)).

The NMDAR activation needs the concomitant binding of glutamate and a co-agonist glycine or D-serine(Le Bail, Martineau et al. 2015). While it is blocked by endogenous Mg^{2+} in a voltage dependent way. Significant depolarization only happens upon the relief from Mg^{2+} block and Ca^{2+} entry through NMDAR channels(Nikolaev, Magazanik et al. 2012)

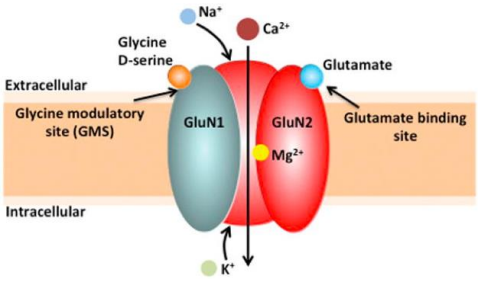

Figure 1.5: NMDA receptor structure and activation (Balu 2016).
When glutamate binds to the GluN2 subunit, post-synaptic depolarisation occurs, this relieves the Mg^{2+} blockade of the channel and lead to an influx of calcium (Ca^{2+}) and sodium (Na^{+}) to the neuron, while potassium (K^{+}) exits.

1.7.2. NMDA receptors and cell death.

NR2A subunits don't assemble by themselves into functional units, they need to co-express with NR1 subunit so receptor activation can occur. The combination of NR1 and NR2B subunits is highly permeable to Ca^{2+},it is activated by glutamate and glycine and blocked by Mg^{2+} in a voltage-dependent manner, the NR2B subunit forms the glutamate binding pocket (Loftis and Janowsky 2003). Excessive release of glutamate into the synapses and

extrasynaptic sites results in stimulation of NMDA receptors at both locations and continuous activation of NR1/NR2B subunits of NMDA, which leads to an increase in intracellular Ca^{2+} which is highly neurotoxic and triggers cascades of pathways leading to cell death by apoptosis, necrosis and excitotoxicity (Dong, Wang et al. 2009, Lai, Zhang et al. 2014) .

Experiments performed with free Ca^{2+} indicators have revealed that, as a corollary, blocking NMDA receptors can be neuroprotective against excitotoxic cell death. MK801 is a non-competitive antagonist of NMDA that binds to two sites of the NMDAR causing its blockage in a voltage-dependent manner (Kovacic and Somanathan 2010). MK801 increased survival rate in rats receiving the neurotoxic agent pilocarpine and was found to be neuroprotective (Ormandy, Jope et al. 1989).

Previously it has been suggested that NMDAR can be phosphorylated by the small serine-threonine kinase cyclin-dependent kinase 5 (cdk5) and this might cause glutamate-mediated excitotoxicity (Wang, Liu et al. 2003) and contribute to neurodegeneration in several diseases. Previous work has also shown possible deregulation of cdk5 in human epileptogenic tissue. Therefore, it might be that an alteration in cdk5 signalling could contribute to the neuronal loss seen in pharmacoresistant epilepsy.

1.8. Cyclin-dependent kinase 5 (cdk5).

Cdk5 was isolated in early 1990 from bovine brain. It is a member of the small serine/threonine cyclin-dependent kinase (CDK) family (Dhavan and Tsai 2001). Cdk5 is a ubiquitous proline-directed serine-threonine kinase that phosphorylates a wide range of intracellular proteins and interacts with numerous substrates (Liu, Zhai et al. 2017). It is expressed in all tissues, but its highest expression and associated kinase activity are detected in the nervous system (Dhavan and Tsai 2001, Ledee, Gao et al. 2005). Monomeric cdk5 by itself has no activity for which it needs association with its activators p35 or p39. p35 and p39 expression are mainly limited to neurons, and consequently, cdk5 activity is predominantly restricted to neurons (Dhavan and Tsai 2001, Gupta and Tsai 2003).

Cdk5 has essential functions in neuronal development, synaptic function, neuronal migration, cytoskeletal dynamics, synaptic vesicle exocytosis, as well as in endocytosis and neuronal plasticity (Chae, Kwon et al. 1997, Dhavan and Tsai 2001, Gupta and Tsai 2003).

Several studies have shown that cdk5 has a significant role in controlling neurotransmitter release in mammalian neurons (Kim and Ryan 2010) and it has been demonstrated that cdk5 has a role as well in regulating neurotransmitter release in the presynaptic terminals (Tomizawa, Ohta et al. 2002).

1.8.1. Deregulation of cdk5 by p25.

p35 is subject to rapid ubiquitin-mediated proteasomal degradation and is also phosphorylated by cdk5. It has a short half-life of approximately 20-30 minutes (Dhavan and Tsai 2001). Neurotoxic stimuli including oxidative stress, excess Ca^{2+}, and glutamate can trigger the calpain-mediated cleavage of p35 to p25. P25 contains all the necessary elements to bind cdk5, but it lacks the myristylation motif present at N-terminus of p35. Therefore, p25 localises to the cell soma and nucleus, while p35 is membrane bound. p25 is more stable than p35 and has a longer half-life and therefore can cause hyperactivation of cdk5 and eventually excitotoxicity (Dhavan and Tsai 2001, Gupta and Tsai 2003). The p25-cdk5 complex phosphorylates the NMDA receptor subunit NR2A on the Ser1232 site causing glutamate-mediated excitotoxicity (Figure 1.6; Dhavan and Tsai, 2001). p25-cdk5 complex also phosphorylates several other substrates (including the nuclear transcription factor, myocyte enhancer factor (MEF2), tau, p53, as well as the retinoblastoma protein pRb (Camins, Verdaguer et al. 2006) that might interfere with survival mechanisms such p25-cdk5 plays a vital role in necrosis and apoptosis (Li, Zhang et al. 2002, Camins, Verdaguer et al. 2006, Chow, Guo et al. 2014).

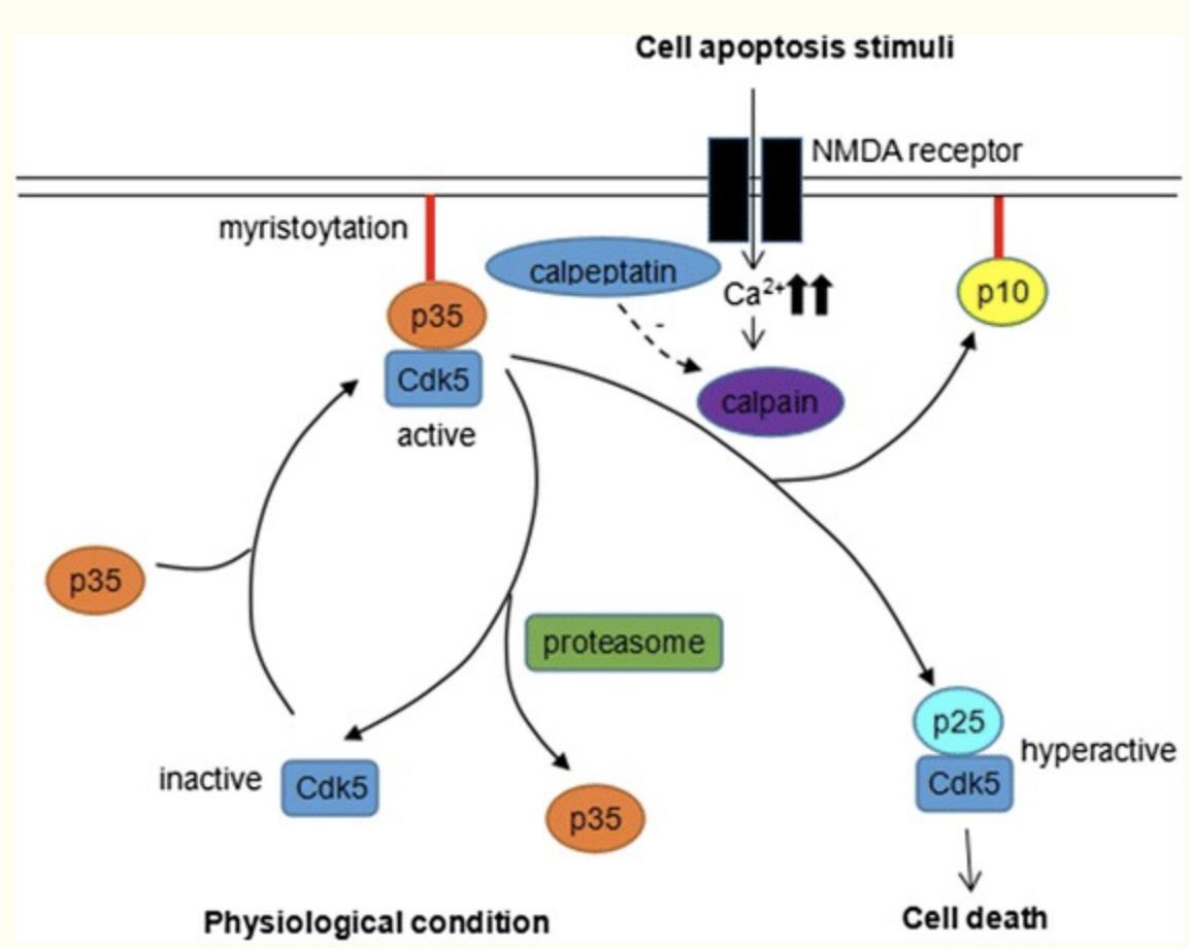

Figure 1.6: Deregulation of cdk5 by p25.
Cdk5 needs its physiological activator p35 to be activated. Any neurotoxic stimuli such as oxidative stress, excess calcium, or glutamate can trigger the calpain-mediated cleavage of p35 to p25. p25 has a longer half-life and therefore can cause hyperactivation of cdk5 and eventually excitotoxicity through a mechanism that might involve NMDA phosphorylation. Adapted from(Liu, Li et al. 2017).

1.8.2. Neurodegeneration and p25-cdk5.

Deregulation of p25-cdk5 activity has neurotoxic effects and has been shown to contribute to the pathogenesis of neurodegenerative disorders such as Alzheimer's disease (Patrick, Zukerberg et al. 1999, Alonso, Zaidi et al. 2001, Monaco 2004, Kurbatskaya, Phillips et al. 2016), amyotrophic lateral sclerosis (Zarei, Carr et al. 2015), Parkinson's disease (Triarhou 2002, Recasens and Dehay 2014, Reeve, Simcox et al. 2014), as well as to ischemia (Wang, Liu et al. 2003) and human hippocampal sclerosis (Sen et al., 2006, Sen et al., 2007).

In Alzheimer's disease, p25 has been found accumulated in neurons in the brains of patients. This accumulation was correlated with an increase in cdk5 kinase activity, and abnormal hyperphosphorylated forms of tau (Patrick, Zukerberg et al. 1999). Elevated cytosolic Ca^{2+} concentrations lead to activation of calpain which leads to calpain-mediated cleavage of p35,

to p25 and dysregulation of cdk5 which abnormally phosphorylates the microtubule protein tau (Monaco 2004, Kurbatskaya, Phillips et al. 2016). Hyperphosphorylation of tau can result in self-assembly of tangles of paired helical filaments and straight filaments, which will contribute to the formation of neurofibrillary lesions and subsequent neuronal loss in Alzheimer's disease (Alonso, Zaidi et al. 2001, Monaco 2004, Mushtaq, Greig et al. 2016).

There is also evidence that the p25-cdk5 might have a role in the pathogenesis of Parkinson's disease as well. Increased p25-cdk5 expression has been demonstrated in the brains of patients (Camins, Verdaguer et al. 2006) and experimental studies performed in neuronal cell culture models of Parkinson's disease have indicated that p25-cdk5 plays a prominent role in apoptosis. Moreover, an apoptotic pathway, via an intracellular Ca^{+2} increase following calpains activation and p25-cdk5 formation, has been suggested (Camins, Verdaguer et al. 2006, Smith, Mount et al. 2006). Similar phenomenon have been suggested in amyotrophic lateral sclerosis pathogenesis, with studies showing that p25-cdk5 activity leads to cdk5 hyperphosphorylated tau and neurofilament proteins leading to cellular apoptosis and neuronal cell death in this disease (Bajaj 2000, Nguyen, Lariviere et al. 2001).

P25-cdk5 complex has also been found to be the leading cause of neuronal death in rodent models of stroke as well. Inhibition of p25-cdk5 during ischemia resulted in blocking of excitotoxicity and protected against neuronal loss (Meyer, Torres-Altoro et al. 2014).

1.9. Inhibiting the cdk5 pathway.

As deregulation of cdk5 is linked to neurodegeneration, inhibiting the cdk5 pathway with the purpose of achieving neuroprotection is becoming a prominent feature of recent studies. Current research is investigating neuroprotective mechanisms with the aim to develop selective, safe and effective cdk5 inhibitors, that might be used in the treatment of neurodegenerative disorders. Previous research has shown that suppressing the p25-cdk5 pathway has neuroprotective effect in neurodegenerative diseases (Alvira, Tajes et al. 2006, Camins, Verdaguer et al. 2006, Sundaram, Poore et al. 2013, Tan, Chen et al. 2015, Mushtaq, Greig et al. 2016).

In an animal and cell culture models of stroke and ischemia, inhibiting p25-cdk5 blocked excitotoxicity (Meyer, Torres-Altoro et al. 2014), and reduced neuronal death by around 80% in a neuronal culture model of ischemia (Osuga, Osuga et al. 2000).

Similarly, in models of Alzheimer's disease, pharmacological inhibition of p25-cdk5 achieved neuroprotection in vivo and in vitro (Alvarez, Toro et al. 1999, Leclerc, Garnier et al. 2001, Chang, Vincent et al. 2012). Protection against neurodegeneration was also obtained in in vivo models of Parkinson's disease and amyotrophic lateral sclerosis through inhibition of the p25-cdk5 formation (Alvira, Tajes et al. 2006, Sundaram, Poore et al. 2013).
Recent research suggests that drugs such as roscovitine, flavopiridol, calpains inhibitors, kenpaullone and indirubin, which inhibit p25-cdk5 formation, may develop into potential drugs for the treatment of neurodegenerative disorders (Camins, Verdaguer et al. 2006). Therefore, it would seem worthwhile to better determine the causes of neuronal loss in models of HS, to evaluate whether pharmacological treatment may lead to neuroprotection in epilepsy.

Although in *vitro* and *in vivo* studies demonstrated neuroprotective effect upon inhibiting cdk5, using those drugs clinically is still questionable. It is also very important to conduct more preclinical research to evaluates the neuroprotective effects of cdk5 inhibitors better, particularly those that are less studied like roscovitine and then to work on developing their properties to become more usable clinically.

Roscovitine is a potent cdk5 inhibitor which shows in vitro and in vivo neuroprotective effects in models of neuronal death. It has been found to be neuroprotective in focal cerebral ischemia in rats (Zhang, Chen et al. 2009) and in a rodent model of stroke (Menn, Bach et al. 2010). The protection does seem related to reduced cdk5 function as roscovitine systemic administration prevents increased p25-cdk5 activity (Menn, Bach et al. 2010). However, relatively few studies have been performed to evaluate the role of roscovitine on preventing neuronal loss in neurodegenerative diseases, and further, the spread and effect of injection of roscovitine into animal models of disease are poorly delineated. Therefore, it would seem worthwhile to better determine the causes of neuronal loss in models of HS, to evaluate the pharmacokinetics of roscovitine administration in animal models of epilepsy and to determine thereby whether roscovitine may offer neuroprotection in epilepsy.

Hypothesis:

Phosphorylation of the NMDA receptor by the cyclin-dependent kinase-5 (cdk5) complex is responsible for NMDA receptor-mediated excitotoxicity in hippocampal sclerosis (HS), thereby leading to the pathogenesis and the cognitive deficits seen in this condition.

Aims:

Using two common rodent epilepsy models (pilocarpine and kainate) and resected tissue from human hippocampal sclerosis, this project aims to evaluate the role of NMDARs and their cdk5-mediated modulation in the subfield-specific neuronal loss in pharmacoresistant epilepsy.

Detailed aims of the project are to:

1- Investigate the role of cdk5 in NMDAR- mediated hyperfunction and NMDAR dependent cell death in rodent epilepsy pilocarpine and kainate models.

2- Study whether resected the sclerotic human hippocampus shows evidence of increased cdk5 levels and facilitated NMDARs expression or phosphorylation.

3- Test whether inhibition of cdk5 reduces the neuronal loss in a rodent model of HS.

4- In the long term to link the project data with emerging research suggesting that clinically approved cdk5 inhibitors may contribute to treatment in patients with pharmacoresistant.

Chapter 2: Pharmacokinetics of roscovitine after i.c.v injection.

2.1. Introduction.

Deregulation of cyclin-dependent kinases (CDKs) has a role in neurodegeneration. In recent research, increased p25-cdk5 expression has been demonstrated to have a role in many neurodegenerative diseases (Camins, Verdaguer et al. 2006). The potential role of inhibition of CDKs in mediating neuroprotective effects is the subject of much previous work and experiments (Mushtaq, Greig et al. 2016). Drugs that inhibit p25-cdk5 formation are considered potential medications for the treatment of neurodegenerative disorders. Those drugs include, flavopiridol, calpain inhibitors, kenpaullone, indirubin, and roscovitine (Camins, Verdaguer et al. 2006).

In our experiments, we began by examining the role of the cdk5 molecule and the associated p25-cdk5 complex in the neuronal loss seen in hippocampal sclerosis (HS). We then tried to test the effect of suppressing p25-cdk5 signalling with the competitive cdk5 antagonist roscovitine, to better determine whether changes in cdk5 function may be causal to the neuronal loss seen in HS. Although many studies have addressed the role of cdk5 in a range of human neurodegenerative conditions, only limited work investigated its role in HS, or examined the effect of suppressing the pathway pharmacologically in general or using roscovitine in particular. Moreover, there are very few experiments which have investigated the pharmacokinetics of roscovitine and almost none have explored its pharmacokinetics after intraventricular (i.c.v) injection.

In this experiment, we started with studying the localisation of roscovitine and its half-life after i.c.v injection through its effect on signalling pathways involved in seizure dependent neuronal loss, to help deciding when to inject the drug before induced neuronal loss.

2.1.1. Roscovitine: general introduction.

Roscovitine which is also known as (R)-Roscovitine, CY-202, and Seliciclib, was named after Roscoff—a French town, where the laboratory that developed the compound is based. The chemical formula is $C_{19}H_{26}N_6O$, molecular weight—354.45 kDa. Roscovitine is a tri-substituted purine analogue (Figure 2.1). As a member of the purine family, it shares the basic ring structure with biologically relevant molecules such as ATP, cyclic AMP, NAD, FAD, adenine and guanine (Cicenas, Kalyan et al. 2015). Roscovitine is currently studied as a potential drug to treat cancers, neurodegenerative diseases, viral infections, and glomerulonephritis (Bach, Knockaert et al. 2005).

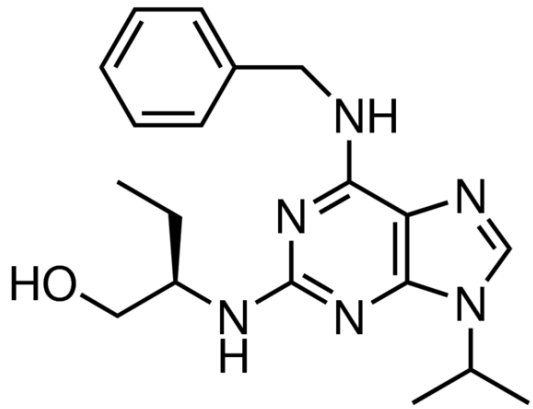

Figure 2.1: Roscovitine structure.

Roscovitine is a purine analogue that shares basic ring structure with essential molecules such as ATP (Cicenas, Kalyan et al. 2015).

2.1.2. Mechanism of action.

Roscovitine is a selective inhibitor of CDKs. It is a potent inhibitor of CDK 1, 2, 5, 7, 9 and signal-regulated kinases (Erk1/2), it is, though, a weak inhibitor of CDK4, CDK6 and CDK8 (Bach, Knockaert et al. 2005, Cicenas, Kalyan et al. 2015). Roscovitine inhibits CDKs by competing with ATP for binding site at the ATP-binding site of CDKs. Roscovitine interacts with the amino acids that bind to the CDK catalytic domain. The benzyl ring of roscovitine is adjacent to the outside of the ATP-binding pocket. This interaction prevents ATP from attaching to the kinase, and thus catalytic reaction cannot be performed (De Azevedo, Leclerc et al. 1997, Cicenas, Kalyan et al. 2015).

Independent of the mechanism by which roscovitine inhibits CDKs, roscovitine was found to suppress mRNA synthesis in human cells, resulting in RNA synthesis inhibition, which in turn can result in the accumulation of nuclear p53 (Ljungman and Paulsen 2001). Roscovitine has also been shown to inhibit DNA synthesis, and to have an effect on voltage-activated calcium channels in central neurons (Yakisich, Siden et al. 1998).

Previous experiments have demonstrated that roscovitine alters the voltage-dependent gating of calcium channels in a cdk5-independent manner. In central neurons, extracellular application of roscovitine severely slows the deactivation kinetics of P/Q-type calcium channels prolonging its opening state and increasing Ca^{+2} influx through these channels. Roscovitine potentiates glutamate release at presynaptic terminals of cultured hippocampal neurons (Yan, Chi et al. 2002). Roscovitine can also affect the N-type calcium channels in a

cdk5 related mechanism as well. Phosphorylation of N-type calcium channel by cdk5 significantly increased calcium-current density and the probability of the channel opening (Su, Seo et al. 2012). Calcium signalling is involved in many pathophysiological conditions. Calcium disruption is an essential factor in epileptogenesis, and seizures link to disruption of various calcium signalling pathways (Steinlein 2014). This would therefore suggest that roscovitine might affect seizures.

2.1.3. Pharmacokinetics of roscovitine.

Several studies have shown that systemic injections of roscovitine are rapidly absorbed, widely distributed to peripheral tissues, rapidly metabolised and eliminated with a half-life ranging from 30 minutes in adult rats to 3 hours in humans. Roscovitine also crosses the blood-brain barrier and the concentration in the brain found to be about 30% of that observed in plasma (Ljungman and Paulsen 2001, de la Motte and Gianella-Borradori 2004, Gherardi, D'Agati et al. 2004, Hahntow, Schneller et al. 2004, Vita, Abdel-Rehim et al. 2005).

Using high-performance liquid chromatography, liquid chromatography/tandem mass spectrometry and nuclear magnetic resonance spectroscopy, Vita et al. identified the structures of three roscovitine metabolites as the carboxyl derivate, hydroxyl derivate, and the demethylated derivate of the parent drug. They studied roscovitine and its metabolites distribution in blood, lungs, kidney, liver, testis, adipose tissue, spleen and brain plasma tissue samples. The secondary carboxyl metabolite (M1) was detected mainly in plasma and lower levels in all other tissues. M1 identifies as conversion of the hydroxyl group at C2 to carboxylic acid (MW = 368). The hydroxyl metabolite (M2) was detected mainly in liver and kidney, and the demethylated derivate in several organs (Vita, Abdel-Rehim et al. 2005).

2.1.4. Preclinical and clinical studies in use of roscovitine.

The effects of roscovitine have been studied in several diseases. The majority of pre-clinical studies to date have evaluated roscovitine on a wide variety of cancer cell lines. Generally, there have been two significant observations: 1) roscovitine causes cancer cell cycle arrest at all phases of cell cycle, and 2) roscovitine can initiate apoptosis in cancer cells (De Azevedo, Leclerc et al. 1997, Raynaud, Whittaker et al. 2005). In addition, roscovitine has been shown

to have a synergistic effect with other anti-oncogenic agents (Cicenas, Kalyan et al. 2015) and has demonstrated potential benefit in animal models of cancer.

Other studies showed that roscovitine has an effect in other diseases; such as polycystic kidney disease (Bukanov, Smith et al. 2006, Cicenas, Kalyan et al. 2015), glomerulonephritis (Zoja, Casiraghi et al. 2007, Cicenas, Kalyan et al. 2015), ischemia (Aydemir, Abbasoglu et al. 2002) and chronic pain (Zhang, Liu et al. 2012, Liu, Liu et al. 2014).

Oral roscovitine has entered clinical trials in cancer. Phase 1 trials showed no objective tumour response though, but disease stabilisation was observed in some patients (Benson, White et al. 2007, Cicenas, Kalyan et al. 2015). Using roscovitine in combinatorial therapy seems more promising than using it as monotherapy in cancer (Cicenas, Kalyan et al. 2015). More recent research is investigating more potent derivatives from roscovitine that might achieve better results clinically. For example, 2-(R) -(1-Ethyl-2-hydroxyethylamino)-6-(4-(2-pyridyl) benzyl)-9-isopropylpurine or (CR8) was introduced as a second-generation CDKs inhibitor derived from roscovitine. CR8 is approximately 50-fold more potent compared to roscovitine in inducing apoptosis in different tumour cell lines (Sallam, El-Serafi et al. 2013).

Although a potential role for roscovitine is emerging in oncology, there has been relatively little work in the field of neurodegeneration. This is perhaps surprising given that cdk5 complexes have been implicated in many human neurodegenerative conditions. In particular, the p25-cdk5 complex has been shown to have a possible role in the neuronal loss seen in Alzheimer's disease, Parkinson's disease (Shah and Lahiri 2014) and HS (Sen, Thom et al. 2006, Sen, Thom et al. 2007). It would, therefore, be of interest to evaluate the role of roscovitine in preventing neuronal loss in neurodegenerative diseases. In particular, as most studies have evaluated roscovitine pharmacokinetics after systemic injection, examining roscovitine pharmacokinetics after direct injection into the brain would be of particular value. In this experiment, we determined the spread and effect of i.c.v. injection of roscovitine in rats to provide data from which to support studies of the impact of the drug on neurodegeneration in two experimental models of HS.

2.2. Materials and methods.

2.2.1. Animals.

Experiments were performed on male outbred Sprague-Dawley rats weighing 200–250g. All experimental animals were obtained from Charles River, Cambridge, UK. They were housed in cages as groups, with free access to food and water and maintained in temperature and light controlled rooms (24 °C, 12/12h light/dark cycle with lights on at 07:00). All of the methods used in the present study were approved by the ethical committees at the University of Oxford and carried out following the United Kingdom's Animals (Scientific Procedures) Act of 1986, revised 2012.

2.2.2. Induction of anaesthesia, pre-surgery preparation.

Rats were anaesthetised in an induction box containing isoflurane 5% in oxygen at 1 l/min, then transferred to anaesthetic mask initially 3% isoflurane, and then adjusted according to respiration and pedal reflex. Rats were maintained at a rectal temperature of 36.5 to 37° C with a Harvard Homoeothermic blanket®. Rats were given the first injection of glucose saline and then subsequent doses every 60 minutes; topical anaesthetic was applied to the ears using cotton buds.

2.2.3. Surgery.

Rectal temperature, breathing rate, pedal reflex and other measures were monitored and recorded to control anaesthesia and administration of drugs. Rats were placed on a folded cloth drape over the Harvard heating pad on the stereotaxic frame. Tail was taped with a rectal probe -which was lubricated with KY jelly- using skin-compatible tape (3M), rats were then placed in the stereotaxic frame fitted with an anaesthetic mask.

Aseptic techniques were followed throughout the procedure. The surgeon cleaned their hands in Sterilium and donned sterile gloves, opened the surgical kit and cleaned the rat scalp with Chloraprep® swab (BD Medical, UK) and then dried it. Surgery was started by making an incision in the scalp 2mm to the right of midline and opened the scalp completely with a spring retractor. The skull was then exposed and cleaned. Skull landmarks lambda and bregma were levelled (to within 0.2 mm) using (The Rat Brain in Stereotaxic Coordinates

Paxinos and Charles Watson atlas 7 th edition). One burr hole was drilled at AP –0.8 mm; lateral –1.5 mm. A syringe was manipulated to the centre of burr hole and lowered until the tip touched the cortical surface, the confirmation of correct needle placement was confirmed by the efflux of CSF. The syringe was then lowered 3.5 mm into the brain to reach the left lateral ventricle. 1mM roscovitine, 50 ng in 140 nl of DMSO/saline, or saline over 5 minutes were injected into the right lateral ventricle using a 1 µl Hamilton syringe with a 26-gauge needle. After completion of the infusion, the needle was kept in place for 5 minutes. The surgeon repaired the craniotomy using Prolene sutures placed to tighten scalp margins, and then we injected the final dose of saline, and additional analgesic when needed.

2.2.4. Cardiac perfusion.

Anaesthetised rats were retained on the stereotaxic frame for set periods of 0.5, 1 and 2.0 hours after the end of infusion. Each rat was injected with an overdose of pentobarbitone (1 ml, 100 mg/kg) and then removed from the frame and placed on its back in a perfusion tray. The short period between cessation of administration of isoflurane and the onset of deep pentobarbitone anaesthesia was carefully monitored to confirm continued lack of consciousness. The rat was placed on its back. After confirmation of deep anaesthesia, a midline incision was made over the sternum, continuing to the abdomen. The rib cage was cut to expose the heart. The left ventricle was cannulated, and perfusion was started with chilled saline (0.9% NaCl in distilled water), the vena cava was immediately cut. Perfusion continued until clear liquid flowed. We then removed the cannula.

2.2.5. Brain removal and hippocampus dissection.

A midline incision was made over the skull, with another transverse incision across the back of the skull, which was followed by flexing the neck allowing access to the foramen magnum for the tips of sharp scissors and then cut the sagittal suture. Using Rongeurs skull plates were peeled from the dorsal aspect of the brain, keeping the lower point horizontal and in contact with the underside of the skull to avoid damaging the brain. The dura was removed using scissors and forceps. The brain rostral was transacted to the bony protrusions that separate cerebellum from cerebral cortex using a sharpened spatula. The spatula was slid forwards while pressing the edge down onto the bottom of skull cavity to sever the cranial nerves with small side-to-side movements. The brain was removed on the spatula and placed

initially in ice-cold saline and then on a filter paper on a low platform. The brain was then bisected along its midline using a scalpel and razor.

The hippocampi was dissected out, separating dorsal from ventral ends. Each hippocampal sample was washed in ice-cold isopentane, to avoid a layer of ice forming that might insulate the brain, and placed into appropriate labelled tubes (left dorsal, left ventral, right dorsal, right ventral). Tubes were then returned to dry ice.

Six batches were produced, consisting of six animals each, each batch containing one rat from each time point (0.5, 1 and 2 hours) and injection type (roscovitine or saline). The total number of rats was thirty-six.

2.2.6. Western blotting.

Hippocampal samples were washed with ice-cold PBS and lysed on ice for 30 minutes in cell lysis RIPA buffer with protease and phosphatase inhibitor 1%. Samples were homogenised with a motor pestle on ice for two minutes. Lysates were centrifuged for 15 minutes at 12000 rpm for 20 minutes at 4°C. We stored cell homogenate fractions at −80°C before use.

The bicinchoninic acid assay (BCA assays) was performed. Protein concentrations were used in supernatant fractions using the Bio-Rad Bradford assay (Bio-Rad, Hercules, CA, USA). Equal amounts of protein (6 mg/ml) were boiled in sample buffer and resolved by SDS-PAGE in 10% (wt/vol) gels. The separated proteins were transferred to polyvinylidene fluoride membranes (Immobilon, Millipore, Billerica, MA, USA).

Blots were blocked in 5% milk in 0.1% Phosphate Buffered Saline (PBS) with Tween 20 (PBS Tween). Membranes were probed overnight with primary antibodies (anti–p25/p35 antibody (Rabbit polyclonal to p35; Santa Cruz Biotechnology, CA, USA) 1/100)) in Tris Buffer Saline Tween 20 and washed with Tris Buffer Saline Tween 20 for an hour. The blot was then incubated with secondary antibody for 1 hour at room temperature. Bands were detected after being immersed in ECL (sensitive, nonradioactive, enhanced luminal-based chemiluminescent substrate for detection of horseradish peroxidase (HRP) on immunoblots) for 5 minutes and then imaged on western blot imaging machine (Bio-Rad, Hertfordshire, UK). Blots were rewashed in PBS Tween for an hour, stripped with 27% H_2O_2 in PBS for 20 minutes, washed again in PBS for 30 minutes. Blots then were probed with β-actin 1:20000

for 1 hour at room temperature. Bands were detected after being immersed in ECL for 1 minute and imaged on the same western blot imaging machine (BIO-RAD, Hertfordshire, UK).

2.2.7. Quantification.

Western blot bands were quantified using Photoshop software (Adobe cc 2015). The relative quantity of protein was quantified in each immunoreactive band by densitometry and normalised to the quantity of β-actin in the same sample. All experiments were performed with samples from all rats in the same batch on the same blot, with the samples being assayed in duplicate or triplicate each time and the average of one data point per animal was taken.

2.2.8. Statistical analysis.

Mean values and standard deviations were calculated for normalised band quantifications (normalised to beta-actin levels). Differences in evaluated variables between roscovitine and control groups were assessed with one-way ANOVA tests by using SPSS (IBM, version 24). The significance criterion was <0.05.

2.3. Results.

To determine where and for how long roscovitine effects after i.c.v injection; we initially studied the pharmacokinetic properties of the impact of roscovitine on the p25:p35 ratio. Western blots probed with anti p25/35 antibody showed a significant decrease in p25:p35 levels (p<0.05, one-way ANOVA) in the rat group injected with roscovitine half an hour before perfusion compared to animals injected with saline in the right dorsal region (injected site) (Figure 2.2). The injection is into the ventricle closest to the right dorsal hippocampus, and the decrease in p25 occurs only in this half of the right hippocampus. There was no significant difference at any other time point in the levels of p25:p35 in the right dorsal half of the hippocampus between roscovitine and saline-treated rats (Figure 2.2).

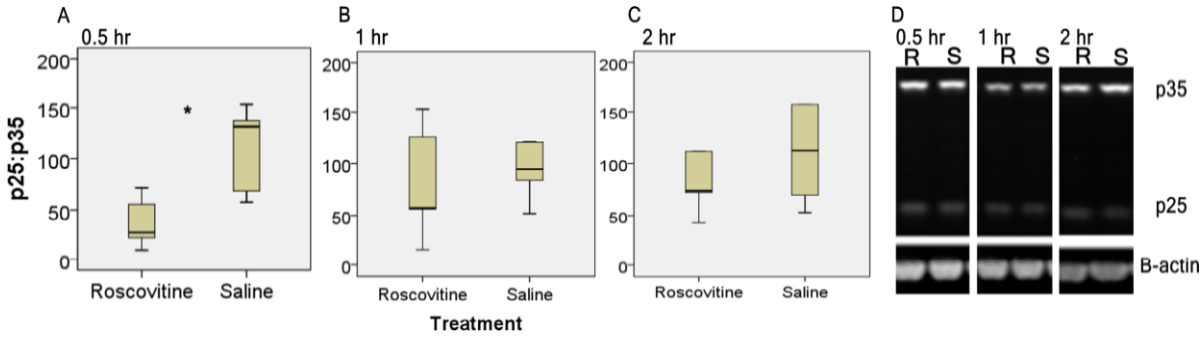

Figure 2.2: p25 and p35 in the right dorsal hippocampus following injection of roscovitine i.c.v.
At 0.5-hour (0.5 hr) time point (A, D), there was a significant decrease in p25:p35 activity level in rats injected with roscovitine compared to rats injected with saline at the right dorsal injected site. There was no difference in the 1-hour (1 hr) time point (B, D) or 2 hours (2hr) (C, D) time point.

In the ventral half of the right hippocampus, there was no significant difference in p25: p35 ratios between roscovitine and saline-treated groups, at any time point (p<0.05, one-way ANOVA; Figure 2.3). There was no significant difference in p25:p35 ratio, between the roscovitine- and saline-injected groups, at any time point in the left hippocampus in both the ventral and the dorsal halves (p>0.05, one-way ANOVA) (Figure 2.4,5). We, therefore, concluded that the effect of roscovitine does not reach far away from the injected site.

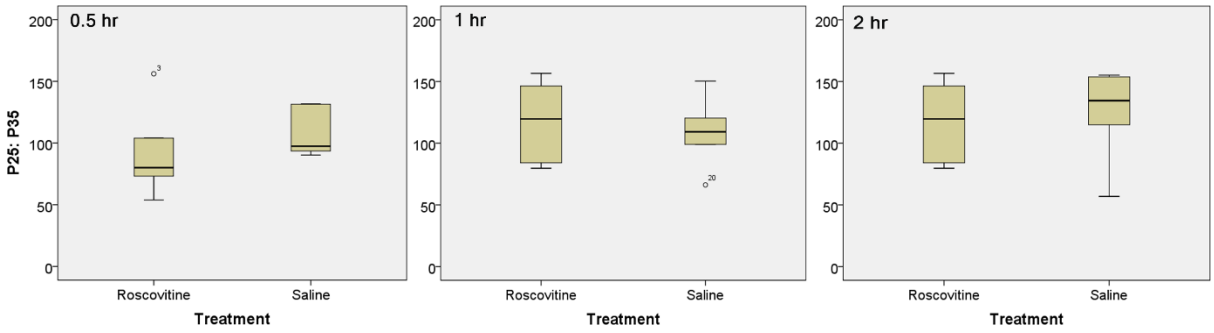

Figure 2.3: p25 and p35 in the right ventral hippocampus following injection of roscovitine into the dorsal right lateral ventricle. At 0.5-hour (0.5 hr) time point, there was no change in p25: p35 activity level in rats injected with roscovitine and rats injected with saline. Similarly, there was no difference in the 1-hour (1 hr) or 2 hours (2 hr) time point.

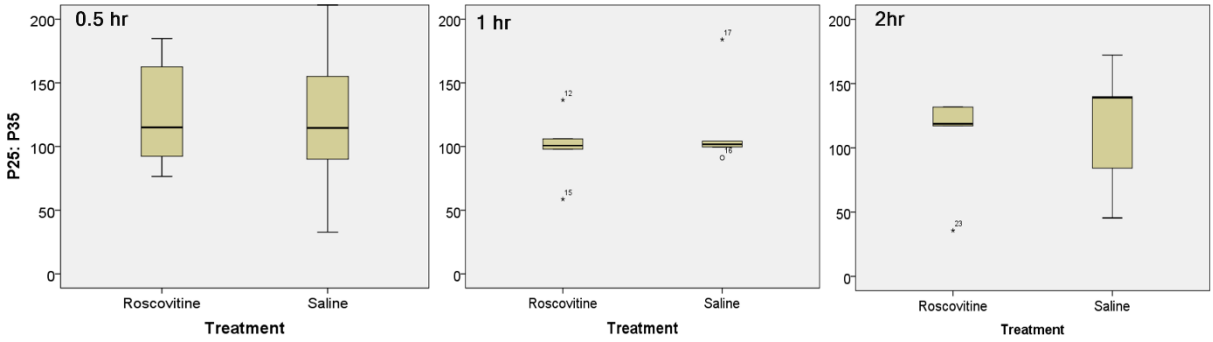

Figure 2.4: **p25 and p35 in the left dorsal hippocampus following injection of roscovitine into the dorsal right lateral ventricle.** There was no difference in p25: p35 activity level in rats injected with roscovitine and rats injected with saline at any time point in the dorsal part of the left hippocampus (non-injected hippocampi).

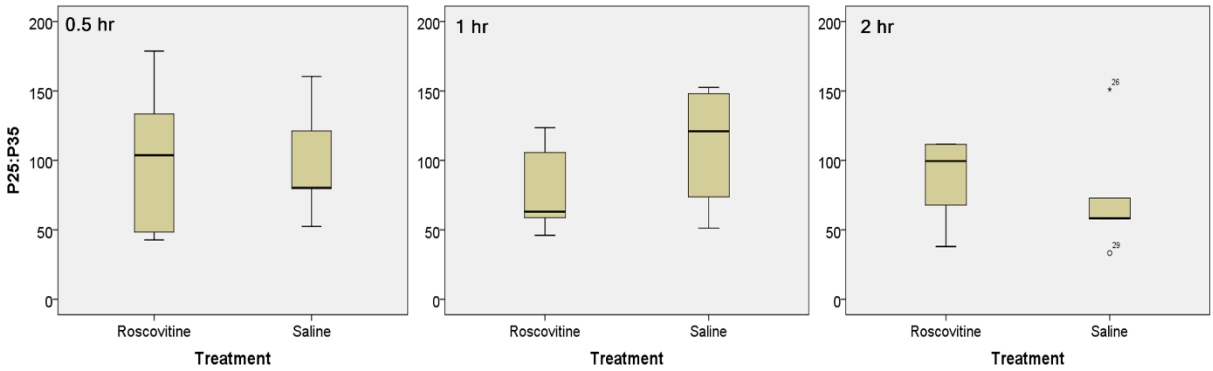

Figure 2.5: p25 and p35 the left ventral hippocampus following injection of roscovitine into the dorsal right lateral ventricle. There was no difference in p25: p35 activity level in rats injected with roscovitine compared to rats injected with saline at any time point in the ventral part of the left hippocampus (non-injected hippocampi).

2.4. Discussion.

Although there are some studies on roscovitine investigating pharmacokinetics after systemic injection, which provides detailed information about roscovitine absorption, distribution and metabolism, to our knowledge, this is the first study to assess roscovitine pharmacokinetics and its effect on the brain after injection directly into the brain.

Initially, we explored the localisation of roscovitine and its half-life after i.c.v. injection through its effect on a signalling pathway potentially involved in the seizure-dependent neuronal loss, the cdk5 pathway. Roscovitine inhibits cdk5, and as a result, it may exhibit a neuroprotective effect.

Here we demonstrate that i.c.v. injection of roscovitine decreases the ratio of p25:p35 half an hour after injection, but only in the part of the hippocampus most proximal to the injection site (right dorsal). This effect is no longer seen by 1 hour after injection; this might suggest that roscovitine is highly distributed in the hippocampus close to the injected site after i.c.v injection, at least for half an hour, and not for more than one hour after injection. Moreover, the relatively short timeframe during which an effect of roscovitine on p25:p35 ratios is seen, might explain why other investigators have not reported an effect of roscovitine after i.c.v. injection. Appreciably this is speculative as there is such scant data on the intraventricular injection of roscovitine.

As roscovitine affected the greatest measured change on p25:p35 levels 30 minutes after administration, we chose this time point for future experiments, with roscovitine being given 30 minutes before either intraperitoneal pilocarpine or intrahippocampal kainic acid**.**

Chapter 3: Cdk5 signalling in the pilocarpine animal model of HS.

3.1. Introduction.

3.1.1. Pilocarpine: general introduction

Pilocarpine is a potent muscarinic agonist originating from the leaves of South America shrubs (Cavalheiro 1995, Kandratavicius, Balista et al. 2014). It is a direct-acting parasympathomimetic agent which mediates its pharmacological action through muscarinic acetylcholine receptor activation (Furman 2013). It is non-selective muscarinic receptor agonist and does not stimulate nicotinic acetylcholine receptors. Clinically it is used to decrease intraocular pressure in glaucoma and in cases of patients suffering from dry mouth to increase salivation. It is used widely in research to stimulate muscarinic receptors selectively.

Pilocarpine use is frequent in creating animal models of epilepsy. The systemic administration of pilocarpine to rodents is one of the earliest and most common animal models of human temporal lobe epilepsy (TLE) (Cavalheiro 1995). A single high dose of systemic pilocarpine is enough to cause widespread damage to the forebrain in rats with the subsequent development of seizures and seizure-related behavioural changes (Cavalheiro, Leite et al. 1991, Cavalheiro 1995).

3.1.2. Pilocarpine animal model is a valid model of human temporal lobe epilepsy (TLE).

Temporal lobe epilepsy (TLE) in human has unique characteristics: (I) the seizure onset is localised to the limbic system, particularly the hippocampus, (II) an initial precipitating injury usually precedes the appearance of temporal lobe epilepsy (TLE), (III) the precipitating injury is followed by a seizure-free period called the latent period and (IV) the occurrence of hippocampus sclerosis (Curia, Longo et al. 2008, Heuser, Tauboll et al. 2009). The systemic pilocarpine model of epilepsy has very similar features with: (I) a rapid induction of acute SE (II) the presence of a latent period that precedes seizures and (III) the occurrence of widespread lesions in multiple brain areas including the hippocampal and parahippocampal regions (Curia, Longo et al. 2008). In particular, administration of pilocarpine results in histological changes in the hippocampus that are very similar to those seen in human HS.

Some studies have shown similarities in the onset zone of spontaneous seizures in patients with temporal lobe epilepsy and pilocarpine-treated rats. The ventral hippocampus and ventral subiculum display the earliest seizure activity in the pilocarpine animal model (Toyoda, Bower et al. 2013), which is the same starting point of seizures in patients (Spencer, Kim et al. 1999). Also, behavioural studies in pilocarpine-injected rats demonstrate that rats have cognitive and memory deficits, which is a common feature found in TLE patients (Kandratavicius, Balista et al. 2014). These features support the model's validity as a representative of human TLE.

3.1.3. Pilocarpine-induced seizures and seizures related behaviours.

Pilocarpine can produce severe seizures and brain damage in rodents when injected in high doses (300-350) mg/kg, or in low dose (30 mg/kg) accompanied with a low dose of Lithium Chloride (LiCl, 3 mEq/kg). The use of LiCl was introduced to increase animal survival rate as with this combination, the dose of pilocarpine can be decreased by about 10-fold (Cavalheiro 1995). Pilocarpine alone at a high dose may not induce consistent SE, so lithium is used to enhance and potentiate the action of pilocarpine and keep consistency of SE (Reddy and Kuruba 2013)

Lithium delay the onset time of SE, reduces seizure susceptibility, mortality and neuronal death in a mechanism that doesn't involve glial activation in the hippocampus but might be through a mechanism involving the influx of Ca^{2+} through the NMDA receptors (Hong, Choi et al. 2017).

The first alterations in behaviour after pilocarpine injection include akinesia, ataxic lurching, facial automatisms and head tremor. After 15-25 min these changes evolve to limbic motor seizures with rearing, forelimb clonus, salivation, intense masticatory movements and falling. Behaviours recur every 2-8 minutes and lead to SE within 60 minutes of pilocarpine administration (Cavalheiro 1995).

After administration of pilocarpine, rodents experience an 'acute period'. The acute period represents the first 24 hours after pilocarpine injection. The lethality rate reaches 30% in this phase. Brain areas are damaged particularly in the hippocampus, thalamus and the

amygdala. Damaged cell morphology characteristics include massive swelling in the dendrites and cell body. A seizure free phase (silent period) follows the acute period, which is then followed by a chronic period. In the chronic period surviving animals suffer from recurrent spontaneous seizures with behaviours including facial automatisms, head nodding and forelimb clonus (Cavalheiro 1995, Leite, Garcia-Cairasco et al. 2002, Scorza, Arida et al. 2009).

3.1.4. Neuropathology of the pilocarpine animal model of epilepsy.

In the systemic pilocarpine model of epilepsy cell damage of a necrotic and apoptotic nature occurs. The cell damage can occur within minutes after pilocarpine injection and results in the process of neurodegeneration that might progress with time (Scorza, Arida et al. 2009). There are cell morphology and function alterations. The damage and histopathological alterations occur in different areas such as the amygdala, hippocampus, neocortex and thalamus. There is evidence that most of the loss and change in cell morphology occurs in the hippocampus where there is more significant damage to primary pyramidal cells and hippocampal granule cells. Severely injured neurons are mainly found in the CA1 and CA3 of the hippocampus (Mello and Covolan 1996, Curia, Longo et al. 2008, Scorza, Arida et al. 2009, Levesque, Avoli et al. 2016).

3.1.5. Mechanisms of the neuropathology of pilocarpine.

Temporal lobe epilepsy (TLE) is related to excessive excitation in the limbic structure against the low function of inhibitory pathways (Scorza, Arida et al. 2009). The hippocampus might be the initiation site of the seizure (Vezzani 2009, Toyoda, Bower et al. 2013). Pilocarpine-induced seizures are initiated via muscarinic receptors and further mediated via NMDA receptors. Pilocarpine mainly induces seizures through direct activation of the cholinergic system in the brain. It activates the M1 receptor which in turn activates the N-methyl-D-aspartate receptor (NMDA). Sustained increases in extracellular glutamate follow, leading to a rise in intracellular Ca^{2+} and activation of lipases, proteases and nucleases. These cascades result in cell death via necrosis and apoptosis (Smolders, Khan et al. 1997, Scorza, Arida et al. 2009).

3.2. Materials and Methods:

3.2.1. Animal production: general remarks.

The pilocarpine-treated animal model of epilepsy was produced in Prof. Matthew Walker's laboratory UCL, Queen Square, London. Sprague Dawley rats (270-330 gm) were ordered at least a week in advance and handled to allow familiarisation with habitat. We placed the rat in an induction box containing isoflurane 5% in oxygen at 1 l/min) and then transferred the rat to anaesthetic mask (initially 3% isoflurane, adjusted according to respiration and pedal reflex). All procedures were produced according to previously published protocols (Chandler, Princivalle et al. 2003).

3.2.2. Animal production: pilocarpine injected rats at different timepoint.

Rats were divided into four experimental groups according to the termination point following pilocarpine injection and recovery (controls n=5, 4 days post-pilocarpine n= 5, 7 days post-pilocarpine n=5 and 21 days post-pilocarpine n=5). Limbic SE was induced in rats by injection of the muscarinic agonist pilocarpine (Sigma Aldrich Co, Irvine, UK), 1 gm in 1 ml of saline, dose 320 mg/kg, i.p.). Scopolamine methyl nitrate (Sigma 1gm dissolved in 1 ml 0.9 saline, dose 1 mg/kg, i.p.) was administered 30 min before and 30 min after pilocarpine to reduce the peripheral effects of cholinergic action. SE was terminated after 120 min by injection of Diazepam (Phoenix Pharma, 10 mg/kg, i.p.).

3.2.3. Animal production: roscovitine and pilocarpine experiment cohort.

Rats were kept under anaesthesia for the whole duration of the roscovitine injection procedure and then allowed to recover prior to pilocarpine injection. They were divided into four experimental groups by the injection type: controls (control injection only n=5), pilocarpine alone (n=5), roscovitine and pilocarpine (n=5). Roscovitine treated rats (n=5) were produced by injecting 50 ng of 1mM Roscovitine i.c.v. into the right hemisphere, half an hour before pilocarpine injection, which we administered according to the protocol mentioned above. Animals were terminated seven days after injection.

3.2.4. Animal production: pilocarpine and MK801 experiment cohort.

The NMDAR antagonist, MK801 (4mg/kg) was administered (s.c.) in a group of animals immediately after termination of acute SE in pilocarpine-injected animals. A separate cohort was administered with pilocarpine alone according to the protocol above, and a naïve group acted as controls.

3.2.5. Perfusion and brain extraction.

In the terminal part of the experiment, anaesthesia was induced with 3% isoflurane and intravenously injected pentobarbitone 1 ml (100 mg/Kg). For each animal, after perfusion with chilled saline (4°C 0.9% NaCl in distilled water) through the aorta, the brain was removed and spilt along the corpus callosum. We fixed one hemisphere by immersion in 4 % paraformaldehyde (PFA), and the other was snap frozen. The brain hemisphere that we fixed was kept in 4% PFA for 48 hours.

3.2.6. Processing tissue for histology.

Fixed samples were sliced into blocks 0.5 mm thick and placed into tissue processing microcassettes. The following day, the samples were embedded in paraffin and subsequently cooled on a cold plate for 1-hour. Paraffin-embedded tissue was sectioned using a standard microtome at a thickness of 7 µm (the cutting was serial with 50 µm difference between each slide). Sections were placed in warm distilled water (40°C) and allowed to equilibrate at this temperature before being placed on Super Frost slides. Slides were then allowed to dry in the air for 1 hour and then in a 37°C oven for another hour.

3.2.7. Fluoro Jade-C (FJ-C) staining.

FJ-C, a polyanionic fluorescein derivative that can sensitively and selectively bind to degenerative neurons (Schmued, Stowers et al. 2005), was applied to examine dying neurons in hippocampus from the pilocarpine-treated rats.

Before staining, paraffin-embedded slides were put in a 60 °C oven for 20 minutes. Slides were then dewaxed in xylene (2x5 minutes) and rehydrated through graded ethanol baths (5 minutes in each of 100% ethanol, 100% ethanol, 95% ethanol, 80% ethanol). Slides were washed in PBS for 5 minutes, incubated in 0.06% potassium permanganate solution for 10

minutes and then transferred for 10 minutes to a 0.0001% solution of FJ-C (Millipore Inc.) dissolved in 0.1% acetic acid vehicle. The working solution was used within 2 hours of preparation.

After staining the slides with FJ-C as above, slides were incubated in 1 µM TO-PRO (TO-PRO®-3 iodide; life technologies) dye in PBS for 15 minutes. The slides were then rinsed through three changes of distilled water for 1 minute per change. Excess water was drained onto a paper towel, and the slides were then air dried on a slide warmer at 50 °C for at least 5 minutes. The air-dried slides were then cleared in xylene for at least 1 minute and then cover slipped with DPX (Sigma) non-fluorescent mounting media (Schmued et al., 2005).

3.2.8. Western blotting.

All western blot analysis was performed on frozen rodent hippocampal samples. Initial western blots were for NeuN, cdk5 and p25/p35 antibodies. Samples were lysed with RIPA buffer (Sigma Aldrich, UK) containing 2 mg/mL aprotinin, 2 mg/mL leupeptin, 1 mg/ mL pepstatin, 5 mM NaF and 5 mM Na_3CO_3. Ten microgram total protein extracts were separated on SDS-polyacrylamide gels and transferred to a nitrocellulose membrane by electrophoresis. After transfer, the membrane was blocked for one hour in 5% milk solution and then incubated with primary antibody overnight at 4°C. Primary antibodies used were DC17 mouse monoclonal anti-cdk5, (Santa Cruz Biotechnology, CA, USA)) 1/500, NeuN mouse anti-neuronal nuclei (NeuN) monoclonal antibody (Millipore, UK) 1/2000, anti–p35 antibody (Rabbit polyclonal to p35) 1/100. β -actin (Sigma Aldrich, UK) was used as a loading control. studied proteins and β -actin were quantified using Photoshop software.

3.2.9. Quantification and statistical analysis.

FJ-C and NeuN positive cells were directly quantified in hippocampus through manual neuronal count per area unit using Image J analysis software. Images were blinded for quantification.

Data was compiled in Excel (Microsoft Corporation) and statistical analysis was performed using SPSS 24 (IBM Corporation). Images were acquired using Zeiss® microscope and Image lab software.

3.4. Results.

3.4.1. Neuronal loss following SE induced by pilocarpine at different time points.

Cell bodies of most FJ-C positive cells were bright green and easily identified, and extensively distributed through the hippocampal areas of rats treated with pilocarpine and terminated at and after 7 days. There was little FJ-C staining in control tissue, and rats treated with pilocarpine and perfused after 4 days of SE (Figure 3.1 A). Staining with FJ-C showed a significant cell loss at and after 7 days of pilocarpine treatment in all hippocampal areas studied except the CA2 area which is known to be resistant to damage (Nonparametric test, Kruskal-Wallis test followed by Mann -Whitney test $p<0.05$) (Figure 3.1 B).

NeuN immunohistochemistry supported the above results. NeuN immunoreactivity was assessed visually and quantified per area. NeuN staining showed decreased neuronal content and dispersion of the granule cell layer in the hippocampus from animals perfused at or beyond seven days post-pilocarpine-induced SE (Figure 3.1 C). In control animals and animals sacrificed 4 days post-SE, NeuN immunohistochemistry showed a tight band of neurons in the CA1 and CA3 regions and preservation of neurons in hilus. By seven days post SE, neuronal loss in CA1 was evident with clear thinning of the CA1 region. Likewise, we saw the neuronal loss in hilus and CA3. We observed similar staining patterns at 21 days post-pilocarpine-induced SE, with no significant difference in neuronal content from the 7-day time point.

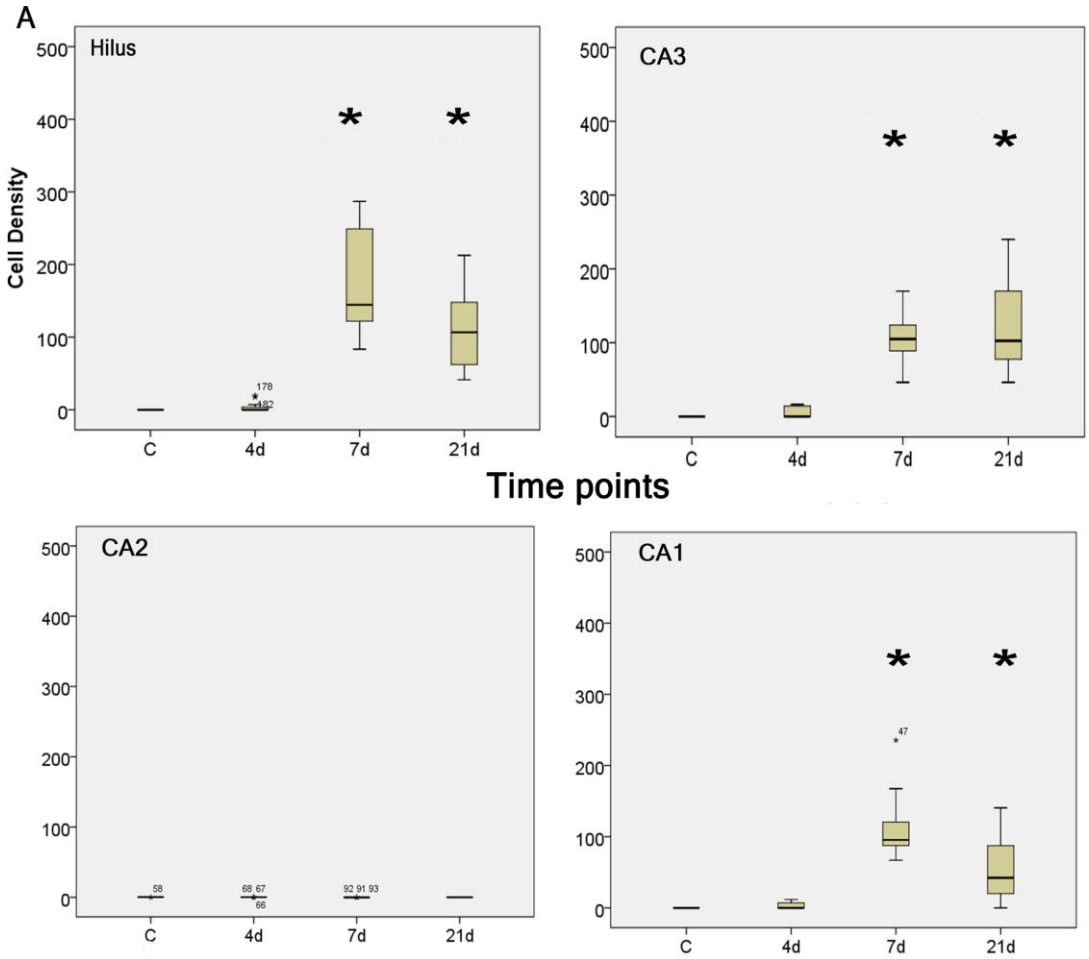
A
Hilus
CA3
CA2
CA1
Cell Density
Time points
C
4d
7d
21d
B
C
4d
Hilus
Hilus
7d
C
C
4d
7d

Figure 3.1: FJ-C staining and NeuN immunohistochemistry in pilocarpine-treated rats terminated at different time points.
We performed FJ-C cell counts in hilus, CA3 and CA1 areas (Figure A, B) of the hippocampus in rats injected with pilocarpine and terminated at 4, 7, 21 days post-SE. Controls were naïve to all treatments. FJ-C staining showed significant cell loss at and after 7 days post SE, NeuN immunohistochemistry confirmed FJ-C results (C). Fig B Scale Bar =100µm. **p<0.05.*

3.4.2. Western blots of cdk5 and p25: p35 in pilocarpine-treated animals at different time points.

Concordant with the immunohistochemistry results, western blot analysis showed a decrease in the expression of NeuN between all pilocarpine treated groups and the control animals. The fall was significant at and after 7 days post induced SE (one-way ANOVA, Dunnett's post hoc test $p<0.05$; Figure 3.2A).

Cdk5 levels were similar at different timepoint ($p=0.057$; one-way ANOVA, Dunnett's post hoc test; Figure 3.2B).

Levels of p35 paralleled that of NeuN and began to fall at and after seven days. Interestingly, p25 levels generally remained constant suggesting that animals terminated beyond seven days after pilocarpine-induced SE exhibit an increase in the ratio of p25: p35 (Figure 3.2 C). When calculated and compared to controls, the ratio of p25: p35 rose significantly at seven days after SE but fell again to non-significant level at 21 days post pilocarpine treatment (one-way ANOVA, Dunnett's post hoc test).

Based on these experiments, the 7-day timepoint was chosen as appropriate to test, in a new cohort of animals, the effect of the anti-cdk5 inhibitor roscovitine and the NMDA antagonist MK801 on the neuronal loss.

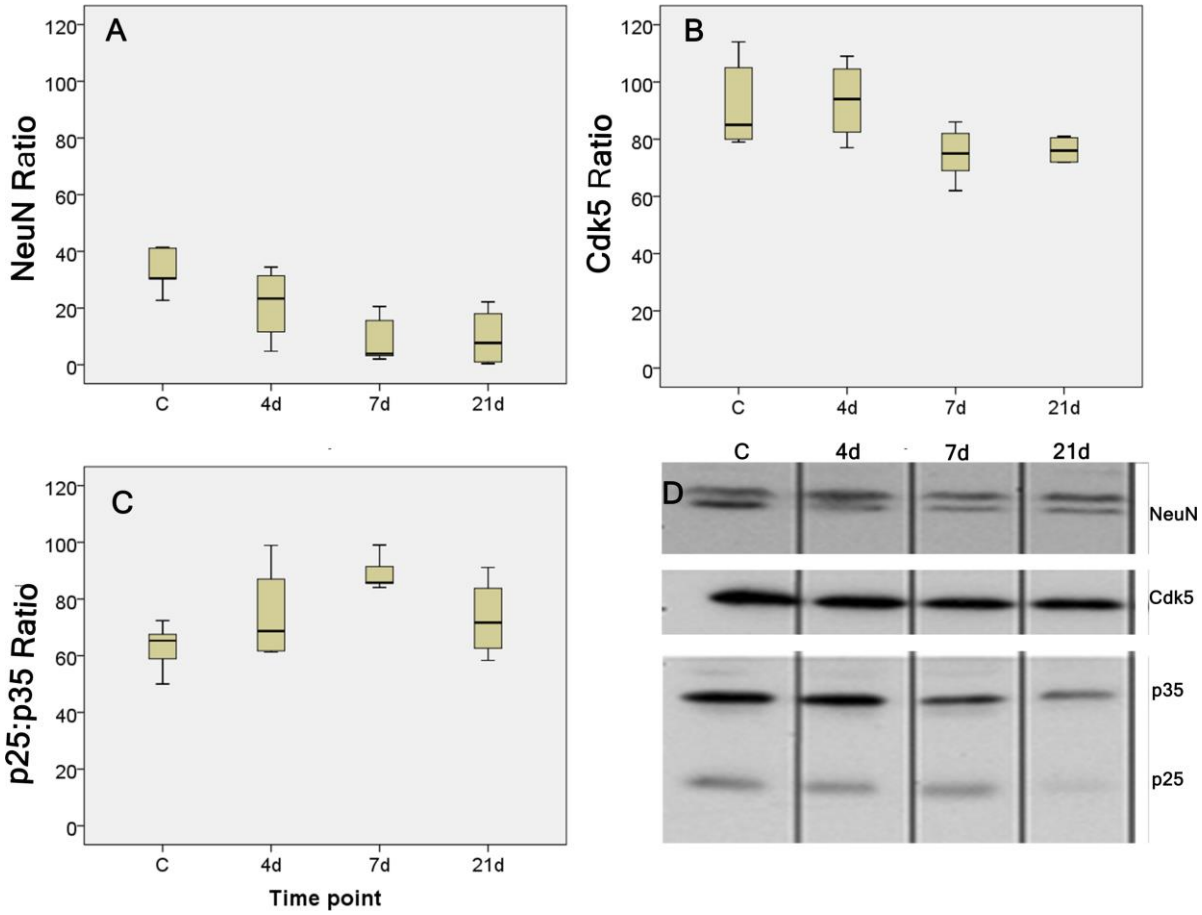

Figure 3.2: Western blot analysis for NeuN, cdk5, p25: p35 ratio in pilocarpine-treated rats terminated at different time points. Graphs represent levels of NeuN (A), levels of cdk5 (B) and the p25: p35 ratio (C) in rats treated with pilocarpine and terminated at different intervals following the induction of SE. An example western blot is also shown (D). This data was provided by Dr Arjune Sen.

3.4.3. The effect of roscovitine on cdk5 activator function and neuronal loss.

FJ-C was used again to examine dying neurons in hippocampal areas in rats treated with pilocarpine alone and rats treated with roscovitine and pilocarpine. Controls were naïve to any treatment.

There was an extensive distribution of FJ-C positive cells in the hippocampal areas of rats treated with pilocarpine alone and terminated at 7 days post-SE.

In animals perfused 7 days post-pilocarpine-induced SE, the cdk5 inhibitor roscovitine significantly reduced neuronal loss as measured by cell counting of FJ-C positive cells in all areas studied (Non-parametric test, Kruskal-Wallis test followed by Mann-Whitney test; $p<0.001$; Figure 3.3). Neuronal loss was evident in the CA1, CA3 and hilus subfields at seven

days following treatment with pilocarpine alone while significant preservation of neurons was evident in all areas in animals treated with roscovitine half an hour before pilocarpine.

NeuN staining results were consistent with FJ-C results. NeuN staining showed neuronal preservation in animals treated with roscovitine prior to pilocarpine (Figure 3.4). NeuN positive cell counts demonstrated that treatment with roscovitine before pilocarpine significantly preserved neurons in CA1, CA3 and hilus subfields (Non-parametric test, Kruskal-Wallis test followed by Mann-Whitney test $p<0.001$; Figure 3.4).

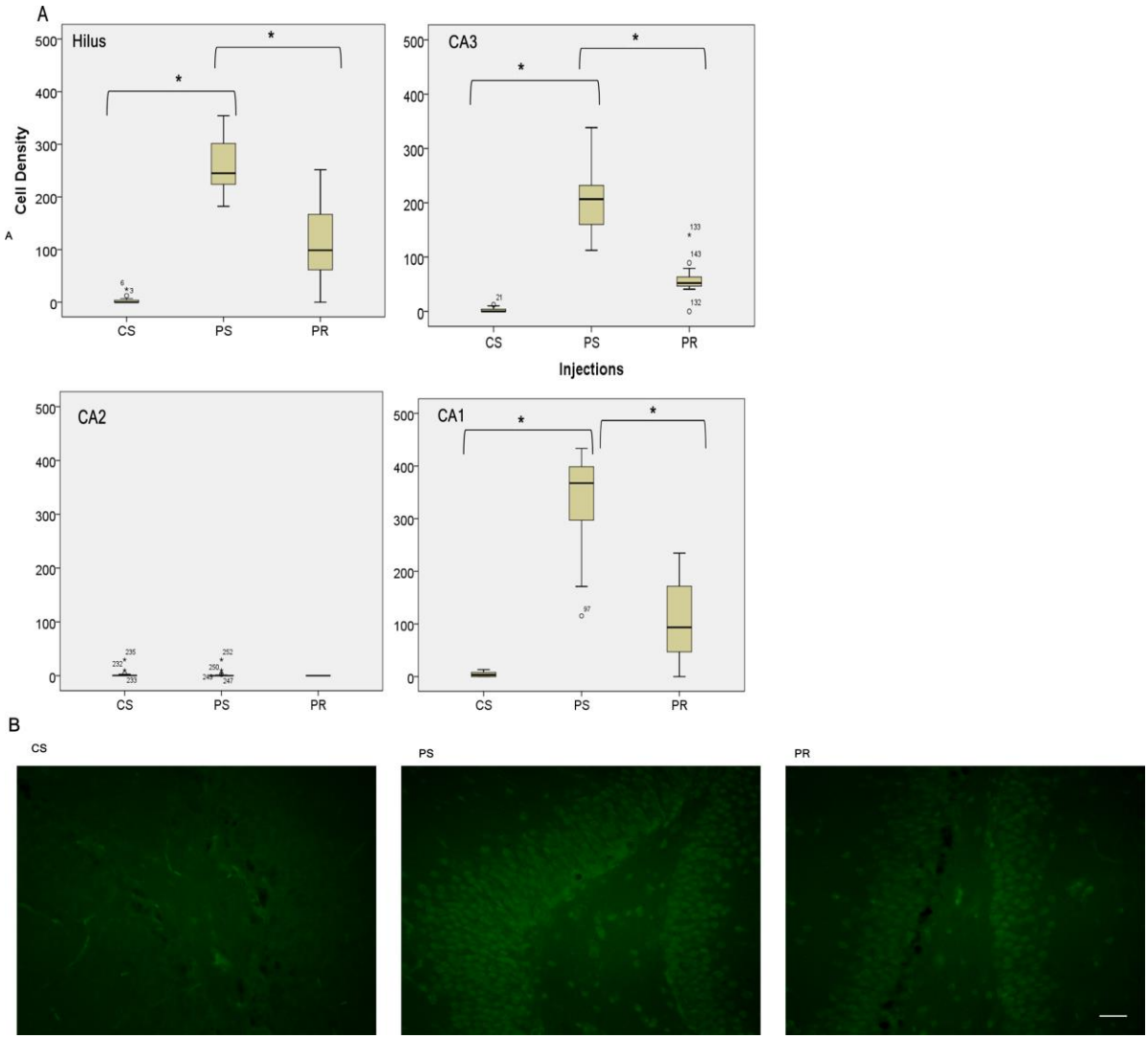

Figure 3.3: FJ-C staining in the hippocampus in pilocarpine alone and pilocarpine & roscovitine. FJ-C staining showed a neuronal loss in rats treated with pilocarpine alone in all areas except CA2, and significant neuronal preservation in rats treated with roscovitine before pilocarpine in all regions studied. Graph B shows a sample

of hilus tissue stained with FJ-C in CS (controls), PS (pilocarpine alone) and PR (pilocarpine and roscovitine). Photos were taken at 20X. Scale Bar=100 µm.

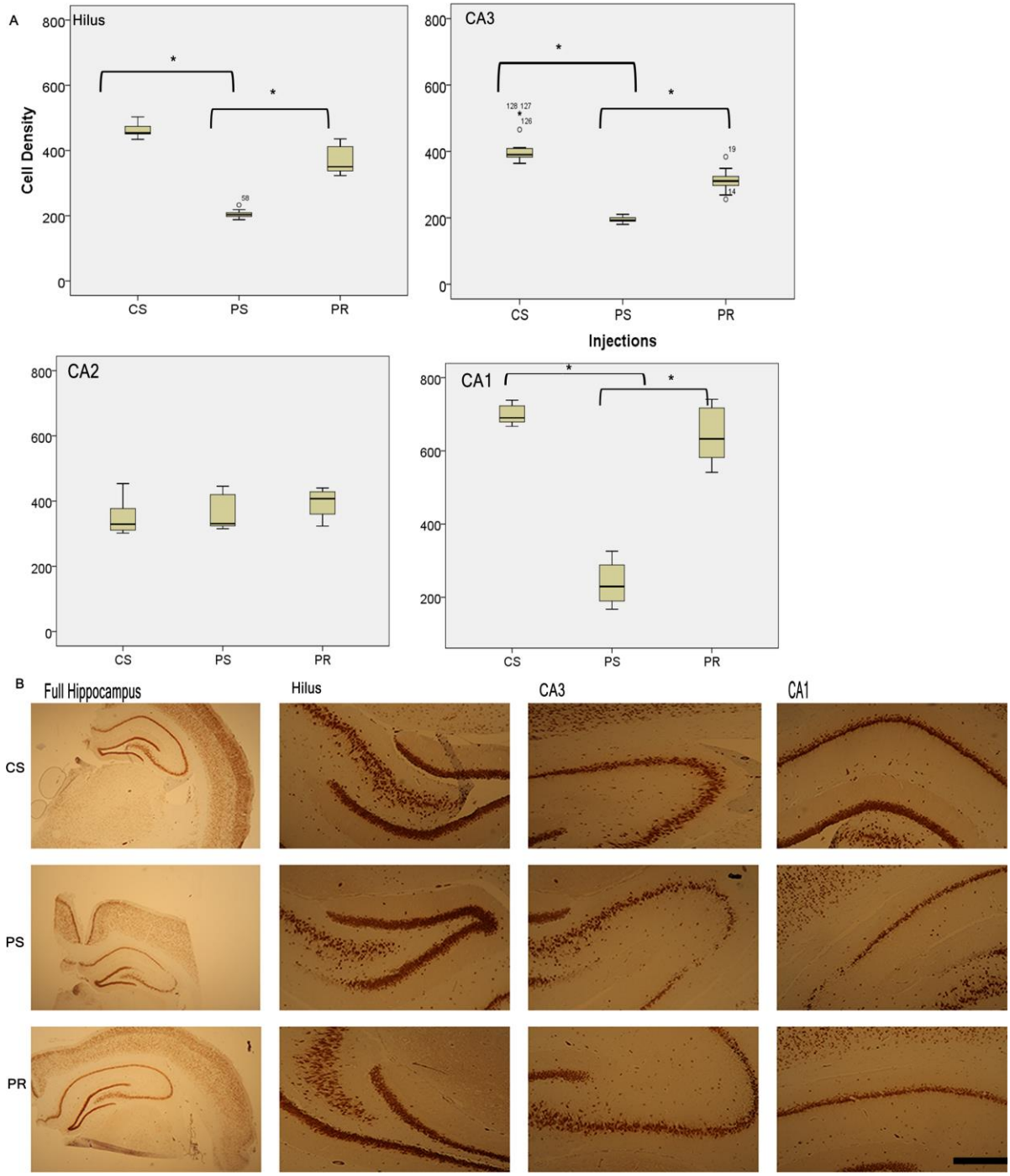

Figure 3.4: NeuN staining in hippocampal areas of rats treated with pilocarpine alone or pilocarpine and roscovitine. NeuN staining confirmed preservation in neurons in rats treated with roscovitine before pilocarpine injection. The full hippocampus image was taken at 2.5X, and other areas were taken at 20X. CS (controls), PS (pilocarpine alone) and PR (pilocarpine and roscovitine). Scale Bar=65 µm.

3.4.4. The effect of MK801 on NMDA receptor function and neuronal loss.

In rats terminated seven days post-pilocarpine-induced SE, we again used NeuN immunohistochemistry and FJ-C staining to assess neuronal loss after additional administration of the NMDA antagonist MK801(4mg/kg s.c).

As before, neuronal loss was evident in all areas studied at seven days following treatment with pilocarpine alone. Additional administration of MK801 provided significant neuronal protection in all hippocampal regions, as measured by cell counting of NeuN and FJ-C positive cells (Non-parametric test, Kruskal-Wallis test followed by Mann-Whitney test,$p<0.001$; Figure 3.5).

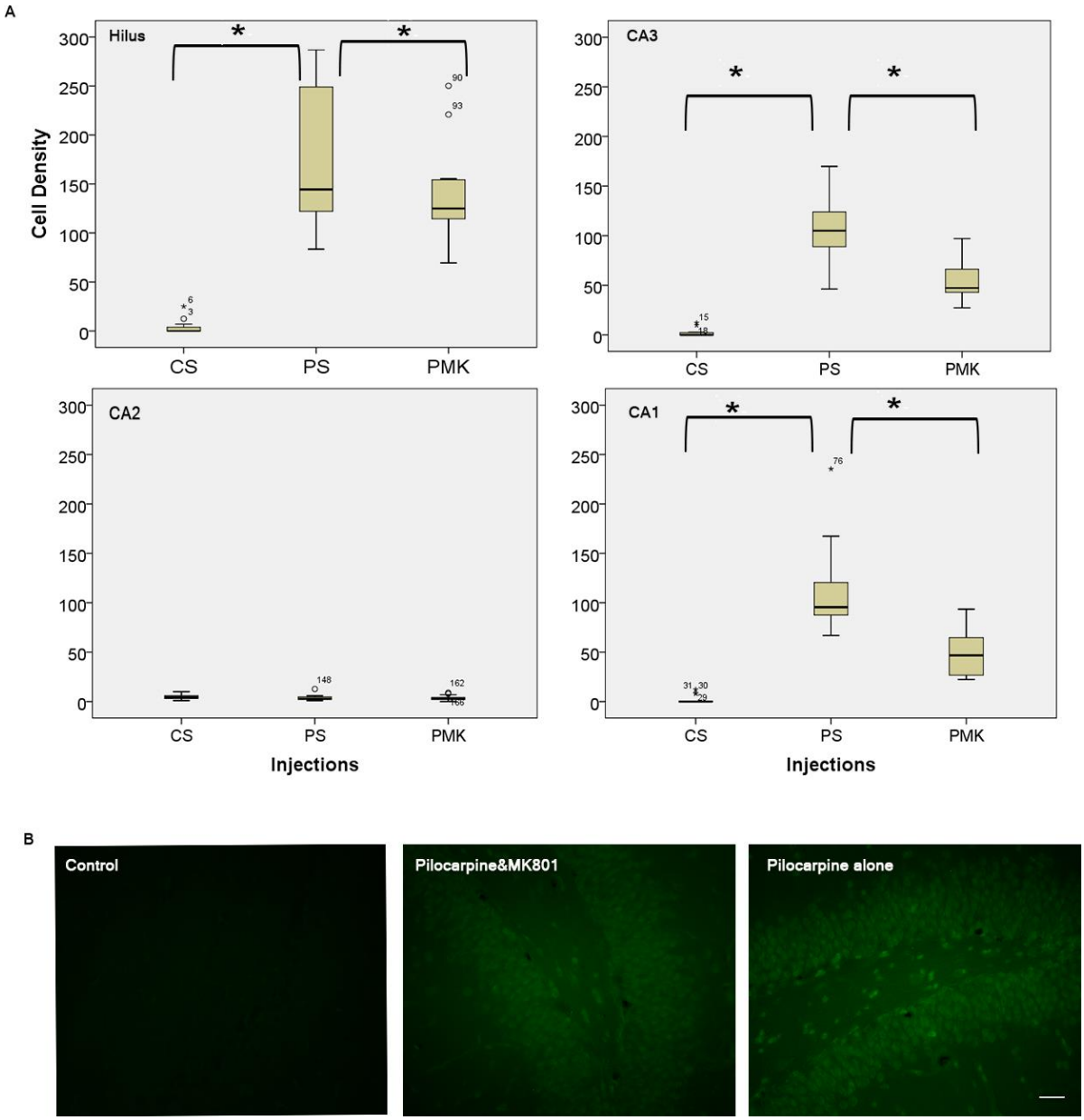

Figure 3.5: FJ-C staining in the hippocampus of rats treated with pilocarpine alone and pilocarpine and MK801. FJ-C staining showed neuronal loss in rats treated with pilocarpine alone in the hilus, CA3 and CA1 regions. A) There was significant neuronal preservation in rats treated with MK801 after pilocarpine in all areas studied (Nonparametric test, Kruskal-Wallis test followed by Mann-Whitney test $p<0.001$). B) sample FJ-C stained sections of hilus in CS (controls), PS (pilocarpine alone) and PMK (Pilocarpine &MK801) treated rats. Scale Bar=100 µm.

3.4.5. The death rate in animals.

The death rate in the pilocarpine-treated rats was high. In each experiment we lost around 30% of animals injected with pilocarpine as a result of pilocarpine-induced seizures. In the roscovitine experiment, the death rate of pilocarpine-treated animals was approximately 90%, so we had to repeat the experiment with producing more animals.

3.5. Discussion:

Our results are consistent with previous research. Systemic injection of pilocarpine in naïve rodents' models human temporal lobe epilepsy (TLE), a seizure-free latent period follows, and then enduring recurrent seizures that continue for the rest of the animal's life (Furman 2013) – a similar time course to that seen in temporal lobe epilepsy (TLE) in patients (Hellier and Dudek 2005, Curia, Longo et al. 2008). Neuropathological changes such as subfield specific neuronal loss are observed in the rat pilocarpine model and are again similar to neuronal loss features in patients with hippocampal sclerosis (Leite, Garcia-Cairasco et al. 2002). There is also evidence that the seizure onset zone in this model is the same as in patients, namely the ventral hippocampus (Toyoda, Bower et al. 2013).

To determine the optimal time point to detect the neuronal loss in the pilocarpine-treated rats, we used different cohorts of animals and terminated them at different time points. Systemic administration of pilocarpine led to repetitive limbic seizures and SE, which lasted until we stopped it pharmacologically. Some studies suggest that at least 1 hour of induced SE is required to produce neuronal damage (Navarro Mora, Bramanti et al. 2009), while others show that cell loss begins after 20 minutes of SE in ventral hippocampal CA1 and CA3 regions, although very few neurons are damaged at this stage. The neuronal damage is still mild 1-hour post-SE and slight-to-moderate 3-hours post-SE and was still slight at 42-hours and 72-hours post SE (Fujikawa 1996).

In our model, we terminated SE after 120 minutes. We did not see any cell loss in the controls, and there were very few dead neurons in the animals perfused four days after injecting pilocarpine. At seven days post-SE there was a significant neuronal loss compared to controls based on immunohistochemistry and western blot analysis.

We also investigated cdk5, p35 and p25 levels at different time points. There was a fall in cdk5 levels in all treated animals potentially consequent to general cell loss as the cdk5 expression is ubiquitous. p35 is a neuronal protein and levels of p35 paralleled that of NeuN with the loss being apparent after 7 days post-SE. However, p25 levels remained relatively

constant throughout suggesting a rise in p25: p35 ratios in latter sacrificed animals. p25: p35 ratios were highest at 7 days post SE.

We, therefore, selected the 7-day post-SE timepoint to further evaluate mechanisms of neurodegeneration in this model. We injected roscovitine thirty minutes before pilocarpine, and MK801 thirty minutes after induced SE and terminated rats at seven days to assess whether these drugs had any effect on neuronal viability.

Our principal finding in this work is that roscovitine significantly prevented neuronal loss in all areas studied in the pilocarpine animal model of HS. The ability of the cdk5 inhibitor roscovitine to preserve neurons in the pilocarpine model suggests that deregulation of the cdk5 pathway might have a role in the neuronal loss associated with epileptogenesis. Notably, injection of roscovitine was focal into the right lateral ventricle, but it still managed to prevent neuronal loss even though seizures are more widespread and longer-lived than the measurable metabolic consequence of the drug.

MK801 is a selective non-competitive NMDA antagonist (Kovacic and Somanathan 2010). Previous studies have shown that pre-treatment of rats with MK-801 (1-10 mg/kg, imp.) prevented neuronal degeneration in the hippocampus caused by direct intracranial injections of NMDA (Foster, Gill et al. 1987, Gill, Foster et al. 1987). Our results are consistent with this and show that MK801 significantly prevented neuronal loss in all areas studied post systemic pilocarpine injection, which suggests that the NMDA receptor has a role in mediating neuronal loss in this epilepsy model and that suppressing NMDA might contribute to neuronal preservation. The fact that it showed an effect on neuronal protection after induced SE offers potential promise for clinical use.

Together with the kainic acid model, the pilocarpine model is one of the two most commonly used animal models of temporal lobe epilepsy (TLE). Prolonged seizures in both models cause neuronal loss, an essential characteristic of HS.
Systemic injection of pilocarpine is a very effective method in producing high numbers of rats in short time. It is a rapid method, and multiple rats can be injected at a similar time. No surgical procedures or implantation of cannulae is required which helps to eliminate post-

surgical complications that could affect the animal's health. However, injecting the drug systemically is not without complications. Although some studies reveal similarities in the onset zone of spontaneous seizures in patients with temporal lobe epilepsy and pilocarpine-treated rats (Toyoda, Bower et al. 2013), injecting pilocarpine systemically raises questions about the validity of the model as a representative of human (TLE). Firstly, there is a lack of control over the lesion and the seizure zone; the fact that pilocarpine is administered systemically makes it hard to take for granted where the seizure onset and the resulting epileptic focus will be located (Jefferys 2014). Secondly, in most rats, both seizure onsets, lesions and neuronal loss were equal in both left and right hemispheres -mostly because of the systemic injection- whereas humans with temporal lobe epilepsy usually have unilateral foci and lesions (Jefferys 2014). Another disadvantage is the high mortality rate in the systemic pilocarpine model. Generally, at least 25% of animals die as result of pilocarpine-induced seizures. This percentage can rise substantially even with only slightly higher doses (Curia, Longo et al. 2008). Different approaches have been tried to overcome this problem, such as injecting multiple lower doses of pilocarpine, but this affected the ability of the model to induce SE (Glien, Brandt et al. 2001). In our experiments, we lost around 30% of animals as a result of pilocarpine-induced seizures, and in one of the cohorts treated with pilocarpine alone, the death rate of animals was approximately 90%. To overcome all these problems and to further study the mechanism of neuronal loss in HS, we continued our investigations using the intrahippocampal kainic acid model of epilepsy.

Chapter 4: The kainic acid rat model.

4.1. Introduction.

4.1.1. Kainic Acid: general introduction.

Kainic acid (KA-in Japanese means the ghost of the sea) was isolated in the early 1950s, from the seaweed Digenea simplex (Levesque and Avoli 2013). The molecular formula of kainic acid is $C_{10}H_{15}NO_4$, and the molar mass is 213.23. It is a potent neurotoxin which causes neuronal cell death through its ability to cause robust depolarisation (Le Duigou, Wittner et al. 2005). Kainic acid is a potent analogue of glutamate and an agonist of ionotropic kainate receptors which are localised pre and postsynaptically in different brain regions including the hippocampus. Administration of KA has been shown to cause excitotoxicity through increased production of reactive oxygen species, mitochondrial dysfunction, and apoptosis in neurons in many regions of the brain, particularly in the hippocampal sub regions of CA1 and CA3, and in the hilus of dentate gyrus (Wang, Yu et al. 2005). The ability of the kainic acid to induce excitotoxic neuronal death extended its use in developing animal models in various neurodegenerative disorders such as Parkinson's disease (Foster, Bezin et al. 2003), Alzheimer's disease (Gilles and Ertle 2000) and multiple sclerosis (Pitt et al., 2000).

4.1.2. Kainate receptors.

Kainate receptors are a class of ionotropic glutamate receptors that are localised pre- and postsynaptically. Postsynaptic kainate receptors contribute to synaptic transmission while the presynaptic receptors modulate transmitter release from excitatory and inhibitory synapses in different brain regions (Lerma 2003). Receptor mapping studies localised kainate receptors in multiple areas of the brain including the amygdala (Rogawski, Gryder et al. 2003), basal ganglia (Jin and Smith 2011), cerebellum (Wisden and Seeburg 1993), and the hippocampus (Lerma 2003).

4.1.3. Hippocampal kainate receptors.

Kainate receptors in the hippocampus are distributed both presynaptically and postsynaptically. They classify into different subtypes: KA1 (GluK 4) subunits which are highly expressed in CA3 pyramidal cells and weakly expressed in CA1 pyramidal cells, KA2 (GluK5)

subunits which are highly expressed in both CA1 and CA3 pyramidal cells, GluR5 (GluK1) which are highly expressed in GABAergic interneurons in both CA1 and CA3 subfields and (GluR6) subunits (GluK2) which are highly expressed in CA3 pyramidal cells. This high expression of kainate receptors in CA3 and CA1 regions explains why those particular regions are highly susceptible to kainic acid induced excitotoxic damage and make the hippocampus the starting point of the seizures in this model (Lerma 2003, Wang, Yu et al. 2005, Bloss and Hunter 2010).

4.1.4. Excitotoxic effect of kainic acid.

Generally, excitotoxic neuronal death happens because of excess calcium influx, which leads to the generation of reactive oxygen species (ROS) and reactive nitrogen species (RNS), which in turn cause damage to intracellular membranes, and triggers apoptotic and necrotic pathways leading to cell death. Kainic acid exerts its neuroexcitotoxic and epileptogenic properties by acting on the ionotropic glutamate kainate receptors (KARs) which have presynaptic modulatory and postsynaptic excitatory actions. Kainic acid induces some cellular events, including the rapid influx of cellular Ca^{2+}, activation of Ca^{2+} dependent enzymes and generation of reactive oxygen species. Together these lead to excessive Ca^{+2} influx, causing a collapse of the mitochondrial membrane potential, opening mitochondrial permeability transition pores, and allowing the release of mitochondrial factors (e.g., cytochrome-c and apoptotic-inducing factor (AIF)) which initiate pathways which will lead to apoptosis. Alternatively, intense Ca^{2+} overload could directly cause mitochondrial swelling and damage, decrease in ATP, and increase in reactive nitrogen species, which oxidises protein, lipid, and DNA, causing acute neuronal necrosis (Figure 4.1) (Wang, Yu et al. 2005,)

.

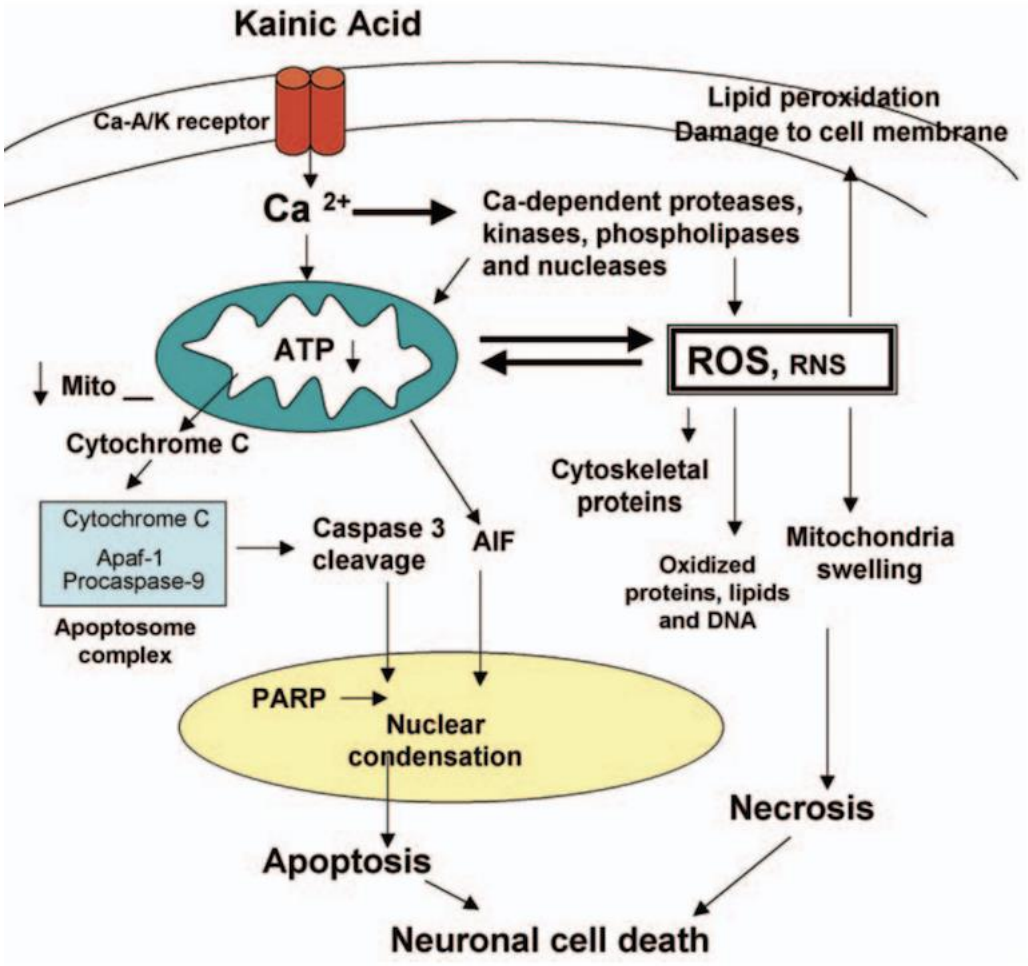

Figure 4.1: Kainic acid-induced cell death.
The diagram explains mechanisms of necrosis and apoptosis induced by kainic acid that will lead to neuronal cell death (Wang, Yu et al. 2005).

4.1.5. Kainic acid animal models of hippocampal sclerosis (HS).

Experimental animal model studies using different routes of administration show that kainic acid injection can induce seizures, seizure-related behaviour changes and irreversible neuronal damage. Injection of kainic acid in animals closely mimics human temporal lobe epilepsy (TLE) (Lothman and Collins 1981, Ben-Ari 1985), as, similar to human cases, it causes an initial precipitating injury that is followed by a latent period and then the appearance of recurrent seizures.

Injection of kainic acid systemically or intracerebrally in the hippocampus or amygdala induces seizures and seizure-related behaviours (Levesque and Avoli 2013). At a histological

level, kainic acid causes severe neurotoxicity and neuronal damage following injection in the CA1, CA2, CA3 and the hilus region of the hippocampus and in extratemporal regions (Ben-Ari 1985, Wang, Yu et al. 2005, Benkovic, O'Callaghan et al. 2006).To avoid the disadvantages of systemic injection - that were discussed in the previous chapter- and to obtain more control over lesion we decided to progress to the intrahippocampal kainic acid animal model of HS.

4.2. Materials and methods.

4.2.1. Animals.

Experiments were performed on male outbred Sprague-Dawley rats and male inbred Fischer- 344 rats weighing 250-300 g. All experimental animals were obtained from Charles River, Cambridge, UK. They were housed in group cages with free access to food and water and maintained in a temperature and light controlled rooms (24 °C, 12/12h light/dark cycle with lights on at 07:00). All the methods used in the present study were approved by the ethical committees at the University of Oxford and carried out under the United Kingdom's Animals (Scientific Procedures) Act of 1986, revised 2012.

Rats were ordered a week in advance and handled to allow familiarisation with habitat and were given small portions of Ribena® and jelly (Hartleys ®, Leeds, UK) three days before surgery.

4.2.2. Pre-surgery preparation and induction of anaesthesia.

One hour before surgery rats were given Vetergesic (0.05 mg/kg), Metacam (1 mg/kg; 2 mg/ml solution), and saline (10 ml/kg /h). Subsequent doses of saline were given every 60 minutes and applied a topical anaesthetic to the ears using cotton buds. Rats were placed in induction box containing isoflurane 5% in oxygen at 1 l/min) and then transferred to anaesthetic mask (initially 3% isoflurane, adjusted according to respiration rate and pedal reflex). Rectal temperature, breathing rate and pedal reflex were monitored and recorded during the surgery.

A folded large cloth drape was placed over the Harvard heating pad on the frame and taped down. The surgical kit was aseptically opened. Each rat was placed on its front on the drape over the heating pad, and a rectal probe lubricated with KY jelly and taped to tail using skin-compatible tape was inserted. The rat was placed in the stereotaxic frame fitted with an anaesthetic mask.

4.2.3. Cannula implantation stereotaxic surgery.

Surgery was performed under aseptic conditions. The Surgeon cleaned their hands in Sterilium and changed to sterile gloves, they cleaned the scalp with Chloraprep® (BD Dispensing, UK), and covered the frame, head, neck and dorsal thorax with sterile drapes exposing only the operating area. The surgeon made an incision in the scalp 2 mm to the right of midline, and levelled skull landmarks lambda and bregma (to within 0.2 mm). The surgeon drilled burr holes at AP –4.5 mm; lateral –4.6 mm for (22 gauge) guide cannula (stainless steel, diameter = 0.008 inch and 8 mm height) with recording (3 mm projection and electrodes 1 mm further projection) and AP –0.8 mm; lat –1.5 mm for (28 gauge) guide cannula (stainless steel, 8 mm height) projecting 4.6 mm further (Figure 4.2). Cannulas were bought from Plastic Ones Inc Roanoke VA, through Bilaney Consultants Sevenoaks, UK. The surgeon drilled another three burr holes for anchoring screws and then inserted bone screws.

The surgeon lowered both cannulas 2 mm below the cortical surface and cemented these in place using Refobacin® Plus bone cement with Gentamicin (Biomet UK Ltd, Swindon UK). The bone cement was built up to a low plinth, and the scalp was sutured to pull it against the wall of the plinth.

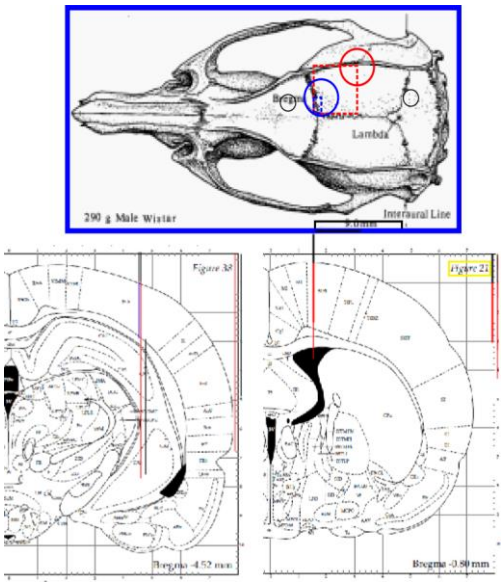

Figure 4.2: stereotaxic surgery coordinates.

4.2.4. Recovery and post-surgery care.

After surgery, rats were placed in a recovery cage with half of the cage on a heating pad. The cage contained a red plastic hut, bedding and a granular substrate to avoid foreign bodies entering wounds. It also contained a variety of wet and dry food such as gel and mash. Rats were continuously monitored until they were able to move and to protect their airways, and only then were they transferred to a recovery box.

Rats were then frequently monitored -every 10 minutes- until seen to be eating, drinking and fully mobile. They were given post-operative drugs for 5 days following surgery; Vetergesic (buprenorphine) (0.05 mg/kg twice daily), Metacam (1 mg/kg; 2 mg/ml once daily) and saline (10 ml/kg/h every 6 or 12 hours as required). Rats were assessed at least once a day (usually 2-3 times daily) until body weight plateaued. Measurements were recorded and observations with drugs administered were documented onto a score sheet. Rats were provided with appealing foods at floor level (e.g. muesli, Cheerios, fruit, mash, gels) to assist feeding and hydration. Pain and discomfort were assessed through observing animal postures, mobility, responsiveness, grooming and other behaviours. Each animals' condition were recorded on a chronic epilepsy score sheet.
After the rats started having seizures, some (notably the Fischer -344 strain) became hard to handle. In such cases, weighing was stopped to reduce stress to animals and used other indicators of well-being.

After 10 to 14 days, when rats had recovered entirely, regained their original weight and were restored to a good condition, they were prepared for injection.

4.2.5. Injections.
We made injections in (towelled) restrained conscious rats, first of the treatment of control or roscovitine and 30 minutes later kainic acid or control.

The first injection of 1mM roscovitine (Sigma, 50 ng in 140 nl of DMSO) or vehicle (140 nl saline/DMSO) was made over 5 minutes. A (24 gauge) inner cannula was placed into the rostral guide cannula and connected by flexible tubing to a (1 μl) Hamilton syringe mounted

on a (22 gauge) syringe pump. The inner cannula was left in place for 5 minutes before removing it and replacing the cap. Thirty minutes after the end of injection, rats were restrained again. The cap was removed from the caudal guide cannula with electrodes, and an inner (28 gauge) cannula -connected by flexible tubing was inserted to the Hamilton syringe mounted on the syringe pump- into the caudal guide cannula. We connected a recording cable to the socket attached to the guide cannula and electrode combination. We injected kainic acid (Sigma, 400 ng in 200 nl salines) or saline (200 nl) at 50 nl / min, (4 minutes) and then left cannula in place for 5 minutes. We recorded for at least 1 hour. We terminated convulsive seizures after 120 minutes using ketamine (50 mg/kg) and diazepam (20 mg/kg).

The above procedures were performed in two different strains of rats, Fischer-344 and Sprague Dawley. Each strain of rats was divided into four experimental groups by the injections made into the rostral and caudal cannulae: vehicle & kainic acid (V Kainic acid), roscovitine & kainic acid (R Kainic acid), roscovitine control (R Control) and vehicle control (V Control). The design used cohorts of 4 rats, one for each experimental condition, prepared as close in time as possible, where possible with the roscovitine and corresponding control in parallel.

4.2.6. Monitoring behaviour after intrahippocampal kainic acid-induced SE.

Twenty non-anaesthetised rats (from both strains) were restrained by a towel and were injected with vehicle& kainic acid (V Kainic acid), roscovitine & kainic acid (R Kainic acid), roscovitine control (R Control) and vehicle control (V Control) using a cannula placed in the right hippocampi. Seizure behaviours were witnessed in rats by witnessing them by eye and the experiment was not blinded.

Racine's scale (RS) - which is one of the most commonly used tools to evaluate the intensity of a seizure in rodent models of experimental epilepsy (Luttjohann, Fabene et al. 2009)- was used. Racine’s scale categorises six stages of intensity based on the behavioural range of the animals during a seizure.

According to Racine’s scale seizure intensity stages are classified into:

Stage 1	Sudden behavioural arrest and/or motionless staring.
Stage 2	Facial jerking with muzzle or muzzle and eye.
Stage 3	Neck Jerks.
Stage 4	Clonic seizure in a sitting position.
Stage 5	Convulsions including clonic and/or tonic-clonic seizures while lying on the belly and/or pure tonic seizures/ rearing and falling.
Stage 6	Convulsions including clonic and/or tonic-clonic seizures while lying on the side and/or wild jumping/circular running.

(Luttjohann, Fabene et al. 2009)

Hellier and Dudek's proposed modified Racine's scale applicable to chemo-convulsant acute seizure models (i.e. kainic-acid and pilocarpine) was used as well. They list the stages as: "head nodding" (1), "wet-dog shakes" (2), "forelimb clonus" (3), "forelimb clonus with rearing" (4), "stage 3 and 4 seizures with animals falling to the side" (5) and "jumping" (6) (Hellier and Dudek 2005).

4.2.7. Terminal procedures.

For the terminal part of the chronic kainic acid, anaesthesia was induced with 3% isoflurane and injected pentobarbitone 1 ml (100 mg/Kg). After perfusion with chilled saline (4°C 0.9% NaCl in water) through the aorta, the heart and brain were removed and kept in 4% Paraformaldehyde (PFA) (room temperature) for 24 hours before immersing them in sucrose 30% solution for 7 days at 4 °C.

4.2.8. Preparing sections for histology.

Frozen brain sections were prepared for histology, and sectioned using a cryostat (Bright, Bright Instruments Ltd, Bedfordshire, UK).

4.2.9. Nissl staining.

Sections were incubated in PBS-T (0.1%) for 10 minutes, washed in PBS for (5 minutes) twice, and incubated in 1:200 Nissl stain (NeuroTrace530/615) and 300 nM DAPI solution for 20 minutes. Sections were rewashed in PBST for 10 minutes, PBS for 5 minutes twice and were given a final wash with PBS for 2 hours at room temperature then mounted on gelatine slides and were blinded for quantification.

4.2.10. Quantification and statistical analysis:

Images were acquired using a Zeiss® microscope and Image lab software and data was compiled in Excel (Microsoft Corporation). SPSS 24 (IBM Corporation) was used to perform statistical analysis.

4.3. Results.

4.3.1. Comparing results of both strains.

Results in both strains were similar. Kainic acid resulted in a neuronal loss in all areas studied (hilus, CA3 and CA1) except CA2. Roscovitine injection before kainic acid administration resulted in neuronal protection in all areas. However, there was a significant difference in result values between the two strains such they could not be combined for the analysis of the effects of roscovitine; non-parametric test, Kruskal-Wallis test followed by Mann-Whitney test, $p<0.001$). However, outliers might account for this problem as one Sprague Dawley rat treated with kainic acid exhibited minor neuronal loss and another one treated with roscovitine before kainic acid manifested dramatic neuronal loss, substantially different to the results from other animals (Figure 4.3).

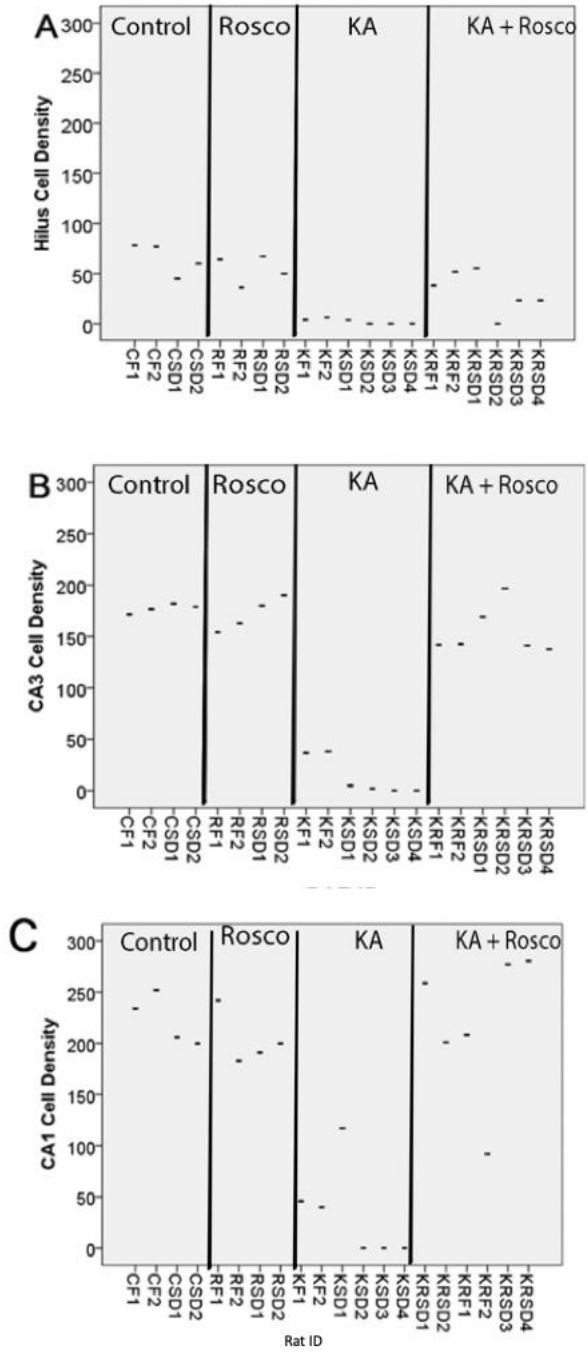

Figure 4.3: Cell density in different hippocampal areas in individual rats.
These plots represent Nissl stained cell counts per area in individual rats in hilus, CA3 and CA1 in control group (Control), Roscovitine alone group (Rosco), kainic acid alone group (KA) and kainic acid and roscovitine injected group (KA + Rosco) in two strains of rats, Fischer-344 and Sprague Dawley (SD). Fischer-344 controls (CF), SD controls (CSD), Fischer-344 roscovitine controls (RF), SD roscovitine controls (RSD), Fischer-344 kainic acid alone (KF), SD kainic acid alone (KSD), Fischer-344 roscovitine & kainic acid (KRF) and SD roscovitine & kainic acid (KRSD).

4.3.2. Neuropathological changes and neuronal loss following intrahippocampal injection of kainic acid.

Neuronal loss was evident at seven days post kainic acid injection. Pre-treatment with roscovitine rescued neuronal loss in rats post kainic acid-induced SE.

The hippocampus in both strains was highly susceptible to neuropathological changes and neuronal loss following intrahippocampal injection of kainic acid, which caused a significant neuronal loss in the hilus, CA3, CA1 regions of the hippocampus, but left the CA2 region and the dentate gyrus almost intact. The unilateral intrahippocampal administration of kainic acid produces cell loss throughout the whole injected right hippocampi, though kainic acid injection was performed in the distal site.

Kainic acid model in Fischer-344 strain:

After terminating rats 7 days post SE, the brains of four vehicle & kainic acid (V Kainic acid) rats, four roscovitine & kainic acid (R Kainic acid) rats, two roscovitine control (R Control) rats and two vehicle control (V Control) rats were processed for histology to assess for neuronal loss. We used Nissl labelling to encompass neuronal cell losses and DAPI as a counterstain.

In Fischer-344 rats, kainic acid administration resulted in a significant neuronal loss in CA1, CA3 and hilus of hippocampal subfields (non-parametric test, Kruskal-Wallis test followed by Mann-Whitney test, $p<0.001$). We did not notice any loss in control rats nor those treated with roscovitine alone. Administration of roscovitine before kainic acid was associated with preservation of neuronal cell counts in CA1, CA3 and the hilus (Nonparametric test, Kruskal-Wallis test followed by Mann-Whitney test, $p<0.001$; comparing neuronal cell count kainic acid and roscovitine vs kainic acid alone). The figure below shows representative photographs of brain sections illustrating treatment-related cell loss in the hippocampal formation (Figure 4.4).

Kainic acid model in Sprague Dawley rats:

We obtained similar results in Sprague Dawley rats. The same histological approach was used with Nissl staining and DAPI to study neuronal loss. Brains of four vehicle & kainic acid (V Kainic acid) rats, four roscovitine & kainic acid (R Kainic acid) rats, two roscovitine control (R Control) rats and two vehicle control (V Control) rats were processed for histology to assess for neuronal loss. There was a significant loss (Non-parametric test, Kruskal-Wallis test followed by Mann-Whitney test $p<0.001$) of hippocampal neurons in animals injected with kainic acid alone in the hilus, CA3 and CA1 areas; CA2 area showed neuronal preservation.

There was no neuronal loss in control or roscovitine-alone injected rats. Nissl count cells in hilus, CA3 and CA1 regions were higher in animals injected with roscovitine before kainic acid than in the animals injected with kainic acid alone, again suggesting neuronal preservation in the roscovitine-treated group (Figure 4.4) (Non-parametric test, Kruskal-Wallis test followed by Mann-Whitney test $p<0.001$).

4.3.4. Comparison between Fischer-344 and Sprague Dawley rats.

Initially, we experimented with the inbred strain Fischer- 344. Our choice to use Fischer-344 rat was based on previous experiments showing that inbred strains have less variability and are more sensitive to epilepsy (Golden, Smith et al. 1995). However, we had to consider changing the strain as Fischer-344 rats proved to bleed more during surgery. There was one case where a rat died from a stroke (proved by post-mortem checks) and another because of continuous haemorrhage. Fischer-344 rats took longer recovery time from surgery owing to haemorrhage. It is also worth mentioning that Fischer-344 rats were aggressive and difficult to handle. As a consequence of all these reasons, we decided to change to an outbred strain. We carried on the rest of the experiments using Sprague Dawley rats which proved not to have any of these problems.

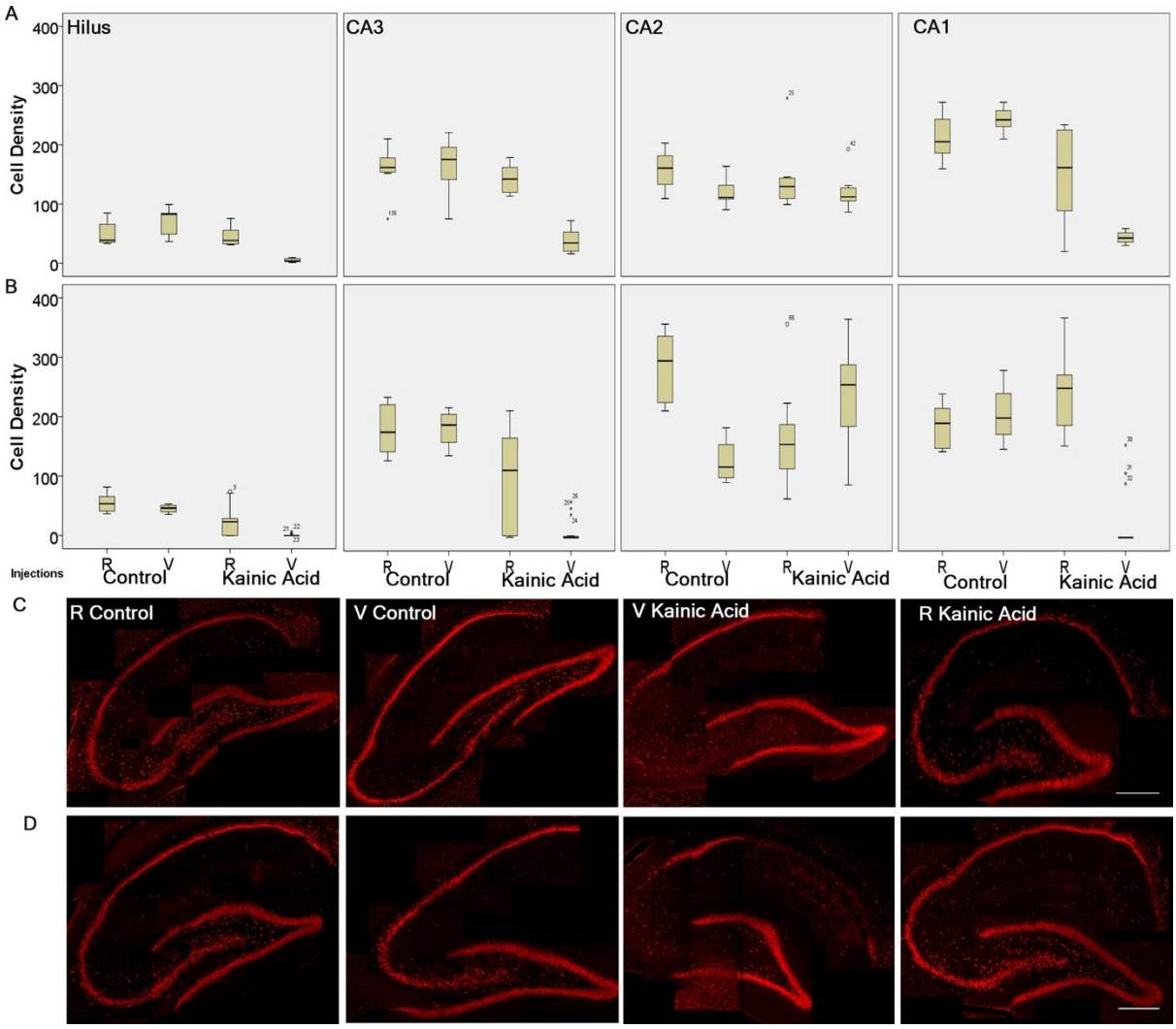

Figure 4.4: Cell counts and histopathological analysis in the kainic acid model of HS.
Graphs representing Nissl stained cell counts per area in hilus, CA3, CA2 and CA1 in controls; V controls (vehicle & control), V kainic acid (vehicle & kainic acid), R kainic acid (roscovitine &kainic acid) and R Control (roscovitine &control) in Fischer-344 strains (A, C) and Sprague Dawley (B, D). The effect of kainic acid was the same in both strains; injecting kainic acid alone (V kainic acid) induced significant neuronal loss in the hilus, CA3 and CA1 sectors. The cell counts significantly increased after injecting roscovitine before kainic acid in all areas suggesting neuronal preservation. Scale bar 500 µm.

The neuropathological changes and neuronal loss following intrahippocampal injection of kainic acid occurred in the injected right hippocampi. The contralateral left hippocampi neurons remained intact (Figure 4.5).

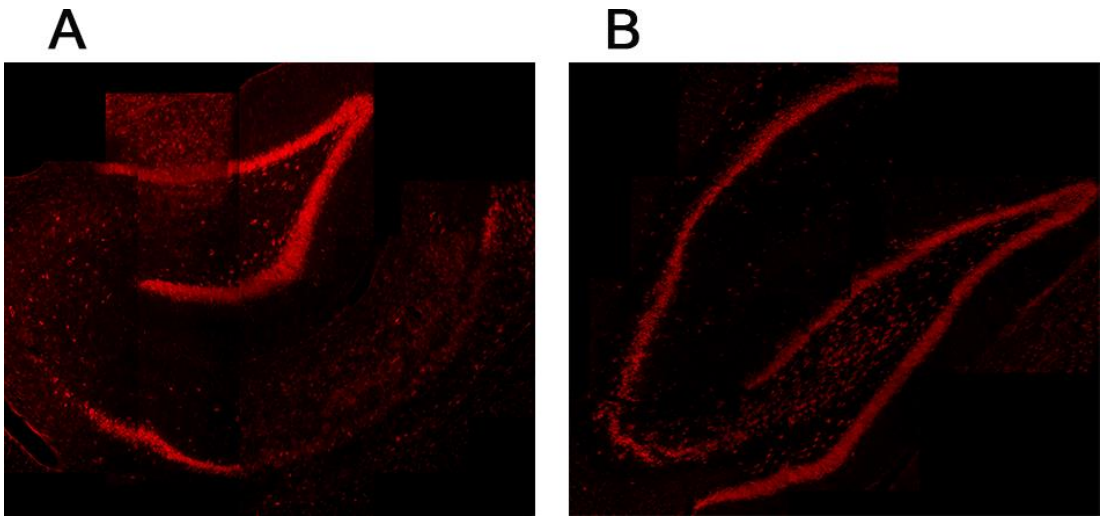

Figure 4.5: Neuropathological changes and neuronal loss in the hippocampus ipsilateral to kainic acid injection. Intrahippocampal injection of kainic acid resulted in a unilateral neuronal loss at the injected site. The neuronal loss in the hippocampus ipsilateral to kainic acid injection, but not in the contralateral hippocampus. The graph shows two hippocampal section taken from a rat injected with kainic acid alone. Image A represents the right injected site while image B represents the left hippocampi.

4.3.5. Seizure-related behavioural changes after intrahippocampal kainic acid injection.

All rats injected with intrahippocampal kainic acid alone (vehicle & kainic acid) in both strains developed SE which led to spontaneous seizures. Some rats injected with roscovitine and kainic acid had SE and showed the same behaviours as rats injected with kainic acid alone. Controls and rats injected with roscovitine alone did not show any epileptic behaviours. Three rats injected with kainic acid alone reached Racine stage 5 and the other four reached stage 6. One rat injected with kainic acid and roscovitine reached stage 5, another one reached stage 3, and three reached stage 2 (Figure 4.6,7).

Statistical analysis (one-way ANOVA, Bonferroni post hoc Test, $p \leq 0.05$) showed a significant difference in the behavioural stage level in the kainic acid alone injected group and the kainic acid and roscovitine group (Figure 4.8).

We conducted behavioural monitoring after the injection started until the end of SE. The mean latency between kainic acid injection and the appearance of the first seizure was 2 minutes (slightly faster for Fischer-344). We observed mouth and facial movements which

included whisker trembling during behavioural arrest and motionless staring (stage1). We noticed head nodding; slight facial jerking expressed with the muzzle or muzzle and eye and wet-dog shakes (stage 2), neck jerks “forelimb clonus” (stage 3); clonic seizures while the animal remained in a sitting position (stage 4) and seizures characterized by rearing and falling and clonic seizures while the animal was lying on its stomach (stage 5), and clonic seizures with the animal lying on its side (stage 6). Some rats started to jump high after kainic acid-induced SE (stage 6). We stopped SE with a combination of diazepam (20 mg/kg) and ketamine (50 mg/kg) after 120 minutes.

Group / **Stage**	**Stage 1**	**Stage 2**	**Stage 3**	**Stage 4**	**Stage 5**	**Stage 6**
K.A	-	-	-	-	**2 rats**	**4 rats**
K.A +Roscov	-	**3 rats**	**1 rat**	-	**2 rats**	-
Roscov	-	-	-	-	-	-
Controls	-	-	-	-	-	-

Figure 4.6: A table is summarising seizure related behavioural changes in single rats from different groups. Two rats from the kainic acid alone group reached Racine stage 5 and the other four reached stage 6. Two rats injected with kainic acid and roscovitine (K.A and Roscov group) reached stage 5, another one reached stage 3 and three reached stage 2. Controls and rats injected with roscovitine alone did not show any epileptic behaviours.

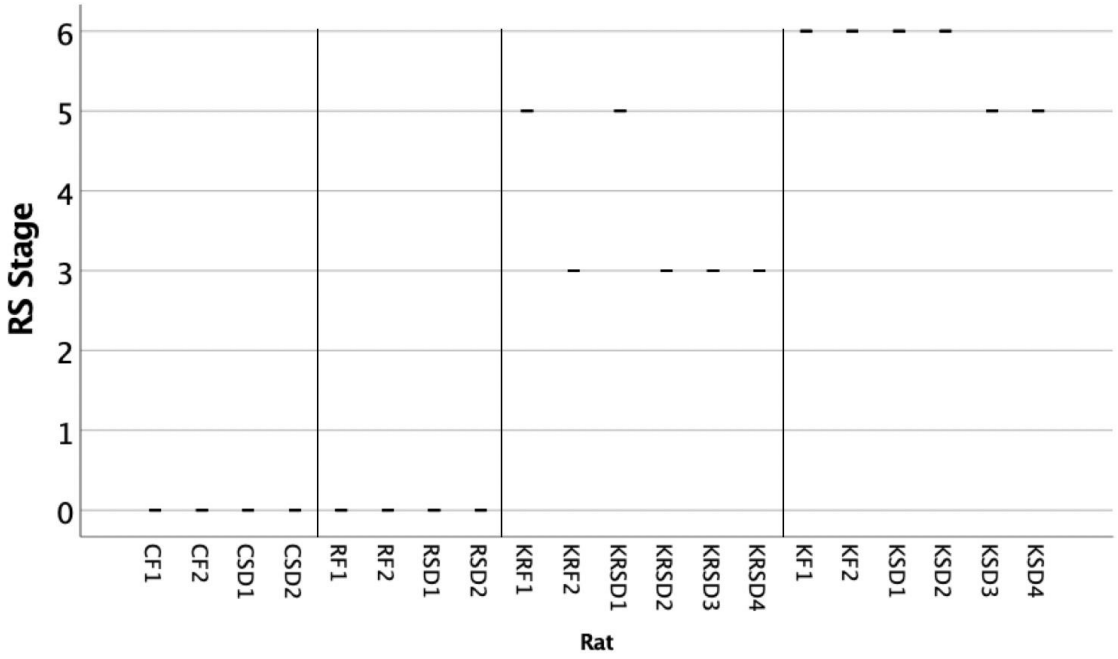

Figure 4.7: Seizure related behavioural changes in single rats from different groups.
Racine (RS) scale classifies seizure-related behaviours into six stages. The following graph represents our observations of behaviours that occurred for each individual rat: Fischer-344 controls (CF), SD controls (CSD), Fischer-344 roscovitine controls (RF), SD roscovitine controls (RSD), Fischer-344 kainic acid alone (KF), SD kainic acid alone (KSD), Fischer-344 roscovitine &kainic acid (KRF) and SD roscovitine & kainic acid (KRSD).

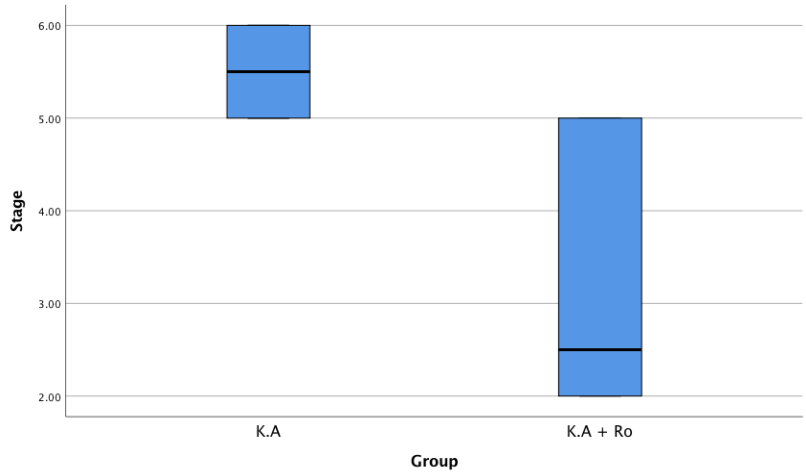

Figure 4.8: Seizure related behaviours. Seizure related behavioural change in Kainic acid alone injected group (K.A), and kainic acid and roscovitine injected group (K.A + Ro). There was a statistically significant difference in behavioural manifestation between kainic acid alone injected group and kainic acid and roscovitine injected group.

The precise electroencephalographic (EEG) and clinical characterisation of spontaneous seizures in this epilepsy model using video-EEG monitoring have been performed for three

pairs of rats in which a rat injected with roscovitine before kainic acid was paired with a rat injected with kainic acid alone. In the three pairs injected with roscovitine before kainic acid, the EEG data showed lower intensity in seizures, which suggest that roscovitine might have an effect on seizures. Figure 4.9 shows an example of a pair of rats in which one was injected with kainic acid alone (rat 2) and the other was injected with roscovitine prior to kainic acid (rat 1).

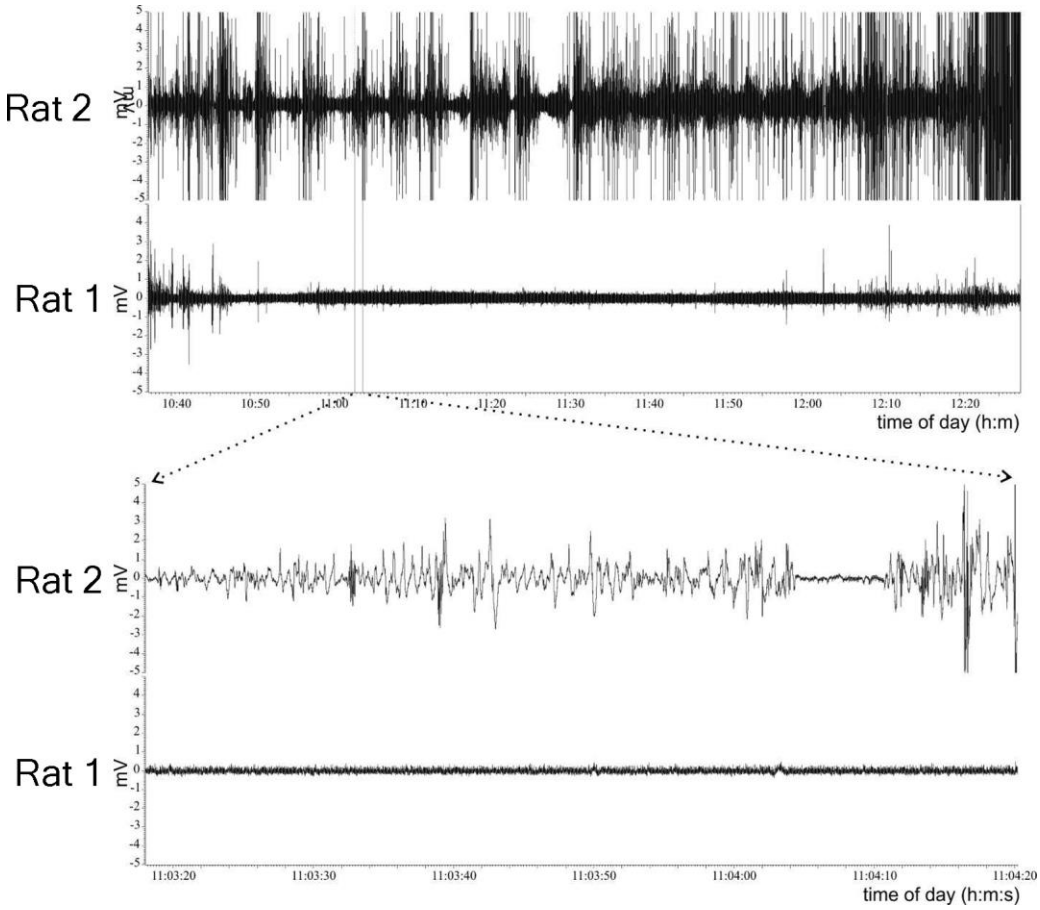

Figure 4.9: EEG graph comparing seizure intensity and duration in rats.

The figure shows an EEG recording in two- pairs of rats, in each pair there is a rat injected with roscovitine before kainic acid (Rat 1) and a rat injected with kainic acid alone (Rat 2) It is obvious that rat 2 had bigger EEG seizures and rat 1 had much smaller seizures that mostly stopped after 11 minutes. Most of the signal in rat 1 from 10:50 to 11:30 (Figure 4.9 A) is an oscillation at 40 Hz, which does not appear to be epileptiform.

4.3.6. Death rate before and after intrahippocampal kainic acid injection and problems related.

Considerable effort was made to reduce mortality. No deaths occurred in rats at the time of injection or during the recovery period after injection. There were two deaths in Fischer-344 rats in the recovery period after cannula implantation surgery because of haemorrhagic complications. In the first case, the rat died from a stroke (proven at post-mortem) and the second because of continuous haemorrhage. We discussed cases with the vets, which led to a joint decision to change the strain.

We had to terminate two additional rats from the Fischer-344 group after implantation surgery, as they had lost their skull caps completely, most likely due to the difficulty of drying the skull during surgery resulting in poor adhesion of the dental cement. We also, therefore, changed from a light-cured glass ionomer to Refobacin bone cement which bonds more strongly to the bone and also contains antibiotics.

A batch of four Sprague Dawleys rats in one cage had to be terminated in the recovery period after implantation, due to damage as one rat, chewed other rats' cannulae making intracranial injections impossible in most of that cohort. The initial cannulae caps were plastic, and so subsequently we changed to using metallic caps that became available around the time we detected that problem.

Discussion:

Our principal finding in this work is that roscovitine significantly prevents neuronal loss in kainic acid animal models of HS although it does not alter the SE induced by Kainic acid. Administration of intrahippocampal kainic alone induced epilepsy and epilepsy-related behaviours from stage 1 to stage 6 on the Racine scale and results in segmental neuronal loss within the hilus, CA3 and CA1 areas of the hippocampus. The effect of the different treatments was similar in Fischer-344 and Sprague Dawley strains. Intrahippocampal administrations of kainic acid provided more control over the bioavailability of the toxin and lesion than is possible with systemic administration of kainic acid or pilocarpine. We also avoided the unwanted effect of additional anaesthesia by injecting all drugs through a guide cannula.

Previous research suggests that injecting kainic acid systemically or intracerebrally in the hippocampus or amygdala could represent a model of TLE since it reproduced the typical histopathological changes seen in people with HS (Levesque and Avoli 2013). Previous studies have shown that systemic injection of high doses of kainic acid-induces seizures and seizure-related behavioural changes. At high doses, intravenous or intraperitoneal kainic acid-induced seizures at the hippocampus. Seizures starts 5 minutes following the injection, and stage 6 seizures related behaviours develops over 1–2 hours. Smaller doses showed different thresholds for these behavioural phenomena but a similar time course of development (Lothman and Collins 1981, Ben-Ari 1985, Van Nieuwenhuyse, Raedt et al. 2015). Systemic treatment with multiple low doses of kainic acid produced chronic epilepsy in rats. Hellier et al. developed this multiple-kainate-injection treatment protocol which resulted in a low mortality rate (15%) and a high percentage (97%) of epileptic rats (Hellier, Patrylo et al. 1998).

There can be severe neurotoxicity and neuronal damage following kainic acid treatment (Benkovic, O'Callaghan et al. 2006). The extent of neuronal damage is significant and occurs bilaterally and in extra-temporal regions. The intrahippocampal neuronal loss happens in the pyramidal cells in the CA1, CA3 and hilus regions of the hippocampus (Ben-Ari 1985, Wang, Yu et al. 2005). The CA3 pyramidal cell loss still occurs, even if kainic acid injections are performed in distal sites (such as CA1), further suggesting that the propagation of ictal activity causes neuronal damage in CA3 to this region (Levesque and Avoli 2013).

Our results suggest that roscovitine might affect seizures; in the kainic acid alone injected group four rats showed stage 6 behaviours and the other three showed stage 5 behaviours. In the roscovitine and kainic acid injected group, four rats showed stage 2 behaviours, one showed stage 3 behaviours, and one showed stage 5 behaviours.

The ability of roscovitine to affect seizures might be a direct result of inhibiting cdk5, which was found to affect voltage-dependent gating of calcium channels in neurons. Previous experiments proved that roscovitine might alter the voltage-dependent gating of calcium channels in a cdk5 dependent way. Cdk5 phosphorylates the N-Type calcium channel causing increased calcium-current density and channel open probability while roscovitine blocks this (Su, Seo et al. 2012).

The advantage of using intrahippocampal administrations of kainic acid is that there is greater control on the bioavailability of the drug and over the lesion that develops. Systemic injection is quicker and can be considered more efficient as multiple rats can be injected at a similar time. It is also less technically demanding, as, for example, implantation of intracranial cannulae is not required.
Our results show that kainic acid model is robust model of HS, and that the anti-cdk5 inhibitor roscovitine is a potential drug that can be used to protect neurons in this case.

Chapter 5: Investigation of NMDA receptor function in human hippocampal sclerosis

5.1. Introduction:

Around 30% of people with epilepsy have seizures that are resistant to current antiepileptic medication (Laxer, Trinka et al. 2014). The burden of epilepsy for these pharmacoresistant cases includes psychological problems, cognitive difficulties, increased morbidity and mortality as well as seizures themselves (Bell, Lin et al. 2011). The most common cause of pharmacoresistant epilepsy in adults is HS (Thom 2014). HS can be easily detected by magnetic resonance brain imaging (Bote, Blazquez-Llorca et al. 2008). A proportion of patients with HS may be suitable for surgical resection and in optimal cases operative intervention may result in 2-year seizure freedom in two thirds of these cases (Malmgren and Thom 2012). However, only 50% of patients who undergo resection for HS remain seizure free for ten years postoperatively (Spencer and Huh 2008). Therefore, enabling new therapeutic opportunities for people with HS is essential, particularly for cases in whom surgical resection is not a viable option or for those whose seizures recur post-operatively.

Histologically, HS is characterised by segmental neuronal loss, gliosis, synaptic reorganisation and dispersion of the granular cell layer (Thom 2014). Typically, in HS, there is massive neurodegeneration in the CA1, CA3 and CA4 areas of the hippocampus and relative sparing of the CA2 area and dentate gyrus. Neuronal loss in CA2 and dentate gyrus still might occur in chronic and severe cases (Proper, Oestreicher et al. 2000).

While HS exhibits features of both necrotic and apoptotic cell death, the underlying mechanisms of this neuronal loss remain elusive (Thom 2014). One protein that is thought to have a role in the mechanisms of neurodegeneration seen in HS is cdk5. The cdk5 monomer has no activity, for which it needs association with its main physiological activator p35 (Corbel, Zhang et al. 2015). p35 is subjected to rapid ubiquitin-mediated proteasomal degradation (Takasugi, Minegishi et al. 2016), and therefore, has a short half-life (approximately 20-30 minutes). Any neurotoxic stimuli including oxidative stress, excess

calcium, excess glutamate or β amyloid treatment of primary neurons can trigger the calpain-mediated cleavage of p35 to p25. p25 contains all the necessary elements to bind cdk5, but it lacks the myristoylation motif present at the N-terminus of p35. Consequently, while p35 is membrane-bound, p25 localises to the cell soma and nucleus. p25 is much more stable than p35 and causes constitutive, mislocalized hyperactivation of cdk5 which can lead to excitotoxicity and neurodegeneration via positive-feedback activation of the NMDA receptor (Humbert, Dhavan et al. 2000, Dhavan and Tsai 2001). For example, a flux of calcium can trigger calpain-mediated cleavage of p35 to p25. The p25-cdk5 complex then phosphorylates the NMDA receptor allowing enhanced calcium entry into the neuron, enabling further cleavage of p35 to p25 and thereby again facilitating NMDA receptor phosphorylation. This cycle of events can culminate in neuronal death. p25 can also play an essential role in apoptosis through directing cdk5 to alternative substrates to initiate apoptotic cell death cascades (Dhavan and Tsai 2001).

Earlier studies showed that changes in the activity of the p25-cdk5 complex associate with neuronal loss in surgically-resected HS (Sen, Thom et al. 2006) and post-mortem cases of HS (Sen, Thom et al. 2007). Here we further investigate the molecular mechanisms underlying the neuronal loss in human tissue. We hypothesise that deregulation of cdk5 by p25 will lead to phosphorylation of the NR2A subunit of the NMDA receptor and subsequent excitotoxic neuronal death

5.2. Materials and Methods:

5.2.1. Human tissue.

The Ethics committee at the University of Munster (responsible for Epilepsy-Zentrum Krankenhaus Mara hospital approved this study; Ethics Vote no 2015-088f-f-S). We obtained all studied tissue following therapeutic operations undertaken to relieve severe refractory epilepsy and was surplus to diagnostic requirement. A written, fully informed consent was obtained in all cases. Pseudoanonymised, fixed, paraffin-embedded 4 um sections were sent from Epilepsie-Zentrum | Krankenhaus Mara, Germany by Prof Dr Christian Bien. Human tissue act regulations were adhered to throughout. A total of 19 cases of HS were studied.

The tissue studied here consisted of the resected hippocampus and the adjacent temporal lobe. Normal human hippocampi are not removed before death, and we decided not to study post-mortem tissue owing to the possibility of upregulation in p25. Adjacent temporal lobe (TL) was used as a control. At the time of original tissue resection, all precautions were made to limit pre-resection hypoxia. Tissue was received fresh from surgery. A coronal slice through the hippocampus and temporal lobe was taken and rapidly placed in paraformaldehyde within a maximum of 30 minutes from removal. Tissue was fixed for 5 to 7 days, sliced, routinely processed, and embedded in paraffin wax. Serial sections were cut at 4-µm thickness. Initial sections were stained with hematoxylin and eosin, Luxol fast blue/cresyl violet and Bielschowsky silver method, allowing diagnosis and HS classification. The pseudonymised data of the patients' details are given in tables for batch 1 and batch 2 in the Appendix section.

5.2.2. Cell loss classification.

The degree of cell loss was classified according to the Wyler scoring system summarised by Thom et al., 2014:

Pathology	**Grade**
No hippocampal pathology.	Garde 0.
Mild damage [gliosis with slight (<10%) or no hippocampal dropout] involving sectors CA1,	Grade I.

CA3, and/or CA4 of the hippocampal pyramidal cell layer.	
Moderate damage [gliosis with moderate (10-50%) neuronal dropout] involving sectors CA1, CA3, and or CA4 of the hippocampal pyramidal cell layer.	Grade II.
Gliosis and neuronal loss in CA4, CA3 and CA1 with sparing of CA2.	Grade III.
Gliosis and neuronal loss in all areas of hippocampus.	Grade IV.

5.2.3. Immunohistochemistry.

We used standard immunohistochemistry techniques with hematoxylin counterstain and development of the immunoreaction with the Envision Detection Systems Peroxidase rabbit/mouse DAKO kit (K4056).

5.2.4. Dewax and rehydration.

We put slides in a 65 °C oven for approximately 20 minutes, and then moved them quickly to Histoclear to clear wax from sections (2X5 minutes). We rehydrated sections through graded alcohol (100%,100%,95%,80%) 5 minutes each and then washed for 5 minutes in washing buffer consisting of 0.05 mol/L Tris-HCl, pH 7.6, containing 0.15 mol/L NaCl and 0.05 % Tween 20.

5.2.5. Immunohistochemistry.

Antigen retrieval was achieved by microwaving in citrate buffer (10 µM citric acid, 0.05% Tween20, pH 6.0) using a 900-watt microwave at high power for 20 to 30 minutes, Endogenous peroxidase activity was blocked by incubating the specimens for 5-10 minutes with dual endogenous enzyme block. Sections were put in Sequenza clips and blocked for non –specific protein binding with 10 % serum in PBST for 1 hour (130 µl/Sequenza clip).

We then incubated sections in primary antibody diluted in 1% serum (goat serum) for 1 hour at room temperature in wash buffer. The following primary antibodies were studied (catalogue number in appendix): DC17 mouse monoclonal anti-cdk5 (Biotechnology, Santa Cruz) 1/100; mouse monoclonal anti-neuronal nuclei (NeuN) monoclonal antibody

(Millipore, UK) 1/1000; anti-p35 antibody rabbit polyclonal to p35, 1/100; rabbit polyclonal p-NR2A which detects the phosphorylated form of NR2A (Biorbyt, UK) 1/100; mouse monoclonal anti NMDANR2A (Sigma, UK) 1/100. After incubation, sections were washed in wash buffer for 3X5 minutes before being incubated with the labelled polymer-HRP (DAKO) for 40 minutes.

5.2.6. Detection.

Sections were washed 3 washes each 5 minutes, in washing buffer and then incubated with DAB+ CHROMOGEN (5-10 minutes) and then washed again in distilled water.

5.2.7. Haematoxylin staining, dehydration and sections mounting.

Sections were incubated in hematoxylin counterstain for 1 minute, rinsed in tap water until clear and then incubated in acid alcohol (200 ul concentrated HCl in 200ml 95% EtOH) for 3 minutes. Sections were rinsed in tap water for one minute, incubated in a bluing agent (Scott's tap water) for 1 minute and then rinsed again in tap water for 1 minute.

Sections were dehydrated through graded alcohol (75%, 95%, 2X100%, 5 minutes each), cleared in xylene/histoclear (2X5 minutes) and then mounted with DePeX permanent mounting medium. In each batch of staining, we included a negative control. TL and HS slides from a given case were stained together to better control for external variables.

5.2.8. Imaging and quantification.

Images were acquired using Zeiss® microscope and Image Lab software. NeuN positive cells were directly quantified in different hippocampal areas through manual neuronal counts per unit area using Image J analysis software. We compiled data in Excel (Microsoft Corporation) and classified HS according to Wyler scoring system mentioned above. The intensity of p-NR2A, NR2A and p35 staining in hippocampal areas was qualitatively compared to their intensity in the adjacent temporal lobe through visual assessment.

Density measurements were performed with ImageJ to quantify the intensity of NR2A and p-NR2A immunohistochemical staining. We used non-counterstained sections for this analysis and subtracted background staining before assessment.

5.3. Results.

A total of 19 cases of HS were studied. Sections were stained with NeuN to classify the degree of neuronal loss and grade HS according to the Wyler classification. There were six cases classified as stage 4, four cases as stage 3, three cases as stage 2 and six cases as stage1.

5.3.1. NR2A/phospho-NR2A immunohistochemistry.

p-NR2A antibody detects the phosphorylated form of the NR2A receptor while NMDANR2A antibody labels the non-phosphorylated form. Qualitatively, in all cases, immunohistochemistry with p-NR2A antibody appeared to demonstrate differences in staining between the hippocampal subfields and the adjacent histologically-normal temporal lobe. All surviving neurons were labelled. However, the intensity of the immunoreaction seemed more significant in surviving neurons within areas of neuronal loss in the hippocampus compared to temporal lobe (TL). This finding applied to cases of mild HS as well as more severe cases. (Figure 5.1,2,4). In contrast to the p-NR2A results, staining for NR2A appeared to show a higher intensity of immunoreaction in the temporal lobe (TL) compared to hippocampal areas (Figure 5.1,3,4).

However, quantitatively, density measurements revealed a significant increase in p-NR2A staining (one-way ANOVA, Bonferroni post hoc test $p<0.05$) in CA4 and CA1 regions compared to TL in patients with stage 4 HS only. There was no significant difference when comparing the other areas and the TL. There was no significant difference in staining intensity between CA4, CA3, CA2, CA1 or TL in cases of stage 1, stage 2 or stage 3 HS (Figure 5.5).

Similarly, there was a significant decrease in NR2A levels in CA4, CA3, CA2 and CA1 to that of the temporal lobe (TL) in stage 4 patients. There was no significant quantitative difference between affected hippocampal areas and temporal lobe (TL) in cases classified with other stages of HS (Figure 5.5).

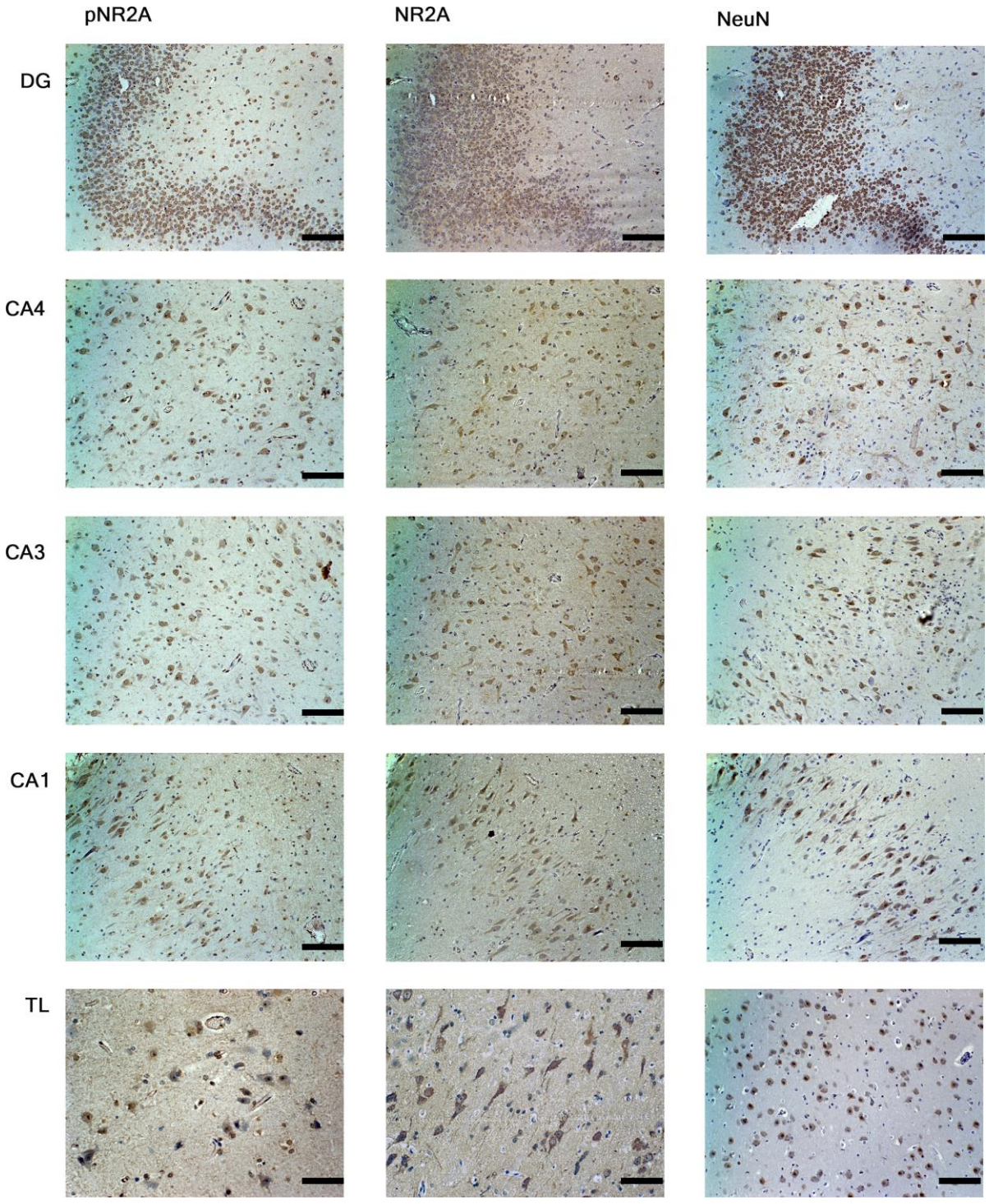

Figure 5.1: Immunohistochemistry with p-NR2A, NR2A and NeuN in the dentate gyrus (DG), CA4, CA3, CA1 and temporal lobe (TL) in human HS (Stage 1). Qualitatively staining with P-NR2A seemed to demonstrate an increased immunoreaction intensity in affected hippocampal areas (CA4, CA3, and CA1) compared to the TL. While staining with NR2A appeared to show increased immunoreactivity in temporal lobe (TL) neurons and less intensity in other hippocampal areas. NeuN staining for the same case is also shown. Images were taken at 10X. Scale bar=150 um.

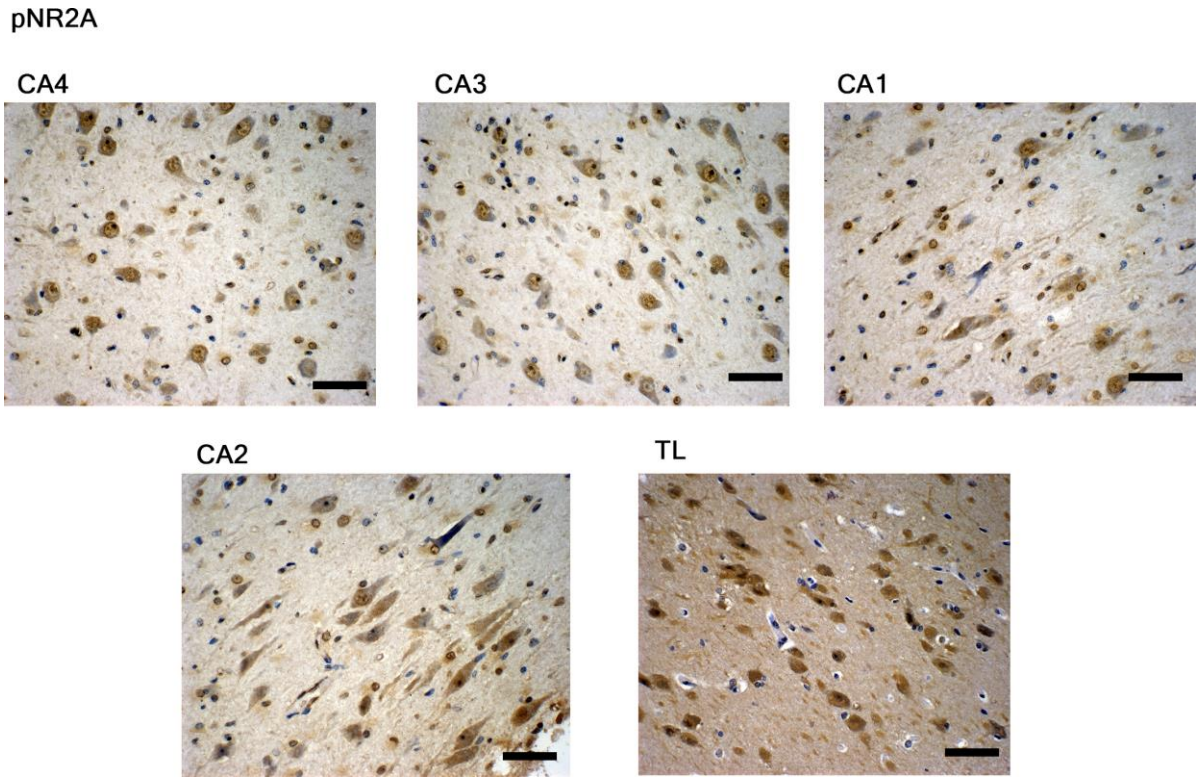

Figure 5.2: Immunohistochemistry with p-NR2A in the dentate gyrus (DG), CA4, CA3, CA2 CA1 and temporal lobe (TL). Qualitatively staining with P-NR2A demonstrated an increased immunoreaction intensity in studied hippocampal areas (CA4, CA3, and CA1) to the reaction in the temporal lobe (TL). Images are from a stage 1 case. Images were taken at 20X. Scale bar= 65 um

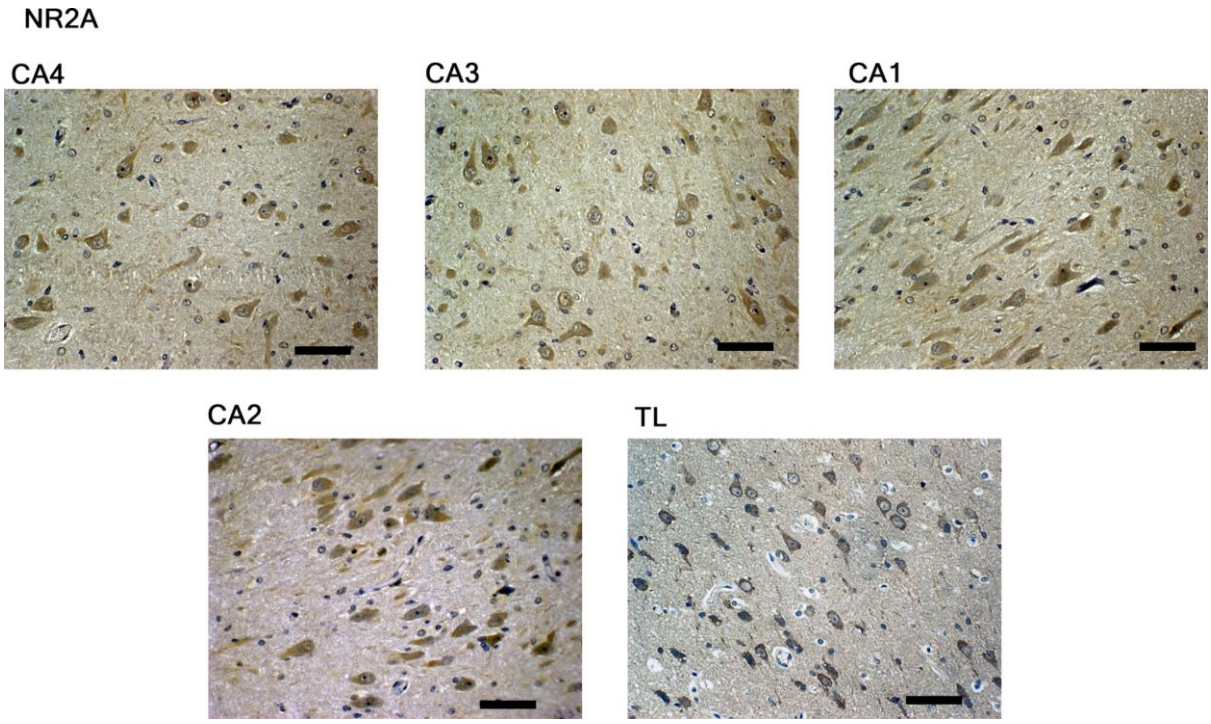

Figure 5.3: Immunohistochemistry with NR2A in the dentate gyrus (DG), CA4, CA3, CA2 CA1 and temporal lobe (TL). Qualitatively staining with RN2A demonstrated an increased immunoreaction intensity in studied hippocampal areas (CA4, CA3, and CA1) to the reaction in the temporal lobe (TL). Images represent a stage 1 case. Images were taken at 20X. Scale bar=65 um.

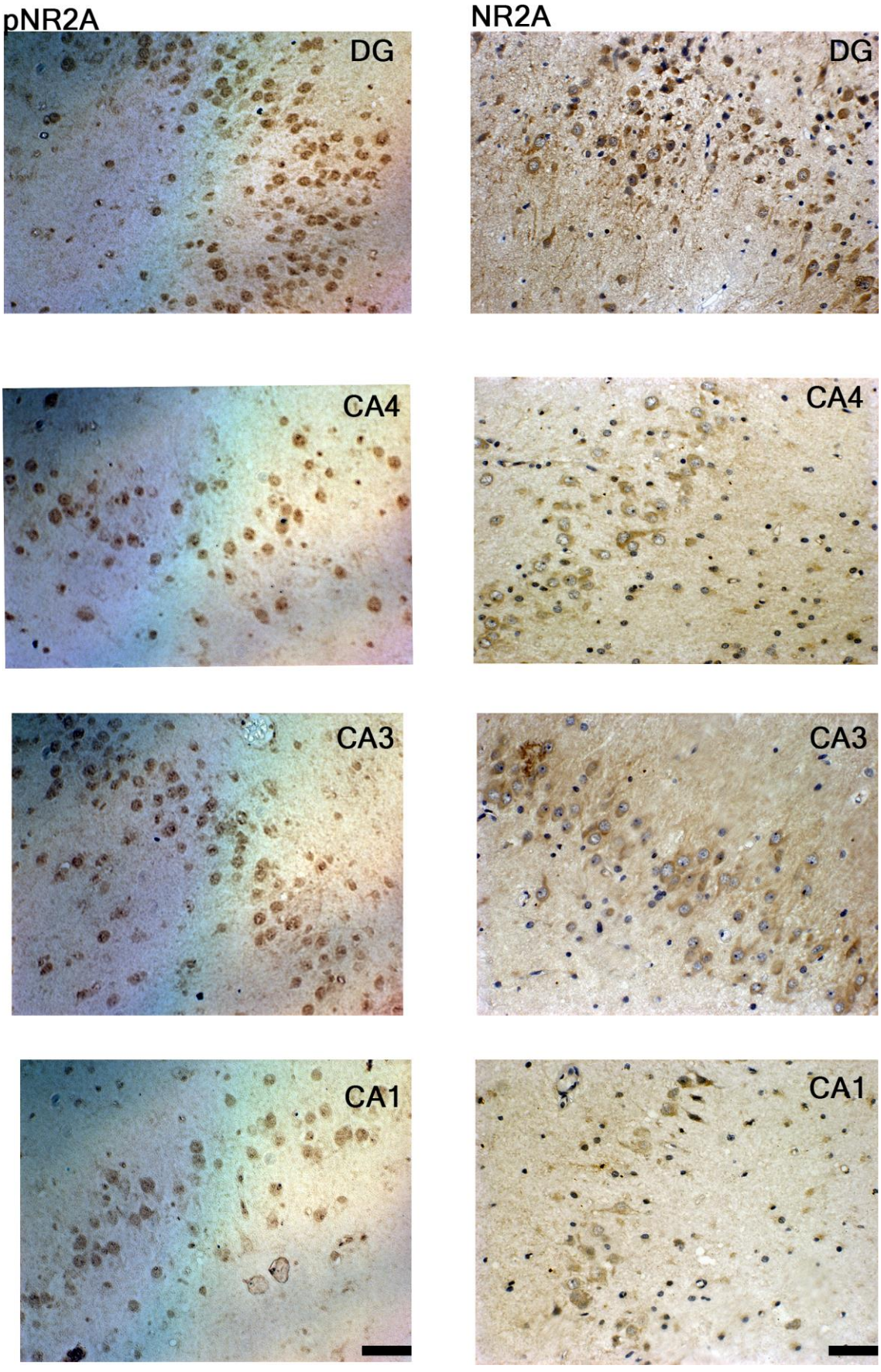
pNR2A
NR2A
DG
DG
CA4
CA4
CA3
CA3
CA1
CA1

Figure 5.4: Immunohistochemistry with NR2A and P-NR2A in the dentate gyrus (DG), CA4, CA3 and CA1 from stage 4 case from a stage 4 case.

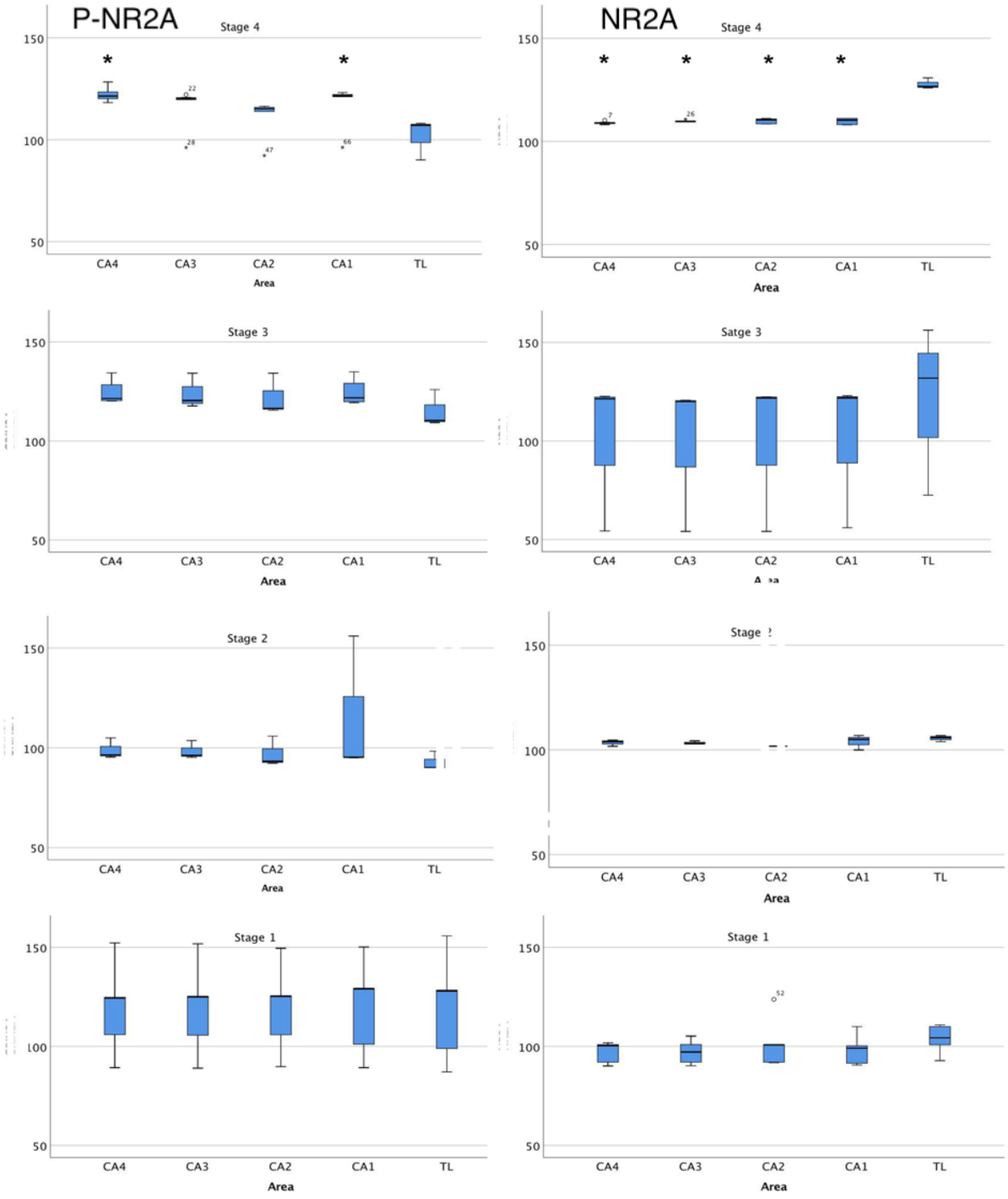

Figure 5.5: Quantitatively, density measurement of the NR2A and p-NR2A immunohistochemical staining. Quantifying immunohistochemical staining by optical density measurement, revealed a significant increase in p-NR2A staining (one-way ANOVA, Bonferroni post hoc test $p<0.05$) in CA4 and CA1 regions compared to temporal lobe (TL) in patients with stage 4 HS. There was no significant difference for the other areas of stage 4 patients when compared to TL. In cases of stage 1, stage 2 or stage 3 HS there was no quantitively difference in staining when comparing hippocampal subfields to the adjacent TL. There was, by contrast, an increase in NR2A immunoreactivity in the temporal lobe (TL) compared to other studied areas in stage 4 patients while there was no significant difference in the other HS stages. *indicates significant difference to TL.

5.3.2. p25: p35 immunoreactivity.

Staining with anti-p25: p35 antibody showed similar staining intensity between the temporal lobe (TL) and hippocampal areas in all cases, both qualitatively and quantitatively (one-way ANOVA *p*>.05) (Figure 5.6,7). However, the pattern of staining between hippocampal areas and temporal lobe neurons (TL) was different. Staining in affected hippocampal areas was more cytoplasmic while staining in the TL was more in nerve terminals and nucleus (Figure 5.6). The antibody used detects p25 and p35, which might suggest that the reaction in the affected area might be of that of p25, though it is not proven quantitatively.

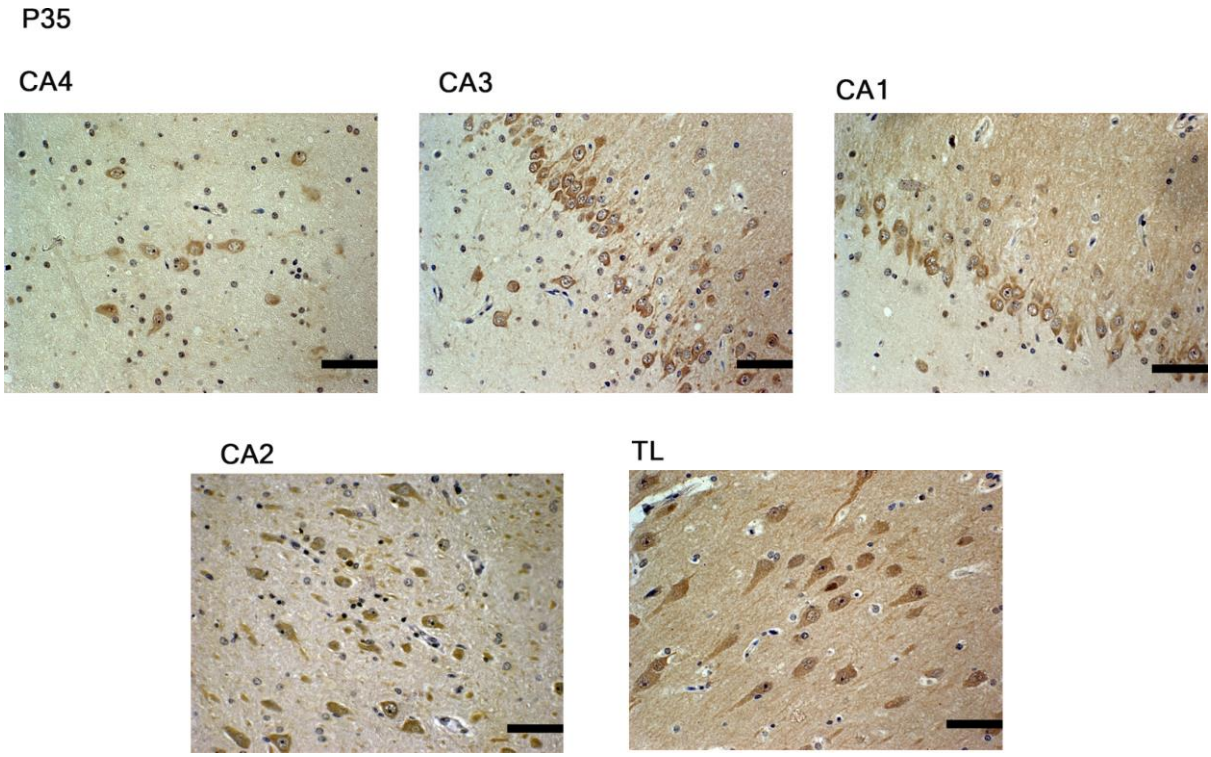

Figure 5.6: Immunohistochemistry with p35 in the dentate gyrus (DG), CA4, CA3, CA1 and temporal lobe (TL). Staining with p35 demonstrated equal immunoreaction intensities in studied hippocampal areas (CA4, CA3, CA2 and CA1) and the reaction in TL. However, the pattern of staining was different; staining in affected hippocampal areas was more in the cytoplasm while staining in the TL in the peripheries and nucleus. Images were taken at 20X. Scale bar=65 um. Images are of Stage 3 case.

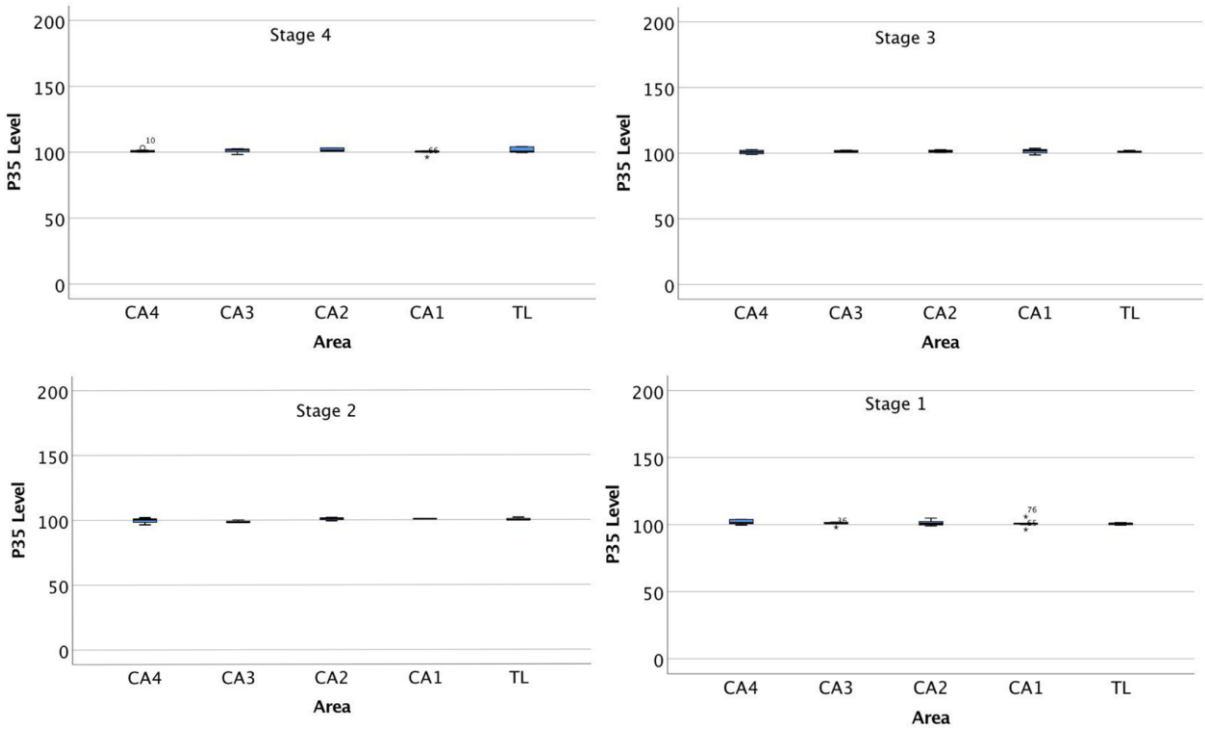

Figure 5.7: Quantitative measurement of p35 immunoreactivity in CA4, CA3, CA2, CA1 and TL. Quantitatively, density measurement of the p35 immunohistochemical staining revealed a similar expression (One Way ANOVA, Bonferroni post hoc test $p<0.05$) in p35 activity between hippocampal areas of CA4, CA3, CA2, CA1 compared to temporal lobe (TL) in patients with HS.

Unfortunately, we could not optimise the cdk5 antibody, so we could not collect data on cdk5 staining (Figure 5.8).

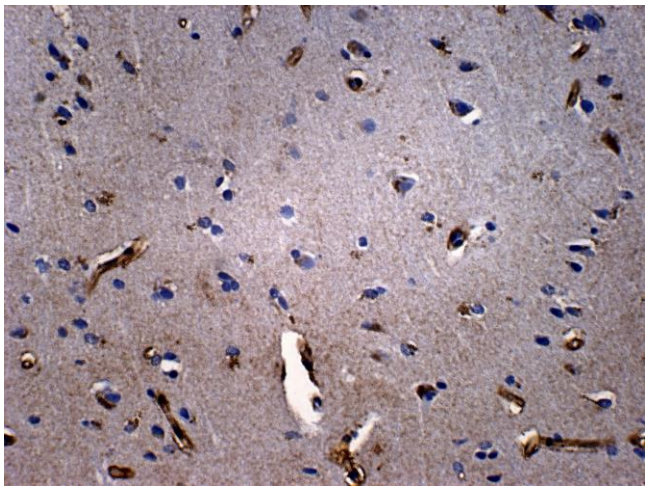

Figure 5.8: Example of attempt at cdk5 staining.
Despite numerous attempts we failed to optimise cdk5 antibody, therefore we couldn't collect data on cdk5 labelling.

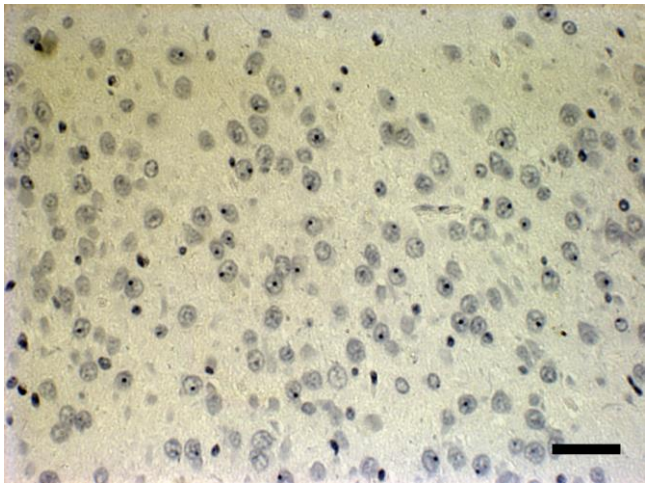

Figure 5.9: Example of a negative control. Scale bar=65 um.
With each batch of immunohistochemistry, negative controls were included. On each occasion there was no immunoreaction

5.4. Discussion.

In this study, we investigated NMDA phosphorylation in human HS. We used surgically resected human tissue to evaluate NMDA phosphorylation and p25/p35 activity.

Staining with anti p25/p35 antibody showed similar staining intensity between the temporal lobe (TL) and hippocampal areas in all cases, irrespective of HS stage. However, there was a difference in the pattern of staining between hippocampal areas and the TL. Staining in affected hippocampal areas was more cytoplasmic while staining in the TL was more in the peripheries and nucleus, this might suggest an active antigen/reaction in the cytoplasm in affected areas with more nuclear staining in the unaffected temporal lobe.

A possible explanation for this might lie in the differential cellular localisation of p25 and p35. The antibody used here binds both p25 and p35. However, p35 is membrane-bound while p25 localises to the cell soma and nucleus. The conversion of p35 to p25 re-localizes the protein from the cell periphery to the cytoplasm. p25 is much more stable than p35 and causes constitutive, mislocalized hyperactivation of cdk5 which may lead to excitotoxicity and neurodegeneration (Patrick, Zukerberg et al. 1999, Dhavan and Tsai 2001). Consequently, the staining pattern demonstrated here might suggest that there is increased p25 in the hippocampal neurons and increased p35 in temporal lobe opening the possibility that the increased phosphorylation of NMDA receptors seen in stage 4 HS is at least contributed to by increased p25-cdk5.

Earlier studies investigating the cdk5 and p35/p25 complex in surgically resected cases of HS with adjacent histologically normal temporal lobe, found increased immunoreactivity for p35/p25 in surviving neurons within areas of neuronal loss compared to the temporal lobe (TL). Western blots showed the ratio of p25 to p35 was greater in affected areas compared to the temporal lobe. Histone-based kinase assays showed increased activity of the p25-cdk5 complex in HS compared with the temporal lobe (TL) despite the neuronal loss in the hippocampal samples, which suggests that p25 is pathologically increased in HS and that deregulation of cdk5 by p25 might contribute to neuronal death in this condition (Sen, Thom et al. 2006).

The main finding in this experiment was that there was a significant increase in NR2A phosphorylation in CA4 and CA1 regions compared to temporal lobe (TL) in patients with stage 4 HS. There was also a significant decrease in NR2A expression in CA4, CA3, CA2 and CA1 compared to temporal lobe (TL) in patients with stage 4 HS. Hence the ratio of p(NR2A):NR2A in Stage 4 HS is significantly higher in affected areas compared to temporal lobe. No difference between areas was found in other stages of HS suggesting that this change in NR2A phosphorylation is only seen in very affected regions of more severe [ca]ses of HS.

NMDAR overactivation is linked to neurodegeneration (Zhou, Hollern et al. 2013). A current theory suggests that synaptic and extrasynaptic NMDAR enforce dramatic effects on cell fate and neuronal cell death is mainly mediated by the activation of external NMDAR (Zhou, Hollern et al. 2013). Activation of the NMDA subtype of glutamate receptor (NMDAR) is the major cause of glutamate excitotoxicity which mediates Ca^{2+} dependent cell death. While physiological activation of NMDAR is proposed to be neuroprotective, excessive or inappropriate activity is harmful (Gupta, Hardingham et al. 2013).

Previous studies have shown that stimulation of NMDA receptors leads to increases in intracellular calcium loads and can trigger cascades of events leading to excitotoxic cell death by apoptosis and necrosis (Dong, Wang et al. 2009, Zhang, Chen et al. 2009). Some studies have also revealed a direct role for p25-cdk5-NMDA mediated excitotoxicity and neuronal loss. Neuronal death in rat models of ischemia share a common pathway that involves p25-cdk5 and NMDA. Inhibition of this pathway was sufficient to reduce neuronal loss (Wang, Liu et al. 2003), suggesting that cdk5 –p25 signalling-mediated phosphorylation of the NMDA receptor is a primary event in the excitotoxicity process in this model of focal ischaemia. Cell death triggered by seizure or ischemic stroke, may therefore be attributed to NMDAR overactivation (Zhou, Hollern et al. 2013).

This study is the first to investigate NMDA phosphorylation in HS. Taken together, our results indicate that cdk5 deregulation and NMDA phosphorylation might contribute causally to neuronal loss in HS, and may in due course, open a potential avenue for pharmacological intervention to prevent neuronal loss in this condition.

Chapter 6: General Discussion and Conclusions

This study investigates the role of the cdk5 pathway in animal models of hippocampal sclerosis and surgically resected human tissue from patients with HS. It aims to evaluate the role of cdk5 and its principal activators in the neurodegeneration seen in HS and to test if inhibiting this pathway pharmacologically might contribute to neuronal preservation. This work is the first to use the cdk5 inhibitor roscovitine to study the effect of suppressing the p25-cdk5 pathway on neurodegeneration in animal models of HS and the first study to evaluate NMDA receptor phosphorylation in human HS tissue.

Our main findings were:

1- There was a hyperactivation of the p25-cdk5 pathway in pilocarpine and kainic acid-treated rodent models of HS suggesting a possible role of this pathway in neurodegeneration.

2- Inhibition of the cdk5 pathway using the cdk5 inhibitor roscovitine protects neurons in rodent models of HS demonstrating for the first time that the cdk5 pathway is causally implicated in the neuronal loss seen in epileptogenic pathologies.

3- There is evidence of increased NMDARs phosphorylation in advanced cases of HS compared to the adjacent histologically-normal temporal lobe (TL), suggesting that the p25-cdk5 pathway might have a role in mediating the neuronal death in HS through NMDA receptor phosphorylation.

Our results are important as they contribute to understanding the mechanism of neuronal loss in HS, in a way that opens a potential avenue for pharmacological intervention to prevent neuronal loss in this condition. Many studies are now targeting the p25-cdk5 pathway with the aim of designing successful therapeutic strategies for several fatal neurodegenerative diseases.

Studies of the p25-cdk5 complex in humans have focussed on archetypal neurodegenerative diseases such as Alzheimer's disease, in which p25 was found

accumulated in neurons in the brains of patients. Studies report that cdk5 is associated with the process of the pathogenesis of Alzheimer's disease and that inhibition of cdk5 activity with inhibitors such as RNA inference (RNAi) could protect from neuronal cell loss through suppressing β-amyloid (Aβ)-induced neurotoxicity and tauopathies (Liu, Wang et al. 2016). The p25-cdk5 complex has also been found to have a role in amyotrophic lateral sclerosis pathogenesis through a mechanism that involves tau hyperphosphorylation and neurofilament proteins which will lead to cellular apoptosis and neuronal cell death (Bajaj 2000, Nguyen, Lariviere et al. 2001). In addition, the role of p25-cdk5 has been demonstrated in the pathology of Parkinson's disease through a mechanism that involves calpain activation after intracellular calcium influx (Camins, Verdaguer et al. 2006). A wide range of studies show that the p25-cdk5 complex plays a role in stroke and ischemia as well and the p25-cdk5 complex is thought to be a leading cause of neuronal death in rodent models of stroke (Osuga, Osuga et al. 2000, Meyer, Torres-Altoro et al. 2014, Tan, Chen et al. 2015, Mushtaq, Greig et al. 2016).

Drugs such as roscovitine, flavopiridol, calpain inhibitors, kenpaullone and indirubin, which inhibit p25-cdk5 formation, are considered potential drugs for the treatment of neurological disorders(Camins, Verdaguer et al. 2006). Inhibition of p25-cdk5 activity was found to be neuroprotective and improved the outcomes of Alzheimer's disease, Parkinson's disease and ischemia both in vivo and in vitro models (Leclerc, Garnier et al. 2001, Alvira, Tajes et al. 2006, Meyer, Torres-Altoro et al. 2014, Ji, Zhuang et al. 2017). With all those studies focusing on the role of cdk5 in neurodegeneration; very few studies investigated the role of cdk5 in HS. Previous studies have shown that the p25-cdk5 complex associates with the neurodegeneration of HS (Sen, Thom et al. 2006, Sen, Thom et al. 2007), but to date, no studies have specifically evaluated NMDA receptor phosphorylation in human HS. Moreover, no previous work has evaluated the effect of inhibiting cdk5 function in animal models of epilepsy to determine better whether the p25-cdk5 complex might be causally implicated in the neurodegeneration seen in HS. The current project set out to address these two key questions.

In our animal models of HS, neuropathological changes such as neuronal loss in several hippocampal subfields is observed in the pilocarpine rat model and kainic acid rat model

which mimics the neuronal loss of that of patients with hippocampal sclerosis. Our principal finding is that roscovitine significantly prevented such neuronal loss in all areas studied in pilocarpine and kainic acid animal models of HS. The ability of roscovitine to preserve neurons and protect against neuronal loss in animal models of HS, suggests that deregulation of the cdk5 pathway might have a role in causing neuronal loss in HS. Injection of roscovitine was focal into the lateral ventricle of the right side, but it still managed to prevent neuronal loss even though seizures are more widespread and longer-lived than the measurable metabolic consequence of the drug. We did, though, have neuronal loss that was more widespread than the zone affected by roscovitine.

We also used MK801 which is a selective non-competitive NMDA antagonist (Kovacic and Somanathan 2010), post pilocarpine treatment in the pilocarpine animal model of HS. Our results showed that MK801 significantly prevented neuronal loss in all areas studied following systemic pilocarpine injection, which supports the hypothesis that NMDA receptor has a role in the pathway of neuronal loss in epilepsy model and that suppressing NMDA might contribute to neuronal preservation.

The main difference between our two animal models was in the route of administration. In the pilocarpine model, injection of pilocarpine was systemic and in the kainic acid model injection of kainic acid was intrahippocampal. The route of administration caused a difference in the extent of the induced neuropathological damage and its location.

Following systemic injection of pilocarpine, there was a loss of cells in the CA1, CA3 and hilus regions of the hippocampus while CA2 and the dentate gyrus were preserved. With pilocarpine, the neuronal loss spread bilaterally and in extra-temporal regions. By contrast, in the kainic acid mode, loss of neurons occurred in the hilus, CA3 and CA1 areas of the right injected hippocampi only. Kainic acid was injected into the distal site, but the neuronal loss spread to the ventral site as well, the left non-injected hippocampi remained intact. The ability of roscovitine to preserve neurons was higher in the kainic acid model than in the systemic pilocarpine one.

The acute behavioural manifestations that follow the intrahippocampal administration of kainic acid are similar in characteristics to those observed following systemic injection of pilocarpine, though they were more intense in the pilocarpine model. We observed behaviours from all the six-stage categories of the Racine scale in both models. However,

while all animals injected with pilocarpine showed stage 6 behaviours, this was not necessarily the case in the intrahippocampal kainic acid model. The mortality rate after pilocarpine-induced SE was high (more than 60% of animals died) while there were no fatalities after kainic acid-induced SE.

In human HS, our main finding was that there was a significant increase in NR2A phosphorylation in CA4 and CA1 regions compared to temporal lobe (TL) in advanced cases of HS. By contrast, there was a significant decrease in NR2A expression in CA4, CA3, CA2 and CA1 compared to temporal lobe (TL) in patients with advanced cases of HS. This shows that there might be an increase in NMDA receptor phosphorylation in neuronal loss area in HS. Although p35 reactivity showed similar staining intensity between the temporal lobe (TL) and hippocampal areas, it was noticeable that there was a difference in morphology and pattern of staining between hippocampal areas and temporal lobe (TL), with the possible explanation that there is increased conversion of p35 to p25 in areas of neuronal loss.

Taken together, our animal model and human tissue results provide evidence that cdk5 deregulation and NMDA phosphorylation might contribute causally to neuronal loss in HS. Our results further link cdk5 and NMDA in epileptogenic pathologies and suggest that phosphorylation of NMDA receptor in HS might be through a mechanism that involves deregulation of the p25-cdk5 pathway. The significant increase in p25: p35 ratio in animal models of HS, the preservation of neurons upon blocking the NMDA receptor and cdk5 pharmacologically in animal models, and the phosphorylation of NMDA receptor in stage 4 hippocampal sclerosis cases, all support this hypothesis.

Conclusion and future work:

Our results further indicate that the p25-cdk5 pathway might have a role in the pathogenesis of neuronal loss in HS and that interfering with this pathway pharmacologically might be a potential approach for the of neuronal loss in this case.

Roscovitine seems a promising drug in protecting neurons. However, we have not studied the effect of roscovitine if injected post excitotoxicity or the effect of other drugs that inhibit p25-cdk5 formation. In the future, we propose to evaluate the effect of roscovitine, and other drugs that inhibit p25-cdk5 formation, on excitotoxic cell loss post induced SE. Cell

culture models and animal models might be used for this purpose. The project could be extended to evaluate neurodegenerative and survival mechanisms, which may contribute to the subfield-specific neuronal loss seen in neurodegenerative diseases with an aim to study the expressions of p35 and p25 and cdk5 kinase activity in-vitro and in vivo following excitotoxic treatment. We could also evaluate the effect of the cdk5 inhibitor roscovitine and other inhibitors like flavopiridol, calpain inhibitors, kenpaullone and indirubin on excitotoxicity and neurodegeneration in cell culture models of other neurodegenerative diseases that might share common mechanisms of neuronal loss to those seen in hippocampal sclerosis.

Appendix

0.06 % Potassium permanganate Solution:

0.6 gm Potassium Permanganate in 1000 ml distilled water.

PBS/T (Wash buffer 0.1%)

1ml Tween-20 per 1L PBS (1L dH20 +10 tablets of PBS)

5% milk solution

2.5g milk solution 50ml PBS-T

MOPS Running buffer (1X SDS Running buffer)

50ml 20x MOPS SDS Running Buffer to 950ml deionized water

Transfer buffer

100ml Methanol 1ml Antioxidant 50ml 20 X Transfer Buffer Made up to 1L with deionized water

Acidified water

400 μl glacial acetic acid

400 ml of water

0.1 % Triton:

(1 ml 5% T x 10 PBS, 9 ml H20, 40 ml PBS)

DAPI and Nissl Double staining

(1/1000 in 0.1 % Triton) 6 ml of DAPI solution in 0.1 % Triton in Nissl Solution (30 μL in Nissl)

Bio Rad Transfer buffer

200 ml of Bio Rad transfer buffer

600 ml of water

200 ml Ethanol.

Citrate buffer

(10 mM **citric acid**, 0.05% Tween 20, pH 6.0)

1.92 g of anhydrous citric acid

1000 ml of distilled water.

Adjust the pH to 6.0 with 1N sodium hydroxide and then add 0.5 ml of Tween 20.

Tris-buffered saline

(TBS) (1X) 6.05 g Tris

8.76 g NaCl

800 mL of H_2O.

pH adjusted to 7.5 with 1 M HCl and volume made up to 1 L with H_2O.

TBS was kept stable at 4°C for 3 months.

Acid alcohol

1% hydrochloric acid in ethanol.

Scott tap water

Magnesium sulfate (MgSO4) 35 gm,

Sodium bicarbonate 20 gm

in 1000 ml distilled eater

AB List

Antibody	Catalogue number
P-NR2A (Phospho-Ser 1232)	Orb221779
Anti-NR2A	75-288
NeuN	MAB377
P35 antibody	Sc-820
Cdk5 (C-8)	Sc-173
Cdk5 (DC17)	Sc-249
Monoclonal Anti-ß-Actin	A3854

Human Tissue Received cases:

Neuropathology No	Sex and DOB	Date of Surgery	Grade and Further remarks
218/15 **IV 1**	F,31st Dec 1982	7th Sept,2015	**IV**
234/15 **IV 1**	M,20th Jan,1967	21st Sept ,2015	**IV**
209/15 **IV 1**	M,24th July, 1963	24th Aug,2015	**IV**
201/15 **I 2**	F,11th Jan,2005	13th Aug,2015	**I**, Rasmussen encephalitis hippocampus resected during functional hemispherectomy

141/15 **III 1**	M,15th July,1988	11th June,2015	**III**
149/15 **III** 1	M,16th July,1988	22nd June,2015	**III**
174/15 IV	M,9th Nov,1976	15th July,2015	IV, Had intrahippocampal depth electrodes

Table summarizing cases of patients with hippocampal sclerosis studied received in BATCH 1.

Patient ID	**Date of Birth**	**Age of**	**Date of Surgery**	**Grade**
60362512	16.07.1980	8	11.11.2013	**II**
60359059	12.07.1990	4	28.10.2013	IV
60010856	08.03.1974	22	26.09.2013	IV
60141415	22.08.1951	6	27.06.2013	**I**
60328030	27.07.1992	4	24.06.2013	**III**
60332027	23.10.1956	5,5	20.06.2013	**III**
60354313	25.06.1988	14	10.06.2013	**I**

60335062	08.05.1972	24	04.06.2013	**II**
60317877	14.03.1952	14	25.04.2013	**II**
60326944	13.03.1968	25	05.03.2013	**I**
60312771	18.03.1952	29	22.01.2013	**I**
60059671	27.09.1984	14	03.01.2013	**I**

Table summarizing cases of patients with hippocampal sclerosis studied received in BATCH 2.

References:

Al Sufiani, F. and L. C. Ang (2012). "Neuropathology of temporal lobe epilepsy." Epilepsy Res Treat **2012**: 624519.

Alonso, A., T. Zaidi, M. Novak, I. Grundke-Iqbal and K. Iqbal (2001). "Hyperphosphorylation induces self-assembly of tau into tangles of paired helical filaments/straight filaments." Proc Natl Acad Sci U S A **98**(12): 6923-6928.

Alvarez, A., R. Toro, A. Caceres and R. B. Maccioni (1999). "Inhibition of tau phosphorylating protein kinase cdk5 prevents beta-amyloid-induced neuronal death." FEBS Lett **459**(3): 421-426.

Alvira, D., M. Tajes, E. Verdaguer, D. Acuna-Castroviejo, J. Folch, A. Camins and M. Pallas (2006). "Inhibition of the cdk5/p25 fragment formation may explain the antiapoptotic effects of melatonin in an experimental model of Parkinson's disease." J Pineal Res **40**(3): 251-258.

Amaral, D. G. and M. P. Witter (1989). "The three-dimensional organization of the hippocampal formation: a review of anatomical data." Neuroscience **31**(3): 571-591.

Arundine, M. and M. Tymianski (2003). "Molecular mechanisms of calcium-dependent neurodegeneration in excitotoxicity." Cell Calcium **34**(4-5): 325-337.

Aydemir, A., O. Abbasoglu, S. Topaloglu, D. Ertoy, A. Ayhan, K. Kilinc, E. Karabulut and I. Sayek (2002). "Protective effect of roscovitine on renal ischemia-reperfusion injury." Transplant Proc **34**(6): 2027-2028.

Bach, S., M. Knockaert, J. Reinhardt, O. Lozach, S. Schmitt, B. Baratte, M. Koken, S. P. Coburn, L. Tang, T. Jiang, D. C. Liang, H. Galons, J. F. Dierick, L. A. Pinna, F. Meggio, F. Totzke, C. Schachtele, A. S. Lerman, A. Carnero, Y. Wan, N. Gray and L. Meijer (2005). "Roscovitine targets, protein kinases and pyridoxal kinase." J Biol Chem **280**(35): 31208-31219.

Bajaj, N. P. (2000). "Cyclin-dependent kinase-5 (CDK5) and amyotrophic lateral sclerosis." Amyotroph Lateral Scler Other Motor Neuron Disord **1**(5): 319-327.

Balu, D. T. (2016). "The NMDA Receptor and Schizophrenia: From Pathophysiology to Treatment." Adv Pharmacol **76**: 351-382.

Beghi, E. (2016). "Addressing the burden of epilepsy: Many unmet needs." Pharmacol Res **107**: 79-84.

Bell, B., J. J. Lin, M. Seidenberg and B. Hermann (2011). "The neurobiology of cognitive disorders in temporal lobe epilepsy." Nat Rev Neurol **7**(3): 154-164.

Ben-Ari, Y. (1985). "Limbic seizure and brain damage produced by kainic acid: mechanisms and relevance to human temporal lobe epilepsy." Neuroscience **14**(2): 375-403.

Benkovic, S. A., J. P. O'Callaghan and D. B. Miller (2006). "Regional neuropathology following kainic acid intoxication in adult and aged C57BL/6J mice." Brain Res **1070**(1): 215-231.

Benson, C., J. White, J. De Bono, A. O'Donnell, F. Raynaud, C. Cruickshank, H. McGrath, M. Walton, P. Workman, S. Kaye, J. Cassidy, A. Gianella-Borradori, I. Judson and C. Twelves (2007). "A phase I trial of the selective oral cyclin-dependent kinase inhibitor seliciclib (CYC202; R-Roscovitine), administered twice daily for 7 days every 21 days." Br J Cancer **96**(1): 29-37.

Bloss, E. B. and R. G. Hunter (2010). "Hippocampal kainate receptors." Vitam Horm **82**: 167-184.

Blumcke, I., M. Thom and O. D. Wiestler (2002). "Ammon's horn sclerosis: a maldevelopmental disorder associated with temporal lobe epilepsy." Brain Pathol **12**(2): 199-211.

Boex, C., M. Seeck, S. Vulliemoz, A. O. Rossetti, C. Staedler, L. Spinelli, A. J. Pegna, E. Pralong, J. G. Villemure, G. Foletti and C. Pollo (2011). "Chronic deep brain stimulation in mesial temporal lobe epilepsy." Seizure **20**(6): 485-490.

Bote, R. P., L. Blazquez-Llorca, M. A. Fernandez-Gil, L. Alonso-Nanclares, A. Munoz and J. De Felipe (2008). "Hippocampal sclerosis: histopathology substrate and magnetic resonance imaging." Semin Ultrasound CT MR **29**(1): 2-14.

Bromfield, E. B. (2006). An Introduction to Epilepsy. An Introduction to Epilepsy. E. B. Bromfield, J. E. Cavazos and J. I. Sirven. West Hartford (CT).

Bukanov, N. O., L. A. Smith, K. W. Klinger, S. R. Ledbetter and O. Ibraghimov-Beskrovnaya (2006). "Long-lasting arrest of murine polycystic kidney disease with CDK inhibitor roscovitine." Nature **444**(7121): 949-952.
Camins, A., E. Verdaguer, J. Folch, A. M. Canudas and M. Pallas (2006). "The role of CDK5/P25 formation/inhibition in neurodegeneration." Drug News Perspect **19**(8): 453-460.
Cavalheiro, E. A. (1995). "The pilocarpine model of epilepsy." Ital J Neurol Sci **16**(1-2): 33-37.
Cavalheiro, E. A., J. P. Leite, Z. A. Bortolotto, W. A. Turski, C. Ikonomidou and L. Turski (1991). "Long-term effects of pilocarpine in rats: structural damage of the brain triggers kindling and spontaneous recurrent seizures." Epilepsia **32**(6): 778-782.
Chae, T., Y. T. Kwon, R. Bronson, P. Dikkes, E. Li and L. H. Tsai (1997). "Mice lacking p35, a neuronal specific activator of Cdk5, display cortical lamination defects, seizures, and adult lethality." Neuron **18**(1): 29-42.
Chang, K. H., F. Vincent and K. Shah (2012). "Deregulated Cdk5 triggers aberrant activation of cell cycle kinases and phosphatases inducing neuronal death." J Cell Sci **125**(Pt 21): 5124-5137.
Chow, H. M., D. Guo, J. C. Zhou, G. Y. Zhang, H. F. Li, K. Herrup and J. Zhang (2014). "CDK5 activator protein p25 preferentially binds and activates GSK3beta." Proc Natl Acad Sci U S A **111**(45): E4887-4895.
Cicenas, J., K. Kalyan, A. Sorokinas, E. Stankunas, J. Levy, I. Meskinyte, V. Stankevicius, A. Kaupinis and M. Valius (2015). "Roscovitine in cancer and other diseases." Ann Transl Med **3**(10): 135.
Corbel, C., B. Zhang, A. Le Parc, B. Baratte, P. Colas, C. Couturier, K. S. Kosik, I. Landrieu, V. Le Tilly and S. Bach (2015). "Tamoxifen inhibits CDK5 kinase activity by interacting with p35/p25 and modulates the pattern of tau phosphorylation." Chem Biol **22**(4): 472-482.
Crespel, A., P. Coubes, M. C. Rousset, C. Brana, A. Rougier, G. Rondouin, J. Bockaert, M. Baldy-Moulinier and M. Lerner-Natoli (2002). "Inflammatory reactions in human medial temporal lobe epilepsy with hippocampal sclerosis." Brain Res **952**(2): 159-169.
Curia, G., D. Longo, G. Biagini, R. S. Jones and M. Avoli (2008). "The pilocarpine model of temporal lobe epilepsy." J Neurosci Methods **172**(2): 143-157.
Das, A., G. C. t. Wallace, C. Holmes, M. L. McDowell, J. A. Smith, J. D. Marshall, L. Bonilha, J. C. Edwards, S. S. Glazier, S. K. Ray and N. L. Banik (2012). "Hippocampal tissue of patients with refractory temporal lobe epilepsy is associated with astrocyte activation, inflammation, and altered expression of channels and receptors." Neuroscience **220**: 237-246.
De Azevedo, W. F., S. Leclerc, L. Meijer, L. Havlicek, M. Strnad and S. H. Kim (1997). "Inhibition of cyclin-dependent kinases by purine analogues: crystal structure of human cdk2 complexed with roscovitine." Eur J Biochem **243**(1-2): 518-526.
de la Motte, S. and A. Gianella-Borradori (2004). "Pharmacokinetic model of R-roscovitine and its metabolite in healthy male subjects." Int J Clin Pharmacol Ther **42**(4): 232-239.
Dhavan, R. and L. H. Tsai (2001). "A decade of CDK5." Nat Rev Mol Cell Biol **2**(10): 749-759.
Dong, X. X., Y. Wang and Z. H. Qin (2009). "Molecular mechanisms of excitotoxicity and their relevance to pathogenesis of neurodegenerative diseases." Acta Pharmacol Sin **30**(4): 379-387.
Dubey, D., J. Kalita and U. K. Misra (2017). "Status epilepticus: Refractory and super-refractory." Neurol India **65**(Supplement): S12-S17.
Engelborghs, S., R. D'Hooge and P. P. De Deyn (2000). "Pathophysiology of epilepsy." Acta Neurol Belg **100**(4): 201-213.
Fisher, R. S., J. H. Cross, J. A. French, N. Higurashi, E. Hirsch, F. E. Jansen, L. Lagae, S. L. Moshe, J. Peltola, E. Roulet Perez, I. E. Scheffer and S. M. Zuberi (2017). "Operational classification of seizure types by the International League Against Epilepsy: Position Paper of the ILAE Commission for Classification and Terminology." Epilepsia **58**(4): 522-530.
Foster, A. C., R. Gill, J. A. Kemp and G. N. Woodruff (1987). "Systemic administration of MK-801 prevents N-methyl-D-aspartate-induced neuronal degeneration in rat brain." Neurosci Lett **76**(3): 307-311.

Foster, J. A., L. Bezin, L. Groc, P. L. Christopherson and R. A. Levine (2003). "Kainic acid lesion-induced nigral neuronal death." J Chem Neuroanat **26**(1): 65-73.
Furman, M. (2013). "Seizure initiation and propagation in the pilocarpine rat model of temporal lobe epilepsy." J Neurosci **33**(42): 16409-16411.
Furukawa, H., S. K. Singh, R. Mancusso and E. Gouaux (2005). "Subunit arrangement and function in NMDA receptors." Nature **438**(7065): 185-192.
Gasull, T., N. DeGregorio-Rocasolano and R. Trullas (2001). "Overactivation of alpha-amino-3-hydroxy-5-methylisoxazole-4-propionate and N-methyl-D-aspartate but not kainate receptors inhibits phosphatidylcholine synthesis before excitotoxic neuronal death." J Neurochem **77**(1): 13-22.
Gherardi, D., V. D'Agati, T. H. Chu, A. Barnett, A. Gianella-Borradori, I. H. Gelman and P. J. Nelson (2004). "Reversal of collapsing glomerulopathy in mice with the cyclin-dependent kinase inhibitor CYC202." J Am Soc Nephrol **15**(5): 1212-1222.
Gill, R., A. C. Foster and G. N. Woodruff (1987). "Systemic administration of MK-801 protects against ischemia-induced hippocampal neurodegeneration in the gerbil." J Neurosci **7**(10): 3343-3349.
Gilles, C. and S. Ertle (2000). "Pharmacological models in Alzheimer's disease research." Dialogues Clin Neurosci **2**(3): 247-255.
Glien, M., C. Brandt, H. Potschka, H. Voigt, U. Ebert and W. Loscher (2001). "Repeated low-dose treatment of rats with pilocarpine: low mortality but high proportion of rats developing epilepsy." Epilepsy Res **46**(2): 111-119.
Golden, G. T., G. G. Smith, T. N. Ferraro and P. F. Reyes (1995). "Rat strain and age differences in kainic acid induced seizures." Epilepsy Res **20**(2): 151-159.
Gupta, A. and L. H. Tsai (2003). "Cyclin-dependent kinase 5 and neuronal migration in the neocortex." Neurosignals **12**(4-5): 173-179.
Gupta, K., G. E. Hardingham and S. Chandran (2013). "NMDA receptor-dependent glutamate excitotoxicity in human embryonic stem cell-derived neurons." Neurosci Lett **543**: 95-100.
Hahntow, I. N., F. Schneller, M. Oelsner, K. Weick, I. Ringshausen, F. Fend, C. Peschel and T. Decker (2004). "Cyclin-dependent kinase inhibitor Roscovitine induces apoptosis in chronic lymphocytic leukemia cells." Leukemia **18**(4): 747-755.
Hellier, J. L. and F. E. Dudek (2005). "Chemoconvulsant model of chronic spontaneous seizures." Curr Protoc Neurosci **Chapter 9**: Unit 9 19.
Hellier, J. L., P. R. Patrylo, P. S. Buckmaster and F. E. Dudek (1998). "Recurrent spontaneous motor seizures after repeated low-dose systemic treatment with kainate: assessment of a rat model of temporal lobe epilepsy." Epilepsy Res **31**(1): 73-84.
Henry, T. R., M. Chupin, S. Lehericy, J. P. Strupp, M. A. Sikora, Z. Y. Sha, K. Ugurbil and P. F. Van de Moortele (2011). "Hippocampal sclerosis in temporal lobe epilepsy: findings at 7 T(1)." Radiology **261**(1): 199-209.
Henshall, D. C. (2007). "Apoptosis signalling pathways in seizure-induced neuronal death and epilepsy." Biochem Soc Trans **35**(Pt 2): 421-423.
Henshall, D. C. and R. P. Simon (2005). "Epilepsy and apoptosis pathways." J Cereb Blood Flow Metab **25**(12): 1557-1572.
Heuser, K., E. Tauboll, E. A. Nagelhus, M. Cvancarova, O. P. Ottersen and L. Gjerstad (2009). "Phenotypic characteristics of temporal lobe epilepsy: the impact of hippocampal sclerosis." Acta Neurologica Scandinavica **120**: 8-13.
Hollmann, M. and S. Heinemann (1994). "Cloned glutamate receptors." Annu Rev Neurosci **17**: 31-108.
Hong, N., Y. S. Choi, S. Y. Kim and H. J. Kim (2017). "Neuroprotective effect of lithium after pilocarpine-induced status epilepticus in mice." Korean J Physiol Pharmacol **21**(1): 125-131.
Humbert, S., R. Dhavan and L. Tsai (2000). "p39 activates cdk5 in neurons, and is associated with the actin cytoskeleton." J Cell Sci **113 (Pt 6)**: 975-983.

Jackson, G. D. (1995). "The diagnosis of hippocampal sclerosis: other techniques." Magn Reson Imaging **13**(8): 1081-1093.
Jefferys, J. G. (2014). "Do seizures in the pilocarpine model start in the hippocampal formation?" Epilepsy Curr **14**(4): 206-207.
Ji, Y. B., P. P. Zhuang, Z. Ji, Y. M. Wu, Y. Gu, X. Y. Gao, S. Y. Pan and Y. F. Hu (2017). "TFP5 peptide, derived from CDK5-activating cofactor p35, provides neuroprotection in early-stage of adult ischemic stroke." Sci Rep **7**: 40013.
Jin, X. T. and Y. Smith (2011). "Localization and functions of kainate receptors in the basal ganglia." Adv Exp Med Biol **717**: 27-37.
Kandratavicius, L., P. A. Balista, C. Lopes-Aguiar, R. N. Ruggiero, E. H. Umeoka, N. Garcia-Cairasco, L. S. Bueno-Junior and J. P. Leite (2014). "Animal models of epilepsy: use and limitations." Neuropsychiatr Dis Treat **10**: 1693-1705.
Karakas, E., M. C. Regan and H. Furukawa (2015). "Emerging structural insights into the function of ionotropic glutamate receptors." Trends Biochem Sci **40**(6): 328-337.
Kim, S. H. and T. A. Ryan (2010). "CDK5 serves as a major control point in neurotransmitter release." Neuron **67**(5): 797-809.
Kini, L. G., J. C. Gee and B. Litt (2016). "Computational analysis in epilepsy neuroimaging: A survey of features and methods." Neuroimage Clin **11**: 515-529.
Kovacic, P. and R. Somanathan (2010). "Clinical physiology and mechanism of dizocilpine (MK-801): electron transfer, radicals, redox metabolites and bioactivity." Oxid Med Cell Longev **3**(1): 13-22.
Kurbatskaya, K., E. C. Phillips, C. L. Croft, G. Dentoni, M. M. Hughes, M. A. Wade, S. Al-Sarraj, C. Troakes, M. J. O'Neill, B. G. Perez-Nievas, D. P. Hanger and W. Noble (2016). "Upregulation of calpain activity precedes tau phosphorylation and loss of synaptic proteins in Alzheimer's disease brain." Acta Neuropathol Commun **4**: 34.
Kwan, P. and M. R. Sperling (2009). "Refractory seizures: try additional antiepileptic drugs (after two have failed) or go directly to early surgery evaluation?" Epilepsia **50 Suppl 8**: 57-62.
Lai, T. W., S. Zhang and Y. T. Wang (2014). "Excitotoxicity and stroke: identifying novel targets for neuroprotection." Prog Neurobiol **115**: 157-188.
Laxer, K. D., E. Trinka, L. J. Hirsch, F. Cendes, J. Langfitt, N. Delanty, T. Resnick and S. R. Benbadis (2014). "The consequences of refractory epilepsy and its treatment." Epilepsy Behav **37**: 59-70.
Le Bail, M., M. Martineau, S. Sacchi, N. Yatsenko, I. Radzishevsky, S. Conrod, K. Ait Ouares, H. Wolosker, L. Pollegioni, J. M. Billard and J. P. Mothet (2015). "Identity of the NMDA receptor coagonist is synapse specific and developmentally regulated in the hippocampus." Proc Natl Acad Sci U S A **112**(2): E204-213.
Le Duigou, C., L. Wittner, L. Danglot and R. Miles (2005). "Effects of focal injection of kainic acid into the mouse hippocampus in vitro and ex vivo." J Physiol **569**(Pt 3): 833-847.
Leclerc, S., M. Garnier, R. Hoessel, D. Marko, J. A. Bibb, G. L. Snyder, P. Greengard, J. Biernat, Y. Z. Wu, E. M. Mandelkow, G. Eisenbrand and L. Meijer (2001). "Indirubins inhibit glycogen synthase kinase-3 beta and CDK5/p25, two protein kinases involved in abnormal tau phosphorylation in Alzheimer's disease. A property common to most cyclin-dependent kinase inhibitors?" J Biol Chem **276**(1): 251-260.
Ledee, D. R., C. Y. Gao, R. Seth, R. N. Fariss, B. K. Tripathi and P. S. Zelenka (2005). "A specific interaction between muskelin and the cyclin-dependent kinase 5 activator p39 promotes peripheral localization of muskelin." J Biol Chem **280**(22): 21376-21383.
Leite, J. P., N. Garcia-Cairasco and E. A. Cavalheiro (2002). "New insights from the use of pilocarpine and kainate models." Epilepsy Res **50**(1-2): 93-103.
Lerma, J. (2003). "Roles and rules of kainate receptors in synaptic transmission." Nat Rev Neurosci **4**(6): 481-495.
Levesque, M. and M. Avoli (2013). "The kainic acid model of temporal lobe epilepsy." Neurosci Biobehav Rev **37**(10 Pt 2): 2887-2899.

Levesque, M., M. Avoli and C. Bernard (2016). "Animal models of temporal lobe epilepsy following systemic chemoconvulsant administration." J Neurosci Methods **260**: 45-52.
Li, B. S., L. Zhang, S. Takahashi, W. Ma, H. Jaffe, A. B. Kulkarni and H. C. Pant (2002). "Cyclin-dependent kinase 5 prevents neuronal apoptosis by negative regulation of c-Jun N-terminal kinase 3." EMBO J **21**(3): 324-333.
Liu, C., X. Zhai, B. Zhao, Y. Wang and Z. Xu (2017). "Cyclin I-like (CCNI2) is a cyclin-dependent kinase 5 (CDK5) activator and is involved in cell cycle regulation." Sci Rep **7**: 40979.
Liu, S. L., C. Wang, T. Jiang, L. Tan, A. Xing and J. T. Yu (2016). "The Role of Cdk5 in Alzheimer's Disease." Mol Neurobiol **53**(7): 4328-4342.
Liu, W., J. Li, Y. S. Song, Y. Li, Y. H. Jia and H. D. Zhao (2017). "Cdk5 links with DNA damage response and cancer." Mol Cancer **16**(1): 60.
Liu, X., Y. Liu, J. Zhang, W. Zhang, Y. E. Sun, X. Gu and Z. Ma (2014). "Intrathecal administration of roscovitine prevents remifentanil-induced postoperative hyperalgesia and decreases the phosphorylation of N-methyl-D-aspartate receptor and metabotropic glutamate receptor 5 in spinal cord." Brain Res Bull **106**: 9-16.
Ljungman, M. and M. T. Paulsen (2001). "The cyclin-dependent kinase inhibitor roscovitine inhibits RNA synthesis and triggers nuclear accumulation of p53 that is unmodified at Ser15 and Lys382." Mol Pharmacol **60**(4): 785-789.
Loftis, J. M. and A. Janowsky (2003). "The N-methyl-D-aspartate receptor subunit NR2B: localization, functional properties, regulation, and clinical implications." Pharmacol Ther **97**(1): 55-85.
Lothman, E. W. and R. C. Collins (1981). "Kainic acid induced limbic seizures: metabolic, behavioral, electroencephalographic and neuropathological correlates." Brain Res **218**(1-2): 299-318.
Luttjohann, A., P. F. Fabene and G. van Luijtelaar (2009). "A revised Racine's scale for PTZ-induced seizures in rats." Physiol Behav **98**(5): 579-586.
Malmgren, K. and M. Thom (2012). "Hippocampal sclerosis--origins and imaging." Epilepsia **53 Suppl 4**: 19-33.
Maragakis, N. J. and J. D. Rothstein (2006). "Mechanisms of Disease: astrocytes in neurodegenerative disease." Nat Clin Pract Neurol **2**(12): 679-689.
Mello, L. E. and L. Covolan (1996). "Spontaneous seizures preferentially injure interneurons in the pilocarpine model of chronic spontaneous seizures." Epilepsy Res **26**(1): 123-129.
Menn, B., S. Bach, T. L. Blevins, M. Campbell, L. Meijer and S. Timsit (2010). "Delayed treatment with systemic (S)-roscovitine provides neuroprotection and inhibits in vivo CDK5 activity increase in animal stroke models." PLoS One **5**(8): e12117.
Meyer, D. A., M. I. Torres-Altoro, Z. Tan, A. Tozzi, M. Di Filippo, V. DiNapoli, F. Plattner, J. W. Kansy, S. A. Benkovic, J. D. Huber, D. B. Miller, P. Greengard, P. Calabresi, C. L. Rosen and J. A. Bibb (2014). "Ischemic stroke injury is mediated by aberrant Cdk5." J Neurosci **34**(24): 8259-8267.
Mushtaq, G., N. H. Greig, F. Anwar, F. A. Al-Abbasi, M. A. Zamzami, H. A. Al-Talhi and M. A. Kamal (2016). "Neuroprotective Mechanisms Mediated by CDK5 Inhibition." Curr Pharm Des **22**(5): 527-534.
Nguyen, M. D., R. C. Lariviere and J. P. Julien (2001). "Deregulation of Cdk5 in a mouse model of ALS: toxicity alleviated by perikaryal neurofilament inclusions." Neuron **30**(1): 135-147.
Nikolaev, M. V., L. G. Magazanik and D. B. Tikhonov (2012). "Influence of external magnesium ions on the NMDA receptor channel block by different types of organic cations." Neuropharmacology **62**(5-6): 2078-2085.
Niquet, J., M. L. Lopez-Meraz and C. G. Wasterlain (2012). Programmed Necrosis After Status Epilepticus. Jasper's Basic Mechanisms of the Epilepsies. th, J. L. Noebels, M. Avoli et al. Bethesda (MD).
Ormandy, G. C., R. S. Jope and O. C. Snead, 3rd (1989). "Anticonvulsant actions of MK-801 on the lithium-pilocarpine model of status epilepticus in rats." Exp Neurol **106**(2): 172-180.

Osuga, H., S. Osuga, F. Wang, R. Fetni, M. J. Hogan, R. S. Slack, A. M. Hakim, J. E. Ikeda and D. S. Park (2000). "Cyclin-dependent kinases as a therapeutic target for stroke." Proc Natl Acad Sci U S A **97**(18): 10254-10259.
Patrick, G. N., L. Zukerberg, M. Nikolic, S. de la Monte, P. Dikkes and L. H. Tsai (1999). "Conversion of p35 to p25 deregulates Cdk5 activity and promotes neurodegeneration." Nature **402**(6762): 615-622.
Proper, E. A., A. B. Oestreicher, G. H. Jansen, C. W. Veelen, P. C. van Rijen, W. H. Gispen and P. N. de Graan (2000). "Immunohistochemical characterization of mossy fibre sprouting in the hippocampus of patients with pharmaco-resistant temporal lobe epilepsy." Brain **123 (Pt 1)**: 19-30.
Rajmohan, V. and E. Mohandas (2007). "The limbic system." Indian J Psychiatry **49**(2): 132-139.
Raynaud, F. I., S. R. Whittaker, P. M. Fischer, S. McClue, M. I. Walton, S. E. Barrie, M. D. Garrett, P. Rogers, S. J. Clarke, L. R. Kelland, M. Valenti, L. Brunton, S. Eccles, D. P. Lane and P. Workman (2005). "In vitro and in vivo pharmacokinetic-pharmacodynamic relationships for the trisubstituted aminopurine cyclin-dependent kinase inhibitors olomoucine, bohemine and CYC202." Clin Cancer Res **11**(13): 4875-4887.
Recasens, A. and B. Dehay (2014). "Alpha-synuclein spreading in Parkinson's disease." Front Neuroanat **8**: 159.
Reddy, D. S. and R. Kuruba (2013). "Experimental models of status epilepticus and neuronal injury for evaluation of therapeutic interventions." Int J Mol Sci **14**(9): 18284-18318.
Reeve, A., E. Simcox and D. Turnbull (2014). "Ageing and Parkinson's disease: why is advancing age the biggest risk factor?" Ageing Res Rev **14**: 19-30.
Rogawski, M. A., D. Gryder, D. Castaneda, W. Yonekawa, M. K. Banks and H. Lia (2003). "GluR5 kainate receptors, seizures, and the amygdala." Ann N Y Acad Sci **985**: 150-162.
Schmidt, D. and S. C. Schachter (2014). "Drug treatment of epilepsy in adults." BMJ **348**: g254.
Schmued, L. C., C. C. Stowers, A. C. Scallet and L. Xu (2005). "Fluoro-Jade C results in ultra high resolution and contrast labeling of degenerating neurons." Brain Res **1035**(1): 24-31.
Scorza, F. A., R. M. Arida, G. Naffah-Mazzacoratti Mda, D. A. Scerni, L. Calderazzo and E. A. Cavalheiro (2009). "The pilocarpine model of epilepsy: what have we learned?" An Acad Bras Cienc **81**(3): 345-365.
Sen, A., M. Thom, L. Martinian, T. Jacobs, M. Nikolic and S. M. Sisodiya (2006). "Deregulation of cdk5 in Hippocampal sclerosis." J Neuropathol Exp Neurol **65**(1): 55-66.
Sen, A., M. Thom, L. Martinian, M. Yogarajah, M. Nikolic and S. M. Sisodiya (2007). "Increased immunoreactivity of cdk5 activators in hippocampal sclerosis." Neuroreport **18**(5): 511-516.
Sendrowski, K. and W. Sobaniec (2013). "Hippocampus, hippocampal sclerosis and epilepsy." Pharmacol Rep **65**(3): 555-565.
Shah, K. and D. K. Lahiri (2014). "Cdk5 activity in the brain - multiple paths of regulation." J Cell Sci **127**(Pt 11): 2391-2400.
Small, S. A., S. A. Schobel, R. B. Buxton, M. P. Witter and C. A. Barnes (2011). "A pathophysiological framework of hippocampal dysfunction in ageing and disease." Nat Rev Neurosci **12**(10): 585-601.
Smith, P. D., M. P. Mount, R. Shree, S. Callaghan, R. S. Slack, H. Anisman, I. Vincent, X. Wang, Z. Mao and D. S. Park (2006). "Calpain-regulated p35/cdk5 plays a central role in dopaminergic neuron death through modulation of the transcription factor myocyte enhancer factor 2." J Neurosci **26**(2): 440-447.
Smolders, I., G. M. Khan, J. Manil, G. Ebinger and Y. Michotte (1997). "NMDA receptor-mediated pilocarpine-induced seizures: characterization in freely moving rats by microdialysis." Br J Pharmacol **121**(6): 1171-1179.
Spencer, S. and L. Huh (2008). "Outcomes of epilepsy surgery in adults and children." Lancet Neurol **7**(6): 525-537.
Spencer, S. S., J. Kim, N. deLanerolle and D. D. Spencer (1999). "Differential neuronal and glial relations with parameters of ictal discharge in mesial temporal lobe epilepsy." Epilepsia **40**(6): 708-712.

Steinlein, O. K. (2014). "Calcium signaling and epilepsy." Cell Tissue Res **357**(2): 385-393.
Su, S. C., J. Seo, J. Q. Pan, B. A. Samuels, A. Rudenko, M. Ericsson, R. L. Neve, D. T. Yue and L. H. Tsai (2012). "Regulation of N-type voltage-gated calcium channels and presynaptic function by cyclin-dependent kinase 5." Neuron **75**(4): 675-687.
Sundaram, J. R., C. P. Poore, N. H. Sulaimee, T. Pareek, A. B. Asad, R. Rajkumar, W. F. Cheong, M. R. Wenk, G. S. Dawe, K. H. Chuang, H. C. Pant and S. Kesavapany (2013). "Specific inhibition of p25/Cdk5 activity by the Cdk5 inhibitory peptide reduces neurodegeneration in vivo." J Neurosci **33**(1): 334-343.
Szydlowska, K. and M. Tymianski (2010). "Calcium, ischemia and excitotoxicity." Cell Calcium **47**(2): 122-129.
Takasugi, T., S. Minegishi, A. Asada, T. Saito, H. Kawahara and S. Hisanaga (2016). "Two Degradation Pathways of the p35 Cdk5 (Cyclin-dependent Kinase) Activation Subunit, Dependent and Independent of Ubiquitination." J Biol Chem **291**(9): 4649-4657.
Tan, X., Y. Chen, J. Li, X. Li, Z. Miao, N. Xin, J. Zhu, W. Ge, Y. Feng and X. Xu (2015). "The inhibition of Cdk5 activity after hypoxia/ischemia injury reduces infarct size and promotes functional recovery in neonatal rats." Neuroscience **290**: 552-560.
Thom, M. (2014). "Review: Hippocampal sclerosis in epilepsy: a neuropathology review." Neuropathol Appl Neurobiol **40**(5): 520-543.
Tomizawa, K., J. Ohta, M. Matsushita, A. Moriwaki, S. T. Li, K. Takei and H. Matsui (2002). "Cdk5/p35 regulates neurotransmitter release through phosphorylation and downregulation of P/Q-type voltage-dependent calcium channel activity." J Neurosci **22**(7): 2590-2597.
Toyoda, I., M. R. Bower, F. Leyva and P. S. Buckmaster (2013). "Early activation of ventral hippocampus and subiculum during spontaneous seizures in a rat model of temporal lobe epilepsy." J Neurosci **33**(27): 11100-11115.
Triarhou, L. C. (2002). "Introduction. Dopamine and Parkinson's disease." Adv Exp Med Biol **517**: 1-14.
Van Nieuwenhuyse, B., R. Raedt, M. Sprengers, I. Dauwe, S. Gadeyne, E. Carrette, J. Delbeke, W. J. Wadman, P. Boon and K. Vonck (2015). "The systemic kainic acid rat model of temporal lobe epilepsy: Long-term EEG monitoring." Brain Res **1627**: 1-11.
Verkhratsky, A., J. J. Rodriguez and V. Parpura (2013). "Astroglia in neurological diseases." Future Neurol **8**(2): 149-158.
Vermeiren, C., M. Najimi, N. Vanhoutte, S. Tilleux, I. de Hemptinne, J. M. Maloteaux and E. Hermans (2005). "Acute up-regulation of glutamate uptake mediated by mGluR5a in reactive astrocytes." J Neurochem **94**(2): 405-416.
Vezzani, A. (2009). "Pilocarpine-induced seizures revisited: what does the model mimic?" Epilepsy Curr **9**(5): 146-148.
Vita, M., M. Abdel-Rehim, C. Nilsson, Z. Hassan, P. Skansen, H. Wan, L. Meurling and M. Hassan (2005). "Stability, pKa and plasma protein binding of roscovitine." J Chromatogr B Analyt Technol Biomed Life Sci **821**(1): 75-80.
Vita, M., M. Abdel-Rehim, S. Olofsson, Z. Hassan, L. Meurling, A. Siden, M. Siden, T. Pettersson and M. Hassan (2005). "Tissue distribution, pharmacokinetics and identification of roscovitine metabolites in rat." Eur J Pharm Sci **25**(1): 91-103.
Wang, J., S. Liu, Y. Fu, J. H. Wang and Y. Lu (2003). "Cdk5 activation induces hippocampal CA1 cell death by directly phosphorylating NMDA receptors." Nat Neurosci **6**(10): 1039-1047.
Wang, Q., S. Yu, A. Simonyi, G. Y. Sun and A. Y. Sun (2005). "Kainic acid-mediated excitotoxicity as a model for neurodegeneration." Mol Neurobiol **31**(1-3): 3-16.
Willard, S. S. and S. Koochekpour (2013). "Glutamate, glutamate receptors, and downstream signaling pathways." Int J Biol Sci **9**(9): 948-959.
Wisden, W. and P. H. Seeburg (1993). "A complex mosaic of high-affinity kainate receptors in rat brain." J Neurosci **13**(8): 3582-3598.

Yakisich, J. S., A. Siden, V. Idoyaga Vargas, P. Eneroth and M. Cruz (1998). "Early inhibition of DNA synthesis in the developing rat cerebral cortex by the purine analogues olomoucine and roscovitine." Biochem Biophys Res Commun **243**(3): 674-677.
Yan, Z., P. Chi, J. A. Bibb, T. A. Ryan and P. Greengard (2002). "Roscovitine: a novel regulator of P/Q-type calcium channels and transmitter release in central neurons." J Physiol **540**(Pt 3): 761-770.
Yuan, G. Q., D. D. Gao, J. Lin, S. Han and B. C. Lv (2013). "Treatment of recurrent epileptic seizures in patients with neurological disorders." Exp Ther Med **5**(1): 267-270.
Zarei, S., K. Carr, L. Reiley, K. Diaz, O. Guerra, P. F. Altamirano, W. Pagani, D. Lodin, G. Orozco and A. Chinea (2015). "A comprehensive review of amyotrophic lateral sclerosis." Surg Neurol Int **6**: 171.
Zhang, Q., C. Chen, J. Lu, M. Xie, D. Pan, X. Luo, Z. Yu, Q. Dong and W. Wang (2009). "Cell cycle inhibition attenuates microglial proliferation and production of IL-1beta, MIP-1alpha, and NO after focal cerebral ischemia in the rat." Glia **57**(8): 908-920.
Zhang, R., Y. Liu, J. Zhang, Y. Zheng, X. Gu and Z. Ma (2012). "Intrathecal administration of roscovitine attenuates cancer pain and inhibits the expression of NMDA receptor 2B subunit mRNA." Pharmacol Biochem Behav **102**(1): 139-145.
Zhou, X., D. Hollern, J. Liao, E. Andrechek and H. Wang (2013). "NMDA receptor-mediated excitotoxicity depends on the coactivation of synaptic and extrasynaptic receptors." Cell Death Dis **4**: e560.
Zoja, C., F. Casiraghi, S. Conti, D. Corna, D. Rottoli, R. A. Cavinato, G. Remuzzi and A. Benigni (2007). "Cyclin-dependent kinase inhibition limits glomerulonephritis and extends lifespan of mice with systemic lupus." Arthritis Rheum **56**(5): 1629-1637.